UNIVERSITY OF BELGRADE
FACULTY OF CHEMISTRY

Kawther Adaila

SYNTHESIS AND CHARACTERIZATION OF Pd(II), Co(III) AND Ni(II) COMPLEXES WITH THE CONDENSATION DERIVATIVE OF 2-(DIPHENYLPHOSPHINO)BENZALDEHYDE AND GIRARD'S T REAGENT

Doctoral Dissertation

Belgrade, 2016

UNIVERZITET U BEOGRADU
HEMIJSKI FAKULTET

Kawther Adaila

SINTEZA I KARAKTERIZACIJA KOMPLEKSA Pd(II), Co(III) I Ni(II) SA KONDENZACIONIM PROIZVODOM 2-(DIFENILFOSFINO)BENZALDEHIDA I ŽIRAROVOG T REAGENSA

doktorska disertacija

Beograd, 2016

Mentor

_____

Full Professor dr Katarina Anđelković

Faculty of Chemistry, University of Belgrade

Commission members

_____

Assistant Professor dr Tamara Todorović

Faculty of Chemistry, University of Belgrade

_____

Assistant Research Professor dr Dragana Mitić

Innovation Center of the Faculty of Chemistry

_____

Full Research Professor dr Dušanka Radanović

Institute of Chemistry, Technology and Metallurgy,

University of Belgrade

Date _____.

Acknowledgements

- It is a genuine pleasure to express my deep sense of thanks and gratitude to **Prof. Katarina Anđelković**, **Dušanka Radanović** and **Tamara Todorović** who helped me to get to this stage.

- I thank profusely my colleagues **Milica Milenković, Božidar Čobeljić** and **Gabrijela Brađan** for their kind help and co-operation throughout my study period.

- I express my deep sense of gratitude to my parents, who exerted their best to complete my educational career.

- It is my privilege to thank my husband **Mr. Osama**, for his constant encouragement throughout my study period.

Synthesis and characterization of Pd(II), Co(III) and Ni(II) complexes with the condensation derivative of 2-(diphenylphosphino)benzaldehyde and Girard's T reagent

SUMMARY

Complexes of Pd(II), Co(III) and Ni(II) with the condensation derivative of 2-(diphenylphosphino)benzaldehyde and Girard's T reagent were synthesized, characterized, and their antimicrobial activities and magnetic properties were evaluated. The ligand, Pd(II) and Co(III) complexes were characterized by elemental analysis, IR and NMR spectroscopy, and X-ray crystallography. Ni(II) complexes were characterized by elemental analysis, IR spectroscopy and X-ray crystallography. In Pd(II) and Co(III) complexes, the deprotonated ligand was coordinated to the metal through the phosphorus, the imine nitrogen, and the carbonyl oxygen atoms. In the octahedral Co(III) complex, two ligand molecules were coordinated to metal ion, while the square-planar environment of Pd(II) complex was constituted of one tridentate ligand and chloride in the fourth coordination place. The ligand and Pd(II) and Co(III) complexes showed moderate antibacterial activity. In all the Ni(II) complexes the ligand is coordinated as tridentate via the phosphorus, the imine nitrogen and the carbonyl oxygen atoms while the remaining coordination positions are occupied with thiocyanato anions. Coordination of deprotonated phosphine ligand results in formation of square-planar complexes, while the octahedral complex was formed with protonated ligand. Results of magnetic measurements analyzed by Curie-Weiss law show paramagnetic behavior of investigated octahedral Ni(II) complex with effective magnetic moment $\mu_{eff} = 3.1$ μ_B.

Sinteza i karakterizacija kompleksa Pd(II), Co(III) i Ni(II) sa kondenzacionim proizvodom 2-(difenilfosfino)benzaldehida i Žirarovog T reagensa

REZIME

Kompleksi Pd(II), Co(III) i Ni(II) sa kondenzacionim proizvodom 2-(difenilfosfino)benzaldehida i Žirarovog T reagensa su sintetisani, strukturno okarakterisani i ispitana su njihova magnetna i antimikrobna svojstva. Ligand, Pd(II) i Co(III) kompleksi su okarakterisani na osnovu rezultata elementalne analize, IC i NMR spektroskopije i rendgenske strukturne analize. Kompleksi Ni(II) su okarakterisani na osnovu rezultata elementalne analize, IC spektroskopije i rendgenske strukturne analize. U kompleksima Pd(II) i Co(III), deprotonovani ligand je koordinovan za jon metala preko atoma fosfora, azometinskog azota i karbonilnog kiseonika. U slučaju oktaedarskog kompleksa Co(III), dva molekula liganda su tridentatno koordinovana za metalni centar, dok u kvadratno-planarnom kompleksu Pd(II) okruženje oko centralnog metalnog jona čine tridentatno koordinovani ligand i hlorido ligand koji zauzima četvrto koordinaciono mesto. Ligand, Pd(II) i Co(III) kompleksi pokazuju umerenu antibakterijsku aktivnost. Kod svih Ni(II) kompleksa ligand je tridentatno koordinovan za jon metala preko P, N i O atoma, a preostala koordinaciona mesta zauzimaju izotiocijanato ligandi. Koordinacija deprotonovanog (cviter-jonskog) fosfinskog liganda dovodi do formiranja kvadratno-planarnih Ni(II) kompleksa, dok je u oktaedarskom Ni(II) kompleksu koordinovan pozitivno naelektrisani jon liganda. Rezultati magnetnih merenja ukazuju na paramagnetična svojstva ispitivanog oktaedarskog Ni(II) kompleksa čiji izmereni efektivni magnetni momenat iznosi 3,1 μ_B.

Ključne reči: Pd(II), Co(III) i Ni(II) kompleksi, 2-(difenilfosfino)benzaldehid, Žirar T reagens.

Naučna oblast: Hemija

Uža naučna oblast: Neorganska hemija

UDK broj: 546

Abbreviations

HLCl·EtOH – (*E*)-2-(2-(2-(diphenylphosphino)benzylidene)hydrazinyl)-*N*,*N*,*N*-trimethyl-2-oxoethan-1-aminium chloride monoethanole

CCDC – Cambridge Crystallographic Data Center

MIC – Minimum Inhibitory Concentration

EtOH – Ethanol

MeOH – Methanol

χ – Magnetic Susceptibility

μ_{eff} – Effective Magnetic Moment

Contents

1. INTRODUCTION

Schiff bases and their metal complexes represent an important class of compounds, not only from a theoretical point of view, but also because of diverse applications in pharmacology, analytical procedures and catalysis [1–3]. Girard's reagents due to their ability to form water soluble hydrazones are often used for the separation of carbonyl compounds from mixtures soluble in non-polar solvents [4–6]. The condensation reaction of Girard's reagents with various carbonyl compounds results in the formation of ligand systems with different coordination properties. Coordination chemistry of Girard's reagent hydrazones is new and not sufficiently investigated area. Some Girard's reagent hydrazones exhibit biological activity [7–9]; hence these compounds are interesting as pharmaceutical agents. In order to more detailed insights in coordination properties as well as biological activity of Girard's reagents hydrazones, in this thesis the synthesis, structural characterization and biological activity of condensation product of 2-(diphenylphosphino)benzaldehyde and Girard's T reagent were described.

References of Introduction

[1] R. Hernandez-Molina, A. Mederos. *In Comprehensive Coordination Chemistry*, J.A. McCleverty, T.J. Meyer (Eds.), Vol. 1, 2nd Edn, Chap. 19, pp. 411–446, Elsevier, Amsterdam (2003).

[2] C.M. da Silva, D.L. da Silva, L.V. Modolo, R.B. Alves, M.A. de Resende, C.V.B. Martins, A. de Fátima, *J. Adv. Res.* **2** (2011) 1.

[3] K.C. Gupta, Alekha Kumar Sutar, *Coord. Chem. Rev.* **252** (2008) 1420.

[4] A. Girard, G. Sandulesco, *Helv. Chim. Acta* **19** (1936) 1095.

[5] J. Heer, K. Miescher, *Helv. Chim. Acta* **34** (1951) 359.

[6] D.F. Godbois, J.M. Mendelsohn, L.J. Ronsivalli, *Anal. Chem.* **37** (1965) 1776.

[7] T. Sedaghat, A. Tarassoli, Z. Ansari-Asl, H. Motamedi, *J. Coord. Chem.* **66** (2013) 2549.

[8] S. Salah, Z.H.A. El-Wahab, R.S. Farag, M.M. Mostafa, *Spectrochim Acta A* **124** (2014) 579.

[9] S.J. Azhari, S. Salah, R.S. Farag, M.M. Mostafa, *Spectrochim Acta A* **136** (2015) 1903.

2. GENERAL PART

Girard's reagents can be considered as *N*-substituted glycine hydrazides. There are three different kind of Girard's reagent (Figure 1):
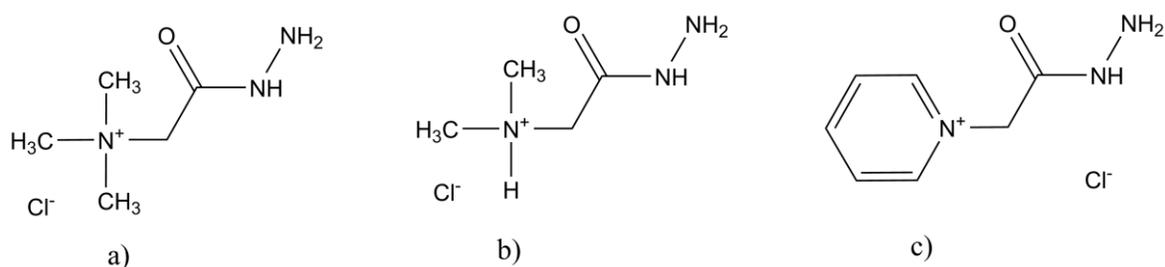

Figure 1: Girard's reagents: a) Girard's T (trimethylacetylhydrazide ammonium chloride) b) Girard's D (*N,N*-dimethylglycine hydrazide hydrochloride) c) Girard's P (pyridinioacetohydrazide chloride)

Girard's T reagent (Figure 1a) is monoprotic acid with the one nitrogen atom from the hydrazine part of a molecule which donates H^+ to a solution and carbonyl oxygen atom serving as potential acceptor. Among the Girard's reagents the largest number of the complexes has been synthesized with the Girard's T reagent. In the synthesized complexes Girard's T reagent was coordinated through terminal hydrazine nitrogen atom and carbonyl oxygen atom, forming a five-membered chelate ring.

Girard's reagent hydrazones are prepared in the reaction of ethanolic or methanolic solutions of Girard's reagents and carbonyl compound in the presence of catalytic amount of acetic acid (Scheme 1).
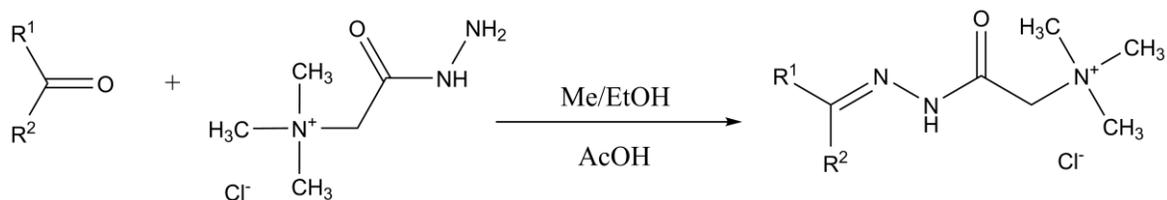
Scheme 1: Synthesis of Girard's T hydrazones

Depending on the nature of the carbonyl reagent used in the synthetic procedure, Girard's hydrazones may have two or more potential donor atoms, i.e. azomethine nitrogen and carbonyl oxygen from acetylhydrazine part of a molecule and donor atoms from derivative carbonyl compound [1]. Previously, synthesized Girard's T reagent hydrazones and their metal complexes are presented in Table 1.

Table 1: Girard's T reagent hydrazones and their metal complexes

Ligand	label	complexes	references
	HL^{1}Cl	[Cu(**HL^1**)Cl$_2$]Cl·H$_2$O [Cu(**HL^1**)$_2$Cl$_2$]Cl$_2$ [Cu(**L^1**)Cl(H$_2$O)$_2$]Cl·H$_2$O	[2]
	HL^{2}Cl	[Cd(**HL^2**)Cl$_2$]·H$_2$O [Cd(**HL^2**)Br$_2$]·5H$_2$O [Hg(**HL^2**)Cl$_2$]·H$_2$O [Cu(**L^2**)$_2$]·4H$_2$O [Co(**L^2**)Cl]·5H$_2$O [Ni(**L^2**)Cl]·3H$_2$O	[3]
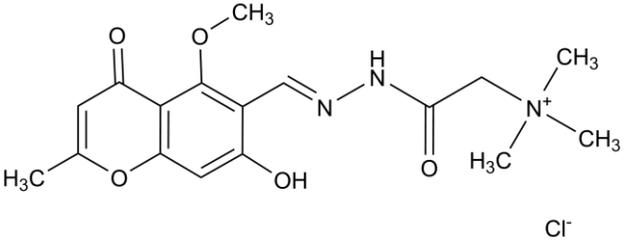
	HL³Cl	[Fe(**HL³**)Cl₂(H₂O)]Cl₂·H₂O [Al(**HL³**)Cl(H₂O)₂]Cl₃ [Sb(**HL³**)Cl₃]Cl·3EtOH [Sn(**HL³**)(H₂O)₃]Cl₃·2.5H₂O	[4]
	HL⁴Cl	[Fe(**HL⁴**)(EtOH)₃]Cl₄ [Al(**HL⁴**)Cl₂(EtOH)₂]Cl₂·1.5H₂O [Sb(**HL⁴**)Cl₂(H₂O)]Cl₂·2H₂O [Sn(**HL⁴**)(EtOH)₂(H₂O)₂]Cl₃	[5]
	H₂L⁵Cl	[Fe(**L⁵**)(NCS)₂(H₂O)] [Fe(**L⁵**)Cl₂]	[6]
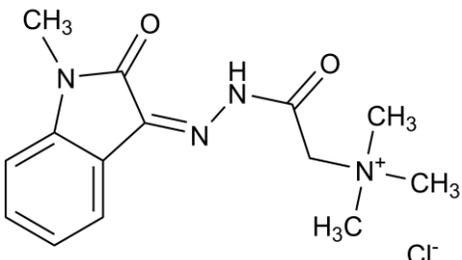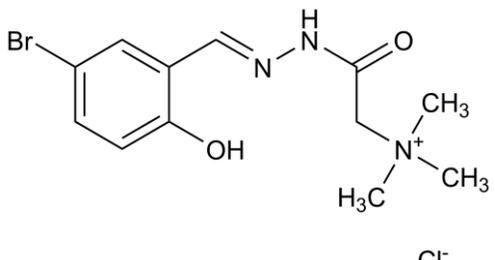
	H₂L⁶Cl	[Cu(**HL⁶**)Cl₂]·H₂O [Cu(**HL⁶**)Br₂]·H₂O [Zn(**L⁶**)Cl]·2H₂O [MoO₂(**L⁶**)(CH₃OH)]I [VO₂(**L⁶**)] [**H₂L⁶**][Cr(NCS)₄(NH₃)₂] (**H₂L⁶**)₄[Fe(CN)₆]·8H₂O (**H₂L⁶**)₃[Fe(CN)₆]·2H₂O (**H₂L⁶**)₂[Fe(CN)₅NO]	[7–11]
	H₃L⁷Cl	[Co(**HL⁷**)(NO₂)₃]·H₂O [Co(**L⁷**)(NO₂)₂(NH₃)]·3H₂O [Co(**HL⁷**)₂](PF₆)₃ [Co(**HL⁷**)₂][Cr(NCS)₄(NH₃)₂]₃·8H₂O [Cu(**HL⁷**)Cl₂] [Cu(**HL⁷**)Br₂] [Cu(**HL⁷**)Cl]NO₃	[10–13]
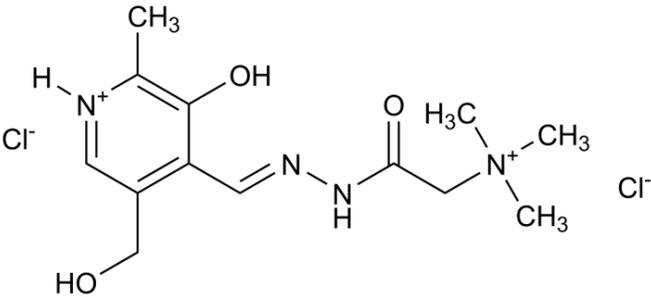
	$H_3L^7Cl_2$	$[Cu(L^7)N_3]$ $[Cu(HL^7)(NCS)_2]$ $[Zn(HL^7)Cl_2]$ $[Zn(HL^7)(NCS)_2] \cdot H_2O$ $[VO_2(L^7)] \cdot H_2O$ $H_3L^7[Cr(NCS)_4(NH_3)_2]_2 \cdot 2CH_3OH$ $(H_3L^7)_2[Fe(CN)_6] \cdot 3H_2O$ $(H_3L^7)_3[Fe(CN)_6]_2 \cdot 2H_2O$ $H_3L^7[Fe(CN)_5NO] \cdot 3H_2O$	
	HL^8Cl	$[Fe(L^8)Cl_3]$ $[Cu(L^8)Cl_2] \cdot H_2O$	[14]
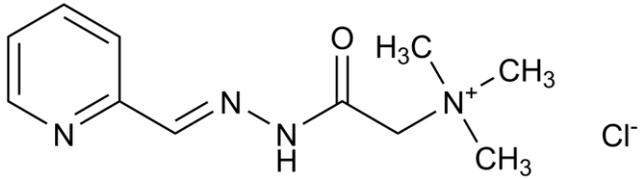
8

	$H_2L^9Cl_2$	$[Mn(H_2L^9)(NCS)_2](NCS)_2 \cdot CH_3OH$	[15]
	$H_2L^{10}Cl$	$[Sn(L^{10})Ph_2Cl]$ $[Sn(L^{10})Me_2Cl]$ $[Sn(L^{10})Bu_2Cl]$	[16]
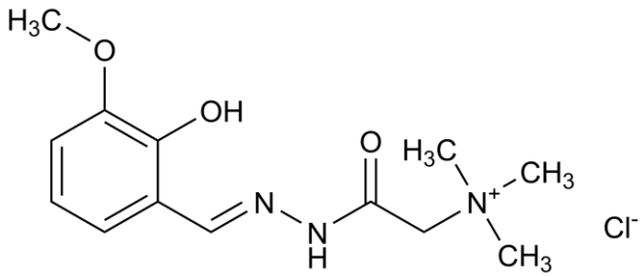
	H₂L¹¹Cl	[Sn(**L¹¹**)Ph₂Cl] [Sn(**L¹¹**)Me₂Cl]	[16]
	HL¹²Cl	[Cu(**HL¹²**)Cl₂]Cl [Fe(**HL¹²**)Cl₃]Cl [Mn(**HL¹²**)₂Cl₂]Cl₂ [Co(**HL¹²**)₂Cl₂]Cl₂	[17]
	HL¹³Cl	(**HL¹³**)₂[ZnCl₄]·MeOH	[18]
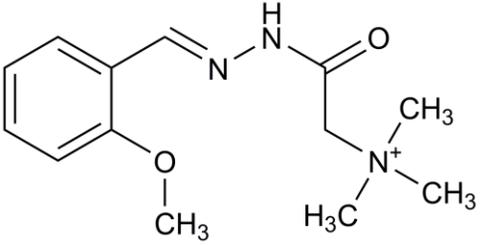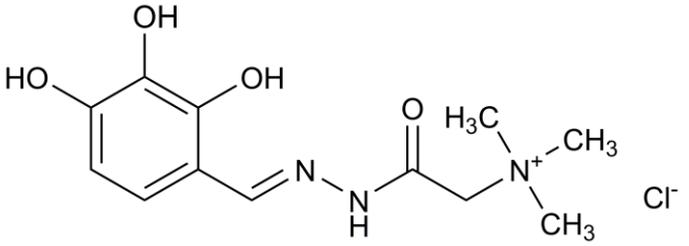
In the reaction of equimolar amounts of **HL^{1}Cl** and CuCl$_2$ three different complexes of Cu(II) were obtained. The nature of the solvent and pH of the reaction solution have influence on geometry and stoichiometry of the reaction products. The square-planar complex [Cu(**HL^1**)Cl$_2$]Cl·H$_2$O crystallized from ethanolic solution. In this complex potentially tridentate ligand is coordinated in a bidentate manner, involving the hydrazone and oxime nitrogen atoms. The reaction performed in an aqueous solution at pH 5, results in the formation of an octahedral bis(ligand) complex [Cu(**HL^1**)$_2$Cl$_2$]Cl$_2$, with bidentate NN coordination of the ligand. Finally, the octahedral mono(ligand) complex [Cu(**L^1**)Cl(H$_2$O)$_2$]Cl·H$_2$O was obtained from an aqueous solution of pH 10. In this complex, the ligand is coordinated as tridentate in monodeprotonated enol form, through the hydrazine and oxime nitrogen atoms and deprotonated oxygen atom of the enolised carbonyl group [2].

The hydrazone **HL^{2}Cl** was prepared in the reaction of equimolar amounts of 2-methyl-5-methoxy-6-formyl-7-bydroxy chromone and Girard's T reagent in ethanol. The complexes of Cu(II), Co(II), Ni(II), Cd(II) and Hg(II) were prepared by mixing equimolar amounts of metal halogenide and **HL^{2}Cl** in ethanol. The complexes were characterized only on the basis of spectrophotometric, conductance, pH and IR measurements [3].

The reactions of isatin Girard's T hydrazone (**HL^{3}Cl**) with Fe(III), Al(III), Sb(III) and Sn(II) chlorides results in the formation of corresponding octahedral complexes. In all the synthesized complexes the ligand is coordinated as tridentate through the two carbonyl groups of Girard's T and isatin parts of the molecule and nitrogen atom of azomethine group. Isatin Girard's T hydrazone complexes exhibited low to moderate antimicrobial activity [4].

Complexes of Fe(III), Al(III), Sb(III) and Sn(II) with *N*-methylisatin Girard's T hydrazone (**HL^{4}Cl**) were prepared in the reaction of ligand with the corresponding chloride salt in ethanol. In all the complexes *N*-methylisatin Girard's T hydrazone is coordinated to the metal ions without deprotonation. In Fe(III) and Sb(III) complexes the ligand is coordinated as tridentate through the carbonyl groups of both *N*-methylisatin and Girard's T

and the nitrogen atom of azomethine group, while in the case of Al(III) and Sn(II) complexes a bidentate manner of ligand coordination was observed. The ligand and complexes showed low to moderate antimicrobial activity [5].

In the reaction of an ethanolic solution of $FeCl_3$ and condensation derivative of the Girard's T reagent and 5-bromosalicylaldehyde (**HL^{5}Cl**) a distorted square-pyramidal Fe(III) complex $[Fe(\mathbf{L^5})Cl_2]$ was obtained. In this complex coordination surroundings of Fe(III) ion consist of ONO coordinated doubly deprotonated Schiff base ligand and two chlorido ligands. Octahedral Fe(III) complex $[Fe(\mathbf{L^5})(NCS)_2(H_2O)]$ with the same Schiff base ligand was formed in the reaction of an aqueous ethanolic solution of the chlorido complex and NH_4NCS. Octahedral environment around Fe(III) consist of the tridentate ONO coordinated organic ligand, two isothiocyanato ligands and one water molecule [6].

In the reactions of methanolic solutions of Et_4NVO_3, and $MoO_2(acac)_2$ (addition of I_2) with tridentate ONO salicylaldehyde Girard's T hydrazone (**H$_2$L^{6}Cl**) dioxovanadium(V) and dioxomolybdenum(VI) complexes of the formulas $[VO_2(\mathbf{L^6})]$ [7] and $[MoO_2(\mathbf{L^6})(CH_3OH)]I$ [8], respectively, were obtained. X-ray analysis of these complexes showed that the ligand was coordinated as tridentate in the monoanionic form, through azomethine nitrogen atom, the oxygen atom of the deprotonated phenolic group and the enolized carbonyl group. The geometry of the dioxovanadium(V) complex is a very deformed square-pyramid, while in the deformed octahedron of dioxomolybdenum(VI) complex coordination surroundings consist of the two oxygen atoms of the dioxomolybdenum(VI), the tridentate chelate ligand and methanol molecule coordinated via oxygen atom.

In the isostructural square-pyramidal complexes of Cu(II) with the same ligand, i.e. $[Cu(\mathbf{HL^6})Cl_2]\cdot H_2O$ and $[Cu(\mathbf{HL^6})Br_2]\cdot H_2O$, the tridentate ONO ligand is coordinated in its monodeprotonated zwitter-ionic form, through the carbonyl oxygen, hydrazine nitrogen and the oxygen of the deprotonated phenolic hydroxyl [9]. Also, the same ligand was used for the preparation of $[Zn(\mathbf{L^6})Cl]\cdot 2H_2O$ complex [11]. In Zn(II) complex, as in the previously described complexes of dioxovanadium(V) and dioxomolybdenum(VI), the ligand is

coordinated in monodeprotonated form. In complexes $H_2L^6[Cr(NCS)_4(NH_3)_2]$, $(H_2L^6)_4[Fe(CN)_6]\cdot 8H_2O$, $(H_2L^6)_3[Fe(CN)_6]\cdot 2H_2O$ and $(H_2L^6)_2[Fe(CN)_5NO]$ the ligand H_2L^6 plays the role of the cation, which is capable of precipitating some voluminous complex anions [10].

The dichloride salt of pyridoxal Girard's T hydrazone dihydrate ($H_3L^7Cl_2$) was obtained in the reaction of an ethanolic solution of the Girard's T reagent and pyridoxal (3-hydroxy-5-(hydroxymethyl)-2-methylpyridine-4-carboxaldehyde) hydrochloride. The first structurally characterized complex with this ligand was obtained in the reaction of aqueous solutions of $Na_3[Co(NO_2)_6]$ and the ligand in a molar ratio of 1:1. In octahedral Co(III) complex $[Co(HL^7)(NO_2)_3]\cdot H_2O$ one molecule of ONO tridentate Schiff base ligand and three monodentate N-bonded NO_2 groups are coordinated to metal ion forming *mer* isomer. Zwitter-ionic form of the ligand (HL^7Cl_2) is accomplished by deprotonation of the coordinated oxygen atom of the phenolic OH group and by enolized form of the carbonyl group [12]. Bis(ligand) cobalt(III) complex $[Co(HL^7)_2](PF_6)_3$ [12] and $[Co(HL^7)_2][Cr(NCS)_4(NH_3)_2]_3\cdot 8H_2O$ [10] were prepared in the reaction of aqueous solutions of $Na_3[Co(NO_2)_6]$ and the ligand in a molar ratio of 1 : 2, in the presence of ammonium salts of PF_6^- or $[Cr(NCS)_4(NH_3)_2]^-$. The reaction of methanolic solution of the complex $[Co(HL^7)(NO_2)_3]\cdot H_2O$ with an excess of $NH_{3(aq)}$ results in the formation of non-electrolyte $[Co(L^7)(NO_2)_2(NH_3)]\cdot 3H_2O$ complex [13]. In this complex one nitro ligand was replaced with an NH_3 molecule, while the pyridoxal ring of the Schiff base ligand was deprotonated. This is the first complex in which the ligand is coordinated in triply deprotonated form. Isostructural, most probably square-pyramidal, complexes of Cu(II), $[Cu(HL^7)Cl_2]$ and $[Cu(HL^7)Br_2]$, were synthesized in the reaction of CuX_2 (X = Cl or Br) with HL^7Cl_2 ligand [11], while the reaction with copper(II) nitrate results in formation of the $[Cu(HL^7)Cl]NO_3$ complex [10]. In two other reported complexes of Cu(II) the ligand is coordinated in triply deprotonated (monoanionic) $[Cu(L^7)N_3]$ or doubly deprotonated (neutral) form $[Cu(HL^7)(NCS)_2]$ [13]. Also, two Zn(II) complexes with this ligand are reported, one of them being the chloride complex of composition $[Zn(HL^7)Cl_2]$ [11] which in the reaction with NH_4NCS gave $[Zn(HL^7)(NCS)_2]\cdot H_2O$ [13]. In the reaction of

ammonium metavanadate with pyridoxal Girard's T hydrazone [VO$_2$(**L**^{7})]·H$_2$O complex was obtained. In the [VO$_2$(**L**^{7})]·H$_2$O complex the Schiff base ligand is coordinated in monoanionic form, formed by deprotonation of the pyridine nitrogen atom. The geometry of [VO$_2$(**L**^{7})]·H$_2$O complex is deformed square-pyramid with two oxo-ligands in the *cis* position [1]. Finally, some anionic complexes of Cr(III) and Fe(II and III) in which pyridoxal Girard's T hydrazone plays the role of the outer-sphere cation are also reported ((**H$_3$L**^{7})[Cr(NCS)$_4$(NH$_3$)$_2$]$_2$·2CH$_3$OH, (**H$_3$L**^{7})$_2$[Fe(CN)$_6$]·3H$_2$O, (**H$_3$L**^{7})$_3$[Fe(CN)$_6$]$_2$·2H$_2$O and **H$_3$L**^{7}[Fe(CN)$_5$NO]·3H$_2$O) [10].

The condensation reaction of 2-formylpyridine and the Girard's T reagent in MeOH yielded **HL^{8}Cl**. This ligand in DMF solution reacted with iron(III) or copper(II) chloride to give the octahedral complex [Fe(**L**^{8})Cl$_3$] and square-pyramidal complex [Cu(**L**^{8})Cl$_2$]·H$_2$O. In both complexes the tridentate NNO organic zwitter-ionic ligand is formally a neutral species, i.e. the positive charge of quaternary ammonium cationic group is compensated by a negative charge of deprotonated enolic tautomer [14].

Leovac *et al*. described a simpler method for the synthesis of 2,6-diacetylpyridine bis(Girard's T hydrazone)dichloride ligand in the form of the tetrahydrate salt (**H$_2$L^{9}Cl$_2$**). This ligand was prepared in the reaction of a warm methanolic solution of the stoichiometric amounts of the Girard's T reagent and 2,6-diacetylpyridine. In the reaction of the ligand and MnCl$_2$ in a mole ratio of 1 : 1 in the presence of an excess of NH$_4$NCS in methanol [Mn(**H$_2$L^9**)(NCS)$_2$](NCS)$_2$·CH$_3$OH complex was obtained. The geometry of the complex is pentagonal-bipyramidal, with the pentadentate N$_3$O$_2$ ligand in the equatorial plane and two isothiocyanato groups in the axial positions [15].

Condensation reaction of Girard's T reagent and 3-methoxysalicylaldehyde or 4-hydroxysalicylaldehyde results in the formation of the corresponding hydrazones **H$_2$L^{10}Cl** and **H$_2$L^{11}Cl** as ammonium quaternary salts. Organotin(IV) complexes were prepared in the reaction of R$_2$SnCl$_2$ (R = Ph, Me or Bu) with the corresponding hydrazone in methanol in the presence of NEt$_3$ as a base. In the six-coordinate and neutral organotin complexes the Schiff base ligands were coordinated as twice-deprotonated through ONO donor atoms.

The synthesized organotin complexes showed significant antibacterial activity against Gram-positive (*B. subtilis* and *S. aureus*) and Gram-negative (*E. coli* and *P. aeruginosa*) bacterial species [16].

In the square-planar copper(II) complex [Cu(**HL^{12}**)Cl$_2$]Cl and square-pyramidal iron(III) complex [Fe(**HL^{12}**)Cl$_3$]Cl, as well as, in octahedral bis(ligand) manganese(II) and cobalt(II) complexes of the general formula [M(**HL^{12}**)$_2$Cl$_2$]Cl$_2$ anisaldehyde Girard-T hydrazone (**HL^{12}Cl**) is coordinated bidentately, through the nitrogen atom of the azomethine group and the carbonyl oxygen atom [17].

In the reaction of equimolar amounts of **HL^{13}Cl** ligand and ZnCl$_2$ (anhydrous) in methanol Zn(II) complex (**HL^{13}**)$_2$[ZnCl$_4$]·MeOH was obtained. Single-crystal X-ray study for this compound showed that the asymmetric unit consists of two Girard's T reagent-based cations, a tetrachloridozincate anion and a molecule of methanol as solvate [18].

References of General Part

[1] LJ.S. Vojinović-Ješić, S.B. Novaković, V.M. Leovac, V.I. Češljević, *J. Serb. Chem. Soc.* **77** (2012) 1129.

[2] M.M. Mostafa, S.M. Hassan, G.M. Ibrahim, *J. Inorg. Nucl. Chem.* **42** (1980) 285.

[3] A.M. Shallaby, M.M. Mostafa, M.M. Bekheit, *J. Inorg. Nucl. Chem.* **41** (1978) 267.

[4] S. Salah, Z.H.A. El-Wahab, R.S. Farag, M.M. Mostafa, *Spectrochim Acta A* **124** (2014) 579.

[5] S.J. Azhari, S. Salah, R.S. Farag, M.M. Mostafa, *Spectrochim Acta A* **136** (2015) 1903.

[6] M.D. Revenco, P.N. Bourosh, O.V. Palamarciuc, J. Lipkowski, M. Gdaniec, Y.A. Simonov, *Russ. J. Inorg. Chem.* **54** (2009) 1581.

[7] X. Wang, X.M. Zhang, H.X. Liu, Inorg. Chim. Acta **223** (1994) 193.

[8] X. Wang, X.M. Zhang, H.X. Liu, *J. Coord. Chem.* **33** (1994) 223.

[9] V.M. Leovac, G.A. Bogdanović, V.I. Češljević, Lj.S. Jovanović, S.B. Novaković, Lj.S. Vojinović-Ješić, *Struct. Chem.* **18** (2007) 113.

[10] Lj.S. Vojinović, Ph. D. Thesis, Faculty of Science, University of Novi Sad, 2005 (in Serbian).

[11] V.M. Leovac, K. Mészáros-Szécsényi, Lj.S. Vojinović-Ješić, V.I. Češljević, S. Markov, T. Wadsten, *J. Therm. Anal. Cal.* **86** (2006) 379.

[12] Lj.S. Vojinović, V.M. Leovac, S.B. Novaković, G.A. Bogdanović, J.J. Csanádi, V.I. Češljević, *Inorg. Chem. Commun.* **7** (2004) 1264.

[13] Lj.S. Vojinović-Ješić, G.A. Bogdanović, V.M. Leovac, V.I. Češljević, Lj.S. Jovanović, *Struct. Chem.* **19** (2008) 807.

[14] O.V. Palamarciuc, P.N. Bourosh, M.D. Revenco, J. Lipkowski, Y.A. Simonov, R. Clérac, *Inorg. Chim. Acta* **363** (2010) 2561.

[15] Lj.S. Vojinović-Ješić, V.I. Češljević, G.A. Bogdanović, V.M. Leovac, K.M. Szécsényi, V. Divjaković, M.D. Joksović, *Inorg. Chem. Commun.* **13** (2010) 1085.

[16] T. Sedaghat, A. Tarassoli, Z. Ansari-Asl, H. Motamedi, *J. Coord. Chem.* **66** (2013) 2549.

[17] M.E.M. Emam, M.A.H. Hafez, M.N.H. Moussa, *J. Thermal. Anal.* **37** (1991) 1005 and references therein.

[18] S.B. Novaković, B.M. Drašković, Lj.S. Vojinović-Ješić, V. I. Češljević, V. M. Leovac, *Acta Crystallogr.* **E66** (2010) m328.

3. EXPERIMENTAL PART

3.1. Materials and methods

2-(Diphenylphosphino)benzaldehyde (97%) and Girard's T reagent (99%) were obtained from Aldrich. Ethanol and methanol were reagent grade and used without purification.

Melting points (uncorrected) were determined using a Büchi instrument. Elemental analysis (C, H, and N) were performed by standard micro-methods using the ELEMENTAR Vario EL III C.H.N.S.O analyzer. IR spectra were recorded on a Nicolet 6700 FT-IR spectrometer using the ATR technique in the region 4000-400 cm^{-1} (vs-very strong, s-strong, m-medium, w-weak). ^{1}H NMR (500 MHz), ^{13}C NMR (125 MHz), and 2-D NMR spectra were recorded on a Bruker Avance 500 spectrometer in DMSO-d_6 using TMS as an internal standard for ^{1}H and ^{13}C. Chemical shifts are expressed in ppm (δ) values and coupling constants (J) in Hz. Molar conductivities were measured at room temperature (23 ^{o}C) on a digital conductivity-meter JENWAY-4009. UV-Vis spectra were recorded at Shimadzu 1800 UV/Vis spectrometer. The temperature dependence of magnetic susceptibility was studied on the powder sample by Quantum Design MPMS-XL-5 SQUID magnetometer in the temperature range 2–300 K, and under applied magnetic field of 1000 Oe.

3.2. Synthesis

*3.2.1 Synthesis of (E)-2-(2-(2-(diphenylphosphino)benzylidene)hydrazinyl)-N,N,N-trimethyl-2-oxoethan-1-aminium chloride monoethanole (**HLCl·EtOH**)*

A mixture of 140 mg (0.48 mmol) 2-(diphenylphosphino)benzaldehyde and 80 mg (0.48 mmol) Girard's T reagent was dissolved, by heating, in 20 mL ethanol and one drop of concentrated hydrochloric acid was added. The mixture was refluxed for 60 min. The reaction solution was left to stand at room temperature while the colorless crystals separated from the solution. Yield: 110 mg (47%); Mp 216 °C. IR (vs-very strong, s-strong, m-medium, w-weak): 3524 (w), 3403 (w), 3308 (w), 3050 (m), 3018 (m), 2970 (m), 2930 (m), 2890 (m), 2817 (w), 1686 (vs), 1657 (m), 1602 (w), 1491 (w), 1475 (s), 1433 (s), 1410 (s),1342 (w), 1306 (s), 1277 (w), 1212 (w), 1133 (w), 1123 (m), 1095(w), 1044 (w), 992 (w), 948 (w), 929 (w), 876 (w), 848 (w), 765 (w), 746 (vs), 699 (s), 620 (w), 585 (w), 505 (w), 481 (w), 437 (w). Results of elemental analysis are given in Table 2.

Table 2. Elemental analysis of **HL**Cl·EtOH.

Element	Anal. Calcd. for $C_{24}H_{27}ClN_3O_2P \cdot EtOH$ (%)	Found (%)
C	64.26	64.17
H	6.84	6.92
N	8.65	8.78

3.2.2 Synthesis of [Pd**L**Cl]Cl complex (**1**)

The ligand **HL**Cl·EtOH (80 mg, 0.16 mmol) was dissolved, by heating at 65 °C, in 35 mL H_2O. After that, a solution of $K_2[PdCl_4]$, prepared by dissolving 60 mg (0.18 mmol) in 5 mL H_2O, was added to it. Right after that, the mixing temperature was decreased to 52 °C, and the mixture was heated at that temperature for 1 h. The reaction solution was evaporated under vacuum, dissolved in 10 mL of methanol, and the solution was filtered. After two days, yellow crystals of Pd(II) complex arose from methanolic solution. Yield: 30 mg (32%). IR: 3391 (m), 3053 (w), 3010 (w), 2959 (w), 1639 (m), 1547 (s), 1484 (m), 1436 (m), 1398 (w), 1369 (w), 1343 (w), 1315 (w), 1275 (w), 1213 (w), 1180 (w), 1139 (w), 1101 (w), 1028 (w), 997 (w), 975 (w), 933 (w), 912 (w), 868 (w), 807 (w), 772 (w), 748 (w), 691 (m), 588 (w), 547 (w). Results of elemental analysis are given in Table 3.

Table 3. Elemental analysis of complex (**1**).

Element	Anal. Calcd. For $C_{24}H_{26}Cl_2N_3OPPd$ (%)	Found (%)
C	49.63	49.74
H	4.51	4.46
N	7.23	7.36

3.2.3. Synthesis of [Co(**L**)$_2$](BF$_4$)$_3$ complex (**2**)

The ligand **HL**Cl·EtOH (140 mg, 0.29 mmol) was dissolved, by heating, in EtOH/H_2O mixture (10 mL/10 mL) and solid Co(BF$_4$)$_2$·6H$_2$O (100 mg, 0.29 mmol) was added. The reaction mixture was heated at 65 °C for 4 h. The color of the solution changed to red. The reaction solution was left to stand at room temperature, while the red crystals

precipitated from the solution. Yield: 50 mg (29%). IR: 3599 (m), 3559 (m), 3473 (w), 3060 (w), 2995 (w), 1619 (w), 1572 (m), 1483 (m), 1436 (m), 1412 (w), 1322 (m), 1222 (w), 1058 (vs), 926 (m), 872 (w), 753 (m), 698 (m), 593 (w), 525 (m), 495(w). Results of elemental analysis are given in Table 4.

Table 4. Elemental analysis of complex (**2**).

Element	Anal. Calcd. For $C_{48}H_{52}B_3CoF_{12}N_6O_2P_2 \cdot 3H_2O$ (%)	Found(%)
C	48.84	48.86
H	4.95	5.04
N	7.12	7.03

*3.2.4. Synthesis of [Ni(**HL**)(NCS)$_3$]·H$_2$O complex (**3**)*

A mixture of 0.08 g (0.23 mmol) Ni(BF$_4$)$_2$·6H$_2$O and 0.11 g (0.23 mmol) of ligand **HL**Cl·EtOH was dissolved in 20 mL methanol and then 0.07 g (0.72 mmol) KSCN was added to it. The mixture was refluxed for 2 h and filtered. The reaction solution was cooled to room temperature and white precipitate (KBF$_4$) was filtered. Filtrate was left to stand at room temperature for three days while purple crystals arose from the solution. Yield 0.07 g (47%) IR: 3304 (w), 3017 (w), 2931 (w), 2764 (w), 2113 (s), 2067 (vs), 1659 (m), 1612 (m), 1475 (w),1435 (w), 1412 (w), 1333 (w), 1298 (w), 1089 (w), 976 (w), 918 (w), 794 (w), 755 (w), 696 (w). Results of elemental analysis are given in Table 5. Λ_M (1 mM, DMSO): 12 Ω^{-1} cm^2 mol^{-1}. λ_{max} (nm) (H$_2$O): 277, 341, 363.

Table 5. Elemental analysis of complex (**3**).

Element	Anal. Calcd. For $C_{27}H_{29}N_6NiO_2PS_3$ (%)	Found (%)
C	49.48	49.36
H	4.46	4.45
N	12.82	12.84
S	14.68	14.65

*3.2.5 Synthesis of [Ni**L**(NCS)]BF$_4$·2H$_2$O complex (**4**)*

A mixture of 0.08 g (0.23 mmol) Ni(BF$_4$)$_2$·6H$_2$O and 0.11 g (0.23 mmol) of ligand **HL**Cl·EtOH was dissolved in 20 mL methanol and then 0.06 g (0.79 mmol) NH$_4$SCN was added to it. The mixture was refluxed for 2 h. The reaction solution was left to stand at room temperature for two days while reddish crystals arose from the solution. Yield 0.09 g (64%) IR: 2071 (m), 1605 (w), 1568 (m), 1477 (w), 1432 (w), 1404 (w), 1343 (w), 1303 (w), 1035 (s), 973 (m), 910 (m), 871 (w), 845 (w), 810 (w), 771 (m), 749 (m), 691 (m), 665 (w). Results of elemental analysis are given in Table 6. Λ_M (1 mM, DMSO): 45.9 Ω^{-1} cm^2 mol^{-1}. λ_{max} (nm) (H$_2$O): 296, 327, 344, 362.

Table 6. Elemental analysis of complex (**4**).

Element	Anal. Calcd. For $C_{25}H_{30}BF_4N_4NiO_3PS$ (%)	Found (%)
C	46.69	46.35
H	4.70	4.74
N	8.71	8.79
S	4.99	5.05

*3.2.6 Synthesis of [Ni**L**(NCS)]SCN·H₂O complex (**5**)*

In the mixture of 0.06 g (0.24 mmol) Ni(AcO)$_2$·4H$_2$O and 0.11 g (0.23 mmol) of ligand **HL**Cl·EtOH in 20 mL methanol 0.07 g (0.72 mmol) KSCN was added. The mixture was refluxed for 2 h. The reaction solution was left to stand at room temperature for two days while reddish crystals arose from the solution. Yield 0.10 g (73 %) IR: 3518 (w), 3382 (w), 3059 (w), 3017 (w), 2959 (w), 2080 (s), 2060 (s), 2005 (w), 1606 (w), 1571 (m), 1480 (m), 1433 (m), 1406 (w), 1344 (w), 1312 (w), 1101 (w), 998 (w), 978 (w), 935 (w), 914 (w), 750 (w), 692 (w). Results of elemental analysis are given in Table 7. Λ_M (1 mM, DMSO): 46.4 Ω^{-1} cm^2 mol^{-1}. λ_{max} (nm) (H$_2$O): 298, 328, 343, 362.

Table 7. Elemental analysis of complex (**5**).

Element	Anal. Calcd. For $C_{26}H_{28}N_5NiO_2PS_2$ (%)	Found (%)
C	52.37	52.56
H	4.73	4.88
N	11.74	11.51
S	10.75	10.53

3.3. X-ray structure determinations

3.3.1 X-ray analysis of ligand **HLCl·EtOH** and complexes (**1**) and (**2**)

Single-crystal X-ray diffraction data were collected using the Mo Kα radiation (λ = 0.71073 Å) at T = 293 K on a SMART diffractometer with Breeze area detector. The collected intensities were corrected for Lorentz and polarization factors and empirically for absorption by using the SADABS program [1]. Structures were solved by direct methods using SIR2011 [2] and refined by full matrix least squares on all F^2 using SHELXL97 [3] implemented in the Olex2 package [4]. Hydrogen atoms were introduced in calculated positions. Anisotropic displacement parameters were refined for all non-hydrogen atoms.

Hydrogen bonds have been analyzed with SHELXL97 [3] and PARST97 [5], and extensive use was made of the Cambridge Crystallographic Data Center packages [6] for the analysis of crystal packing. Compound (**2**) presented problematic data, with a very large unit cell containing many disordered anions and possibly solvent molecules that have not been located in the electron density map. Three independent cations are clearly determined, but they present high thermal mobility and therefore also contribute to poor data quality. The molecular structure of the cations has been restrained, especially for the

trimethylammonium moieties that were not totally visible in the electron density maps. The final structure demonstrates the molecular connectivity, but no further discussion is attempted. Crystals of **(1)** were radiation-sensitive and data were corrected for decay. The structure is made by an ordered and stable part consisting of complex cations and anions and refines very well, and by an unknown disordered part contained in channels. The final structure has been optimized by accounting for disordered density by the masking procedure implemented in Olex2. It was not possible to determine the nature of the disordered content of the crystal. Table 8 summarizes crystal data and structure determination results for **HL**Cl·EtOH and **(1)**, while results for **(2)** are shown in Table 9. Crystallographic data (excluding structure factors) for **HL**Cl·EtOH, **(1)** and **(2)** have been deposited with the Cambridge Crystallographic Data Center as supplementary publications Nos. CCDC 1013634 (**HL**Cl·EtOH), 1013635 **(2)**, and 1013636 **(1)**. Copies of the data can be obtained free of charge on application to CCDC, 12 Union Road, Cambridge CB2 1EZ, UK (Fax: (+44) 1223–336-033; E-mail: deposit@ccdc.cam.ac.uk).

Table 8. Crystal data and structure refinement for **HL**Cl·EtOH and complex **(1)**.

	HLCl·EtOH	complex **(1)**
Empirical formula	$C_{26}H_{33}ClN_3O_2P$	$C_{24}H_{26}Cl_2N_3OPPd$
Formula weight	485.97	580.75
Temperature (K)	296.15	296.15
Crystal system	Triclinic	Triclinic
Space group	*P-1*	*P-1*
a (Å)	8.9862(6)	10.5515(18)
b (Å)	10.7502(8)	12.531(2)
c (Å)	14.923(1)	21.514(4)
α (°)	101.865(1)	98.909(3)
β (°)	104.198(1)	96.810(3)

γ (°)	97.828(1)	98.838(3)
Volume (Å^3)	1341.0(2)	2747.3(8)
Z	2	4
ρ_{calcd} (g cm^{-3})	1.204	1.404
μ (mm^{-1})	0.228	0.948
F(0 0 0)	516.0	1176.0
Crystal size (mm^3)	$0.1 \times 0.08 \times 0.05$	$0.45 \times 0.11 \times 0.042$
Radiation	MoKα ($\lambda = 0.71073$)	MoKα ($\lambda = 0.71073$)
2Θ range for data collection (°)	2.906–60.116	1.94–43.56
Reflections collected	21056	22008
Independent reflections	7796 [$R_{\text{int}} = 0.0278$]	6518 [$R_{\text{int}} = 0.0577$]
Data/restraints/parameters	7796/0/303	6518/0/586
Goodness-of-fit on F^2	1.213	1.005
Final R indexes [$I \geq 2\sigma(I)$]	$R_1 = 0.0525$, $wR_2 = 0.1685$	$R_1 = 0.0346$, $wR_2 = 0.0745$
Final R indexes [all data]	$R_1 = 0.0680$, $wR_2 = 0.1790$	$R_1 = 0.0487$, $wR_2 = 0.0792$
Largest ΔF max/mine (Å^{-3})	0.39/$-$0.28	0.61/$-$0.39

Table 9. Crystal data and structure refinement for complex (**2**).

Empirical formula	$C_{48}H_{52}BCoF_4N_6O_2P_2$
Formula weight	952.63
Temperature (K)	296.15
Crystal system	Monoclinic
Space group	*Cc*
a (Å)	37.583(12)
b (Å)	41.382(13)
c (Å)	10.948(4)
α (°)	90
β (°)	98.501(4)
γ (°)	90
Volume (Å^3)	16841(9)
Z	12
ρ_{calcd} (g/cm^3)	1.127
μ (mm^{-1})	0.414
$F(000)$	5952.0
Crystal size (mm^3)	$0.535 \times 0.14 \times 0.046$
Radiation	MoKα ($\lambda = 0.71073$)
2Θ range for data collection (°)	1.472 to 39.754

Reflections collected	51321
Independent reflections	15324 [R_{int}= 0.0988, R_{sigma}= 0.0954]
Data/restraints/parameters	15324/156/681
Goodness-of-fit on F^2	1.509
Final R indexes [$I \geq 2\sigma$ (I)]	$R_1 = 0.1551, wR_2 = 0.3961$
Final R indexes [all data]	$R_1 = 0.1942, wR_2 = 0.4266$
Largest diff. peak(hole) e Å^{-3}	1.84/-0.62
Flack parameter	0.420(15)

3.3.2. X-ray analysis of complexes (**3**) and (**4**)

Crystal data and refinement parameters of compounds (**3**) and (**4**) are listed in Table 10. The X-ray intensity data were collected at room temperature with Agilent SuperNova dual source with an Atlas detector equipped with mirror-monochromated Mo Kα radiation ($\lambda = 0.71073$ Å). The data were processed using CRYSALIS PRO [7]. The structures were solved by direct methods (SIR-92 [8]) and refined by a full-matrix least-squares procedure based on F^2 using SHELXL-97 [9]. All non-hydrogen atoms were refined anisotropically. The N1 and C6 bonded hydrogen atoms in (**3**) and C6 bonded hydrogen atoms in (**4**) were located in a difference map and refined with the distance restraints (DFIX) with N-H = 0.86 and C-H = 0.98 and with $U_{iso}(H) = 1.2U_{eq}(N)$ or $U_{iso}(H) = 1.2U_{eq}(C)$, respectively. The water hydrogen atoms in (**3**) were also located in a difference map and refined with the distance restraints (DFIX) with O-H = 0.96 and with $U_{iso}(H) = 1.5U_{eq}(O)$. All other hydrogen atoms were included in the model at geometrically calculated positions and refined using a riding model. It is also noteworthy that the thermal parameters of the S3 atom of one of the SCN$^-$ ligands in (**3**) and F4 atom of BF$_4^-$ ion in (**4**) are rather high. Splitting the location of these atoms in two different nearby positions using the PART instruction from the SHELXL routine result in a better agreement factor. Oxygen atoms

belonging to water molecules in **(4)** exhibit large thermal ellipsoids due to the high mobility of the water molecules in the structures.

Table 10. Crystal data and structure refinement details for complexes **(3)** and **(4)**.

	complex **(3)**	complex **(4)**
Formula	$C_{27}H_{29}N_6NiO_2PS_3$	$C_{25}H_{30}BF_4N_4NiO_3PS$
Fw (g mol^{-1})	655.42	643.08
Crystal size (mm^3)	$0.10 \times 0.05 \times 0.05$	$0.50 \times 0.05 \times 0.05$
Crystal color	purple	red
Crystal system	monoclinic	monoclinic
Space group	$P2_1/c$	$P2_1/c$
a (Å)	19.394(2)	13.7978(4)
b (Å)	10.4468(4)	11.5110(3)
c (Å)	17.1915(12)	17.7664(6)
β (º)	116.060(10)	93.241(3)
V (Å^3)	3128.9(4)	2817.26(15)
Z	4	4
Calcd density (g cm^{-3})	1.391	1.516
F(000)	1360	1328
No. of collected reflns	11019	13264
No. of independent reflns	6303	6441

R_{int}	0.0447	0.0376
No. of reflns observed	3733	4389
No. parameters	386	377
$R[I > 2\sigma (I)]^{a}$	0.0527	0.0586
wR_2 (all data)^{b}	0.1028	0.1616
Goof , S^{c}	1.007	1.031
maximum/minimum residual electron density (e Å^{-3})	+0.31/-0.35	+0.69/-0.62

---

[a] $R =\sum||F_o| - |F_c||/\sum F_o|$. [b] $wR_2 = \{\sum[w(F_o{}^2 - F_c{}^2)^2]/\sum[w(F_o{}^2)^2]\}^{1/2}$.

[c] $S = \{\sum[(F_o{}^2 - F_c{}^2)^2]/(n/p\}^{1/2}$ where n is the number of reflections and p is the total

3.3. Antimicrobial activity of ligand **HL**Cl·EtOH **and complexes (1) and (2)**

The antimicrobial activity was investigated on six different laboratory control strains of bacteria, i.e. the Gram-positive: *Staphylococcus aureus* (ATCC 6538), *Bacillus subtilis* (ATCC 6633), and the Gram-negative: *Escherichia coli* (ATCC 10536), *Klebsiella pneumoniae* (NCIMB 9111), *Pseudomonas aeruginosa* (ATCC 9027), *Salmonella abony* (NCTC 6017), and one strain of yeast, i.e. *Candida albicans* (ATCC 10231). All tests were performed in Müller Hinton broth for the bacterial strains and in Sabouraud dextrose broth for the yeast. Overnight broth cultures of each strain were prepared, and the final concentration in each well was adjusted to 2×10^6 CFU/mL for the bacteria and 2×10^5 CFU/mL for the yeast. **HL**Cl·EtOH, **(1)** and **(2)** were dissolved in 1% dimethyl sulfoxide (DMSO) and then diluted to the highest concentration. Twofold serial concentrations of the compounds were prepared in a 96-well microtiter plate over the concentration range 62.5–1000 µg·mL^{-1}. The microbial growth was determined after 24 h of incubation at 37 °C for the bacteria and after 48 h of incubation at 26 °C for the fungi. The MIC is defined as the lowest concentration compound at which no visible growth of microorganism is observed.

References of Experimental Part

[1] (a) SAINT. SAX, Area Detector Integration, Siemens Analytical instruments INC., Madison, WI (2006); (b) G. Sheldrick. SADABS: Siemens Area Detector Absorption Correction Software, University of Göttingen, Göttingen (1996).

[2] M.C. Burla, R. Caliandro, B. Carrozzini, G.L. Cascarano, C. Giacovazzo, M. Mallamo, A. Mazzone, G. Polidori, Sir2011. Istituto di Ricerca per lo Sviluppo di Metodologie Cristallografiche CNR, Bari (2011).

[3] G. Sheldrick. Shelxl97. Program for Structure Refinement, University of Göttingen, Göttingen (1997).

[4] O.V. Dolomanov, L.J. Bourhis, R.J. Gildea, J.A.K. Howard, H. Puschmann, *J. Appl. Cryst.* **42** (2009) 339.

[5] M. Nardelli, *J. Appl. Cryst.* **28** (1995) 659.

[6] (a) F.H. Allen, O. Kennard, R. Taylor, *Acc. Chem. Res.* **16** (1983) 146; (b) I.J. Bruno, J.C. Cole, P.R. Edgington, M. Kessler, C.F. Macrae, P. McCabe, J. Pearson, R. Taylor, *Acta Crystallogr.* **B58** (2002) 389.

[7] Oxford Diffraction, CrysAlis PRO, Oxford Diffraction Ltd., Yarnton, England, 2009.

[8] A. Altomare, G. Cascarano, C. Giacovazzo, A. Guagliardi, Completion and Refinement of Crystal Structures with SIR92, *J. Appl. Crystallogr.* **26** (1993) 343.

[9] G.M. Sheldrick, A short history of SHELX, *Acta Crystallogr. A* **64** (2008) 112.

4. RESULTS AND DISCUSSION

4.1. Synthesis

As a result of the condensation reaction between the Girard's T reagent and 2-(diphenylphosphino)benzaldehyde, the corresponding hydrazone was obtained as an ammonium quaternary chloride salt [(E)-2-(2-(2-(diphenylphosphino)benzylidene)hydrazinyl)-N,N,N-trimethyl-2-oxoethan-1-aminium chloride monoethanole (**HL**Cl·EtOH) (Scheme 2)].

The [Pd(**L**)Cl]Cl **(1)** complex was prepared by substitution reaction starting from $K_2[PdCl_4]$ and the ligand **HL**Cl·EtOH (Scheme 3(a)). The [Co(**L)$_2$**]$(BF_4)_3$ **(2)** complex was obtained by direct synthesis in the reaction of the ligand **HL**Cl·EtOH and $Co(BF_4)_2$·$6H_2O$ (Scheme 3(b)). Square-planar Pd(II) complex is in the cationic form [Pd**L**Cl]$^+$ with the deprotonated ligand coordinated as tridentate via the phosphorius, the imine nitrogen and the carbonyl oxygen atoms, and the chlorido ligand occupying the fourth coordination site. The chloride anion serves as counter ion. The Co(III) complex consists of cation [Co**L$_2$**]$^{3+}$ counterbalanced by three BF_4^- anions. This complex has a bis(trischelate) PNO coordination on the Co(III) center, giving an octahedral geometry.

In order to study the structural modes of coordination complexes of Ni(II) with acylhydrazones of 2-(diphenylphosphino)benzaldehyde a series of new Ni(II) complexes has been synthesized.

In the reaction of the ligand **HL**Cl·EtOH with $Ni(BF_4)_2$·$6H_2O$ and KSCN in molar ratio 1 : 1 : 3 in methanol, the neutral octahedral complex [Ni**(HL)(NCS)$_3$**]·H_2O **(3)** was obtained (Scheme 4). Precipitation of insoluble KBF_4 shifts the reaction equilibrium towards formation of complex **(3)**. In complex **(3)** organic ligand is coordinated as tridentate through phosphorus, imine nitrogen and carbonyl oxygen atoms, while the

remaining three coordination positions are occupied with *mer N*-coordinated thiocyanate anions. When the similar reaction was performed using NH₄SCN instead of KSCN as a source of thiocyanate anion the reaction product was square-planar complex [Ni(**L**)(**NCS**)]BF₄·2H₂O **(4)** (Scheme 4). The cationic complex consisted of one molecule of deprotonated ligand coordinated in a tridentate PNO fashion to Ni(II) and a thiocyanate anion coordinated through nitrogen atom. Reaction of Ni(AcO)₂·4H₂O, **HL**Cl·EtOH and KSCN in molar ratio 1 : 1 : 3 in methanol resulted in the formation of a square-planar Ni(II) complex [Ni(**L**)(**NCS**)]SCN·H₂O **(5)** (Scheme 4). Complex **(5)** possesses the same cationic complex as complex **(4)**, however it is counterbalanced with a thiocyanate anion. In complexes **(4)** and **(5)**, deprotonation of the organic ligand results in the formation of formally neutral zwitter-ionic species. The positive charge of the quaternary ammonium group is compensated by the negative charge produced by the dissociation of the hydrazonic proton and the formation of a negatively charged oxygen atom after tautomerization.

Isothiocyanato complexes of Ni(II) with ethyl (2*E*)-2-[2-(diphenylphosphino)benzylidene]hydrazinecarboxylate [1] and 2-(diphenylphosphino)benzaldehyde 4-phenylsemicarbazone [2] were obtained in the reaction of the corresponding ligand, Ni(AcO)₂·4H₂O and NH₄SCN, while in the reaction of these ligands with Ni(BF₄)₂·6H₂O and KSCN it was not possible to obtain stable octahedral complex (Scheme 5).
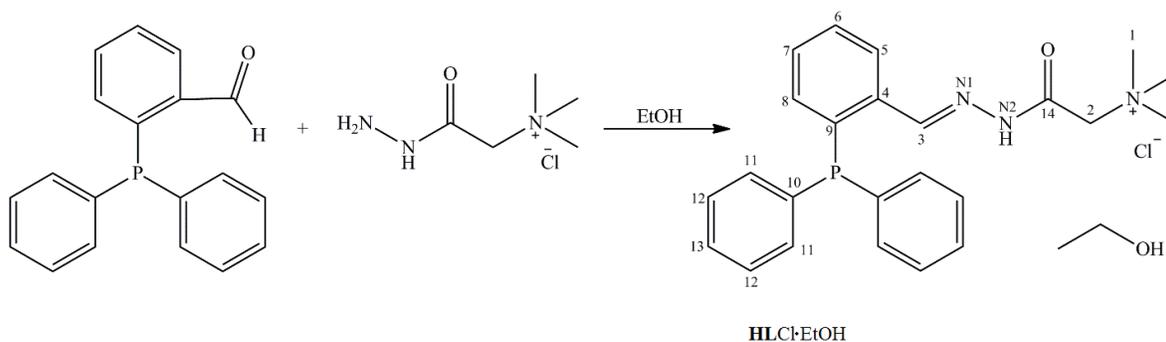
Scheme 2. Synthesis of (*E*)-2-(2-(2-(diphenylphosphino)benzylidene)hydrazinyl)-*N*,*N*,*N*-trimethyl-2-oxoethan-1-aminium chloride monoethanole (**HL**Cl·EtOH)
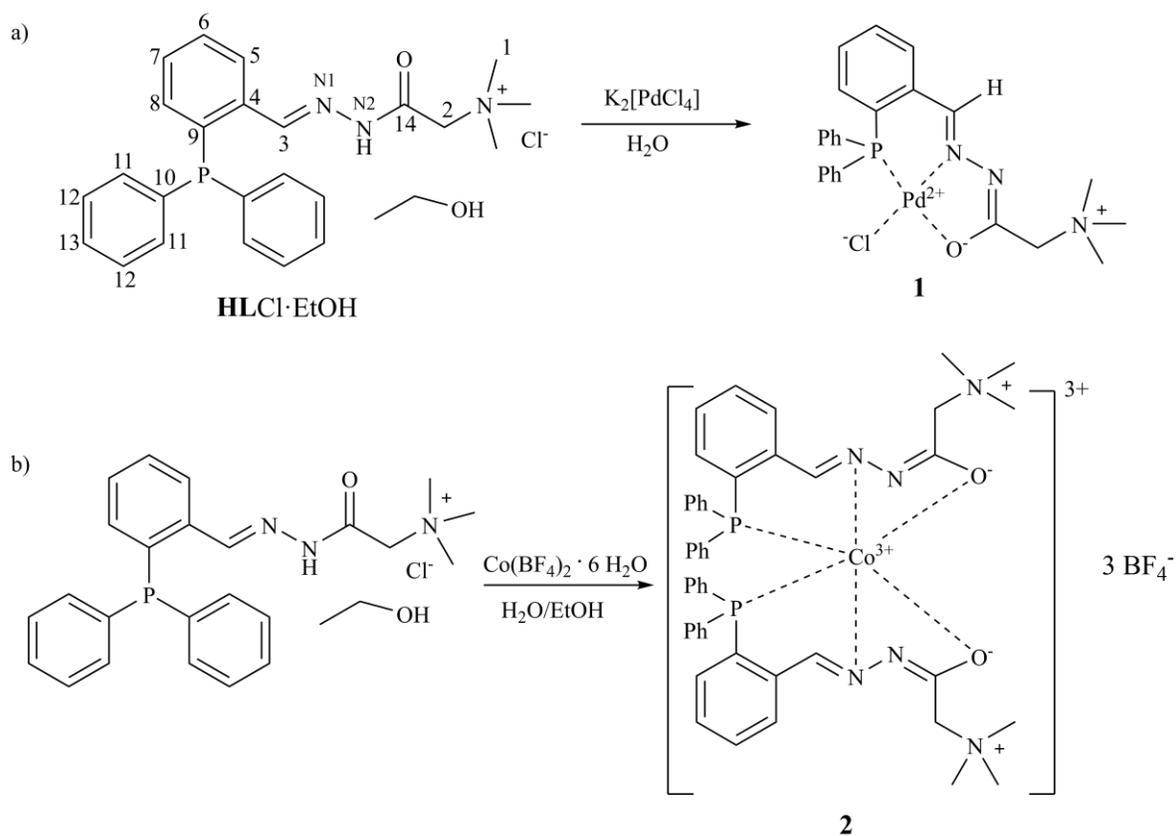
Scheme 3. (a) Synthesis of [Pd(**L**)Cl]Cl complex (**1**); (b) synthesis of [Co(**L**)₂](BF₄)₃ complex (**2**)
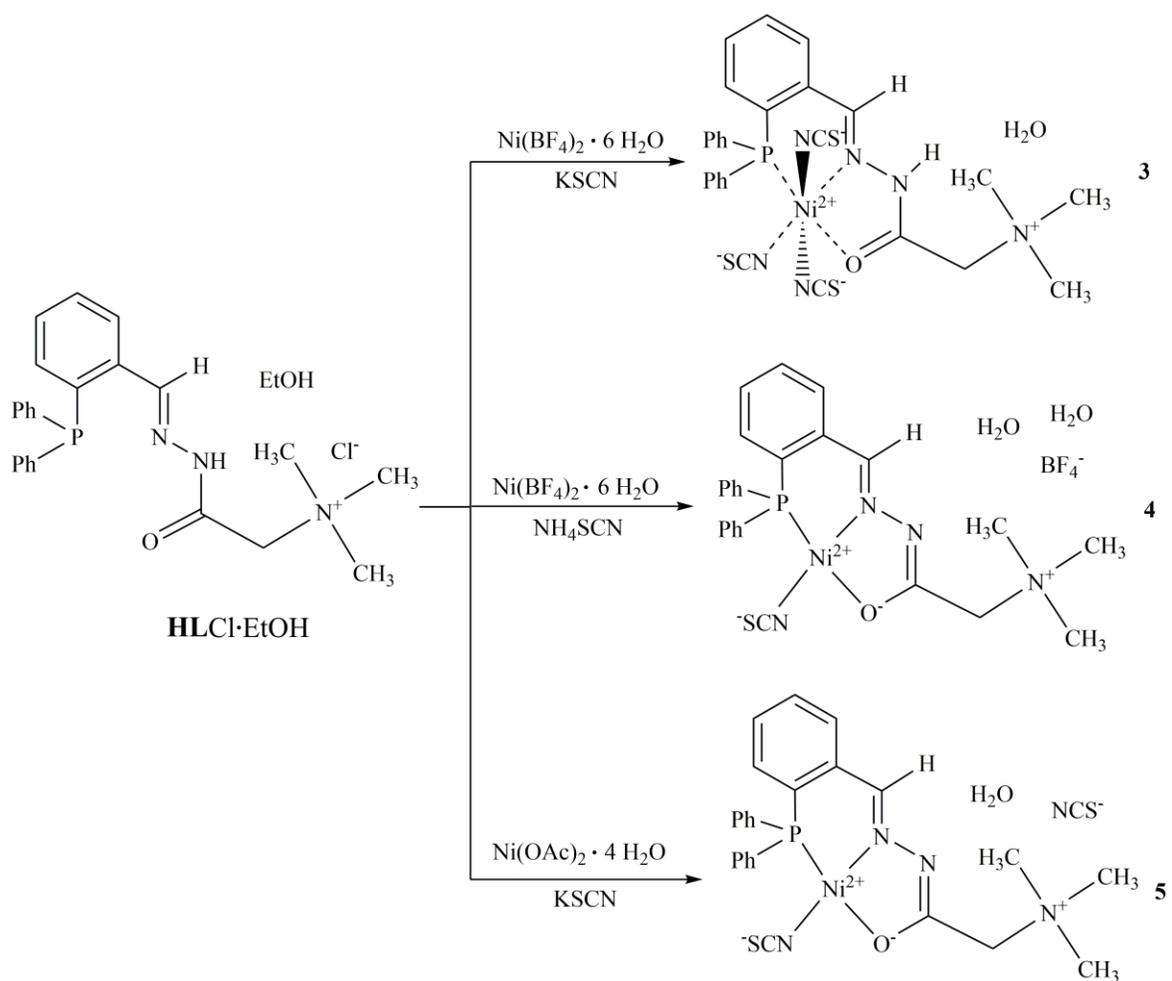
Scheme 4. Synthesis of [Ni(**HL**)(**NCS**)$_3$]·H$_2$O complex **(3)** [Ni(**L**)(**NCS**)]BF$_4$·2H$_2$O complex **(4)** [Ni(**L**)(**NCS**)]SCN·H$_2$O complex **(5)**
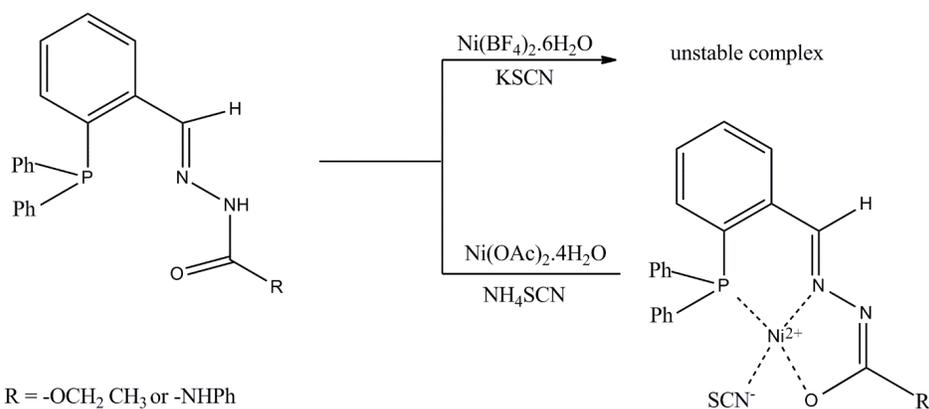
Scheme 5. Synthesis of Ni(II) isothiocyanato complexes with ethyl (2*E*)-2-[2-(diphenylphosphino)benzylidine]hydrazinecarboxylate and 2-(diphenylphosphino)benzaldehyde 4-phenylsemicarbazone.

4.2. Spectroscopy measurments

In the IR spectrum of **HLCl·EtOH**, there is a band at 1657 cm^{-1} originating from the azomethine group (v(C=N)) [3]. In each IR spectrum of complexes (**1–5**) this band appeared at lower wave number: at 1547 cm^{-1} in the spectrum of (**1**), at 1572 cm^{-1} in the spectrum of (**2**), at 1612 cm^{-1} in the spectrum of (**3**), at 1605 cm^{-1} in the spectrum of (**4**), and at 1606 cm^{-1} in the spectrum of (**5**), indicating that imine nitrogen was involved in coordination.

Contrary to the IR spectrum of the ligand **HLCl·EtOH**, in which the carbonyl band was observed at 1686 cm^{-1}, in the IR spectra of the complexes a new band appeared at 1639 cm^{-1} in the spectrum of complex (**1**) [4], at 1619 cm^{-1} in the spectrum (**2**) [4], at 1568 cm^{-1} in the spectrum of complex (**4**), and at 1571 cm^{-1} in the spectrum of complex (**5**) corresponding to v($^-$O–C=N) of the deprotonated hydrazide moiety. The negative shift of the v(C=O) vibration which is in the spectrum of complex (**3**) observed at 1659 cm^{-1} was related to the coordination of the oxygen atom of the carbonyl group.

The position of the band assigned to v(C–P) vibrations is almost constant in the IR spectra of the ligand and the complexes (1433 cm^{-1} in the spectrum of ligand **HLCl·EtOH**, 1436 cm^{-1} in the spectra of complexes **(1)** and **(2)** [4], 1435 cm^{-1} in the spectrum of complex **(3)**, 1432 cm^{-1} in the spectrum of complex **(4)** and 1433 cm^{-1} in the spectrum of complex **(5)**). In the IR spectra of complexes **(2)** and **(4)** the bands at 1058 cm^{-1} [5, 6] and 1035 cm^{-1}, respectively, originate from the tetrafluoroborate anions in the outer sphere of the complexes.

Different coordination modes of thiocyanato anions in complexes **(3)**, **(4)** and **(5)** can be deduced on the basis of the position and number of bands in the v(CN) vibration range of the NCS$^-$group in IR spectra. The presence of two bands in the v(CN) vibration range of the NCS$^-$group in the spectrum of **(3)** confirms the coordination of isothiocyanato ligands in apical (2113 cm^{-1}) and equatorial (2067 cm^{-1}) position. In the IR spectrum of **(4)** a band at 2071 cm^{-1} corresponds to only one NCS group coordinated to Ni(II) *via* the nitrogen atom, while in the spectrum of complex **(5)** two strong v(CN) bands at 2080 cm^{-1}and 2060 cm^{-1} originating from NCS groups are presented. The band at higher energy belongs to the NCS group coordinated through nitrogen atom, while the lower energy band corresponds to a non-coordinated thiocyanate anion [7]. The presence of a non-coordinated thiocyanate anion in complex **(5)** is also confirmed on the basis of the result of molar conductivity measurements.

Electronic spectra of complexes **(3)**, **(4)**, and **(5)** are similar, without electronic transitions below 10000 cm^{-1}indicating square-planar geometry of complexes in solution [8]. Octahedral complex **(3)** is unstable in solution; apical isothiocyanato ligands readily dissociate from metal ion. Final confirmation of the structures of complexes **(3)** and **(4)** in solid state was given by X-ray analysis.

4.3. NMR spectra

Hydrazone can exist as different isomers, due to geometric isomerism related to the imino group (*E*, *Z* isomers) and rotational isomerism as a result of restricted rotation around amide bound (*anti*, *syn* conformers) [9]. Results of X-ray analysis of ligand **HL**Cl·EtOH demonstrated that reaction of 2-(diphenylphosphino)benzaldehyde with the Girard's Treagent results in the formation of its *E* isomer. NMR data for ligand **HL**Cl·EtOH revealed the presence of two stereoisomers *syn* and *anti* in solution.

The ^{1}H NMR spectrum of **HL**Cl·EtOH (Table 11) showed two singlet signals of hydrazide NH at 12.10 and 12.70 ppm [10], corresponding to *syn* and *anti* isomers, respectively [11]. Two singlet signals were observed for azomethine group at 8.79 and 9.02 ppm, corresponding to *syn* and *anti* isomers, respectively [4, 11]. Also, double signals were noticed for methyl, methylene, and aromatic hydrogen atoms H5 and H8. The aromatic protons appeared in the region from 6.83 to 8.05 ppm. Based on integral of hydrogen atom signals, the ratio of *syn*/*anti* isomer of ligand is 0.75 : 0.25. The signal of hydrazide NH in the spectra of both complexes **(1)** and **(2)** is missing, indicating that the ligand **HL**Cl·EtOH is coordinated in deprotonated form [10]. Coordination through imine nitrogen results in downfield shift of H3 in **(2)** [5], while in **(1)** this signal was shifted upfield [10, 12]. In the ^{1}H NMR spectra of complexes signals of most aromatic protons shift downfield, suggesting that coordination occurs through phosphorus atom (Table 11).

In ^{13}C NMR spectrum of **HL**Cl·EtOH, double signals of *syn*and *anti* isomers are also observed (Table 12). The ^{13}C NMR spectrum showed two signals for carbonyl group at 165.5and 160.1 ppm, and two signals for azomethine group at 143.4 and 146.5 ppm corresponding to *syn* and *anti* isomers, respectively. Coordination through carbonyl oxygen atom results in downfield shift of its signal in the spectra of complexes (170.0 ppm in the spectrum of **(1)** and 168.8 ppm in the spectrum of **(2)**) [5, 10, 12]. The signal of imine C3 is shifted downfield in the spectra of complexes due to coordination through imine nitrogen (154.0 ppm in the spectrum of **(1)** and 165.2 ppm in the spectrum of **(2)**) [10]. In **(1)**, signals of aromatic carbon atoms directly bound to phosphorus are shifted upfield due to

coordination through phosphorus atom [5]. In both of the complexes, the chemical shifts of most aromatic carbon atoms have higher values, due to electron withdrawal by the coordinated metal ion.

Table 11. ^{1}H NMR spectral data (chemical shift (ppm), multiplicity, number of H-atoms, coupling constant J in Hz) of **HL**Cl·EtOH and complexes (**1**) and (**2**).

Assignment	**HL**Cl·EtOH *syn*	**HL**Cl·EtOH *anti*	(**1**)	(**2**)
C1	3.30 (s, 9 H)	3.28 (s, 2.7 H)	3.28 (s, 9H)	3.01 (s, 9H)
C2	4.76 (s, 2 H)	4.34 (s, 0.6 H)	4.34 (s, 2H)	3.28 (d, 1H, $J =$ 15 Hz)
C2′				3.58 (d, 1H, $J=$ 15 Hz)
C3	8.79 (d, 1 H, $J = 5.0$ Hz)	9.02 (d,1H, $J = 5.0$ Hz)	8.77 (d, 1H, $J = 5.0$ Hz)	9.39 (s, 1H)
C5	6.83 (m, 1H)	6.86 (m, 0.3 H)	7.48 (dd, 1H, $J=$ 15.0 Hz, $J = 10.0$ Hz)	7.28 (m, 1H)
C6	7.42 (m, 1 H)	7.42 (0.3 H)	7.72 (t, 1H, $J= 8.0$ Hz)	7.63 (t, 1 H, $J= 5.0$ Hz)
C7	7.49 (m, 1 H)	7.49 (m, 0.3 H)	7.85 (t, 1H, $J = 7.5$ Hz)	7.90 (t, 1H, $J = 5.0$ Hz)
C8	8.05 (dd, 1 H, $J = 5.0$ Hz)	7.99 (dd, 0.3 H, $J = 5.0$ Hz)	8.11 (dd, 1H, $J=$ 10.0 Hz, $J = 5.0$ Hz)	8.08 (d, 1H, $J=10.0$ Hz)
C11	7.19 (m, 4 H)	7.19 (m, 1.2 H)	7.55 (m, 4H)	6.99 (dd, 2H, $J= 10.0$ Hz, $J= 5.0$ Hz)
C11′				7.22 (m, 2H)
C12	7.42 (m, 4 H)	7.42 (m, 1.2 H)	7.65 (m, 4H)	7.18 (m, 2H)
C12′				7.37 (m, 2H)
C13	7.42 (m, 2 H)	7.42 (m, 0.6 H)	7.65 (m, 2H)	7.46 (t, 1H, $J= 5.0$ Hz)
C13′				7.53 (t, 1H, $J= 5.0$Hz)
N2	12.10 (s, 1 H)	12.70 (s, 1H)		

Table 12. ^{13}C NMR spectral data (chemical shift (ppm), coupling constant J in Hz) of **HL**Cl·EtOH and complexes **(1)** and **(2)**.

Assignment	**HL**Cl·EtOH *syn*	**HL**Cl·EtOH *anti*	**(1)**	**(2)**
C1	53.4	56.1	53.5	53.4
C2	62.4	63.1	62.4	61.5
C3	143.4 (*J*= 25.0 Hz)	146.5 (*J*= 25.0 Hz)	154.0	165.2
C4	135.4 (*J*= 10 Hz)	135.4 (*J*= 10 Hz)	135.8 (*J*= 17.5 Hz)	134.2
C5	133.2	133.3	134.9 (*J*= 1.25 Hz)	135.4
C6	130.5	130.7	134.3 (*J*= 7.5 Hz)	134.6
C7	129.4	129.6	134.3 (*J*= 7.5 Hz)	134.2
C8	126.3 (*J*= 3.75 Hz)	126.1 (*J*= 3.75 Hz)	138.1 (*J*= 10.0 Hz)	138.8
C9	136.5 (*J*= 18.75 Hz)	136.5 (*J*= 18.75 Hz)	118.2 (*J*= 52.5 Hz)	134.6
C10	137.2 (*J*= 18.75 Hz)	137.2 (*J*= 18.75 Hz)	127.7 (*J*= 62.5 Hz)	134.5
C11	133.5 (*J*= 18.75 Hz)	133.5 (*J*= 18.75 Hz)	129.4 (*J*= 12.5 Hz)	133.3
C12	129.1 (*J*= 7.5 Hz)	129.0 (*J*= 7.5 Hz)	133.9 (*J*= 11.25 Hz)	129.6
C12′				129.1
C13	129.4	129.3	132.6 (*J*= 2.5 Hz)	132.7
C13′				132.1
C14	165.5	160.1	170.0	168.8

4.4. Description of the crystal structures

Compound **HL**Cl·EtOH crystallizes as a quaternary ammonium chloride salt, protonated on the amidic nitrogen and with a chloride counter-anion to balance the total charge, forming a hydrogen bond between these two groups (NH···Cl = 3.264(2) Å, 164(1)°) (Figure 2). The ligand skeleton is skewed, with torsion angles: C13–C18–C19–N1 = 158°, C18–C19–N1–N2 = 176°, C19–N1–N2–C20 = 177°, N1–N2–C20–C21 = −105°. An ethanol molecule completes the asymmetric unit and forms a hydrogen bond with the chloride anion (O–H···Cl = 3.129(3) Å, 179(1)°).

Compound (**1**) crystallizes with two independent cationic complexes in the asymmetric unit (Figure 3), that are not significantly different, and are related by a pseudo-twofold rotation axis, not aligned with the cell edges (Figure 4). The unit cell is completed by two chloride anions, one of which distributed over two positions on inversion centers.
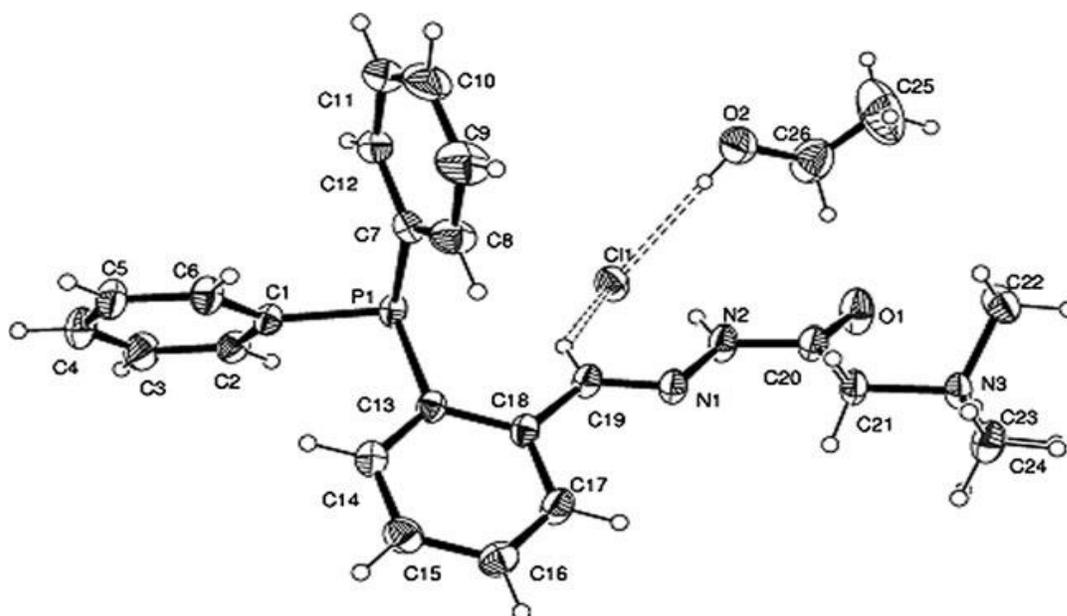
Figure 2. Crystal structure of **HL**Cl·EtOH, with thermal ellipsoids at the 50% probability level. Hydrogen bonds are dashed.
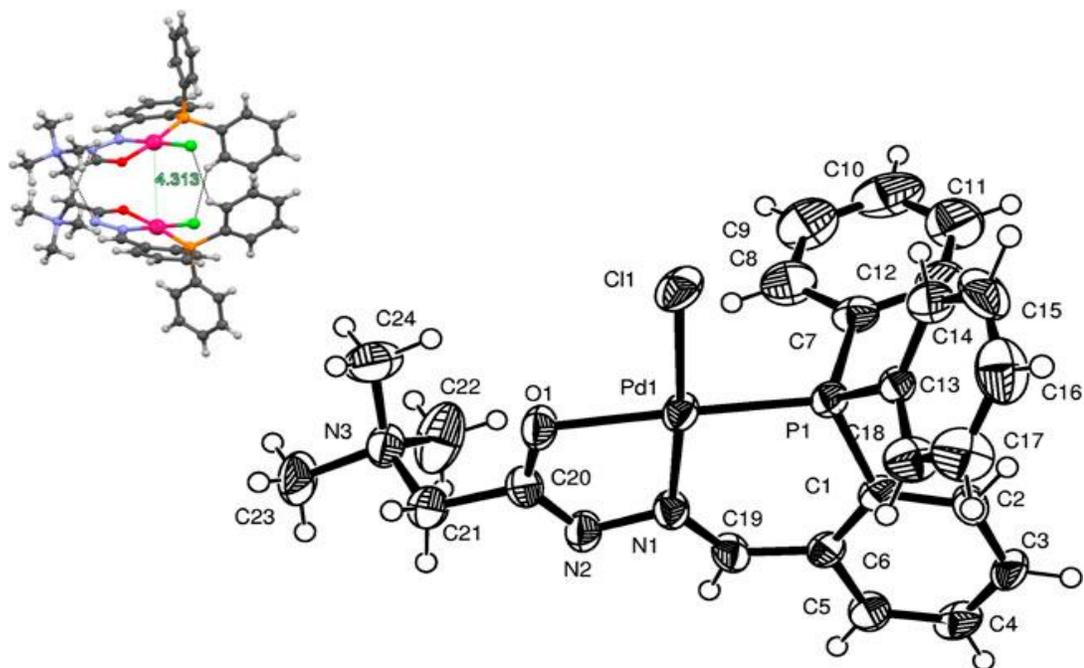
Figure 3. Molecular structure of the [Pd**L**Cl]$^+$ in **(1)**, with thermal ellipsoids at the 50% probability level. Inset: stacking of two crystallographically independent cations in the crystal structure of **(1)**.
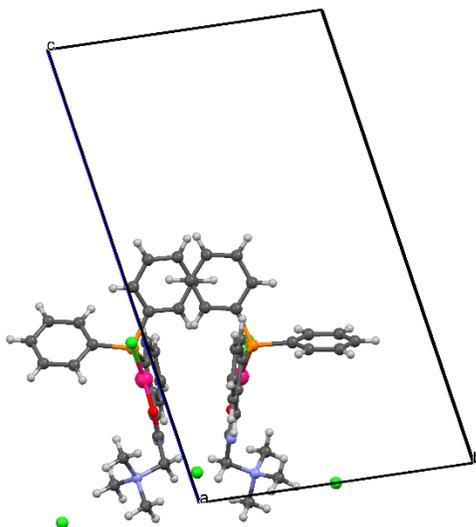
Figure 4. Pseudo twofold rotation relating the two independent molecules of compound **(1)**.

Both complex molecules of **1** (Figure 3) present a square-planar coordination around the metal atom, made by the PNO tridentate neutral zwitterionic ligand and completed by a chloride *trans* to the N atom. Table 13 reports the most relevant bond distances and angles. The phosphorus atom is slightly displaced from the coordination plane, as usually observed for similar families of PNO ligands [13]. Upon coordination of the tridentate ligand, five-membered and six-membered chelation rings are formed, the former planar, the latter slightly puckered due to the above- mentioned hindrance of the phosphorus atom. The trimethylamino cationic tail of the ligand is oriented almost perpendicular to the ligand plane.

Table 13. Relevant bond lengths (Å) and angles (°) for (1), with su's in parentheses.

Bond length (Å)		Bond length (Å)	
C1–P1	1.822(4)	C25–P2	1.796(4)
C7–P1	1.809(5)	C31–P2	1.792(5)
C13–P1	1.803(5)	C37–P2	1.795(5)
C19–N1	1.290(5)	C43–N4	1.293(5)
C20–N2	1.306(6)	C44–N5	1.311(6)
C20–O1	1.282(5)	C44–O2	1.293(5)
C21–N3	1.507(6)	C45–N6	1.496(5)
C22–N3	1.499(6)	C46–N6	1.501(5)
C23–N3	1.486(6)	C47–N6	1.512(6)
C24–N3	1.486(6)	C48–N6	1.480(6)

N1–N2	1.409(5)	N4–N5	1.410(5)
N1–Pd1	1.980(4)	N4–Pd2	1.974(3)
O1–Pd1	2.073(3)	O2–Pd2	2.066(3)
Cl1–Pd1	2.288(1)	P2–Pd2	2.196(1)
Pd1–P1	2.199(1)	Cl2–Pd2	2.290(1)
Bond angle (°)		Bond angle (°)	
N1–Pd1–O1	80.2(1)	N1–Pd1–Cl1	175.0(1)
N1–Pd1–P1	95.3(1)	O1–Pd1–Cl1	95.4(1)
O1–Pd1–P1	174.6(1)	Cl1–Pd1–P1	88.92(5)
Pd1–N1–N2	113.6(3)	Pd1–N1–C19	131.6(3)
N1–N2–C20	111.1(4)	C20–O1–Pd1	107.2(3)
C6–C19–N1	129.3(4)	C19–C6–C1	126.5(4)
C6–C1–P1	122.8(3)	C1–P1–Pd1	111.8(1)
C21–C20–O1	117.4(4)	C20–C21–N3	114.2(4)

Interestingly, the two complex cations are stacked with the coordination planes parallel with a Pd...Pd distance of 4.313 Å (Figure 3, inset), forming other short contacts between the aromatic CH and the chlorides and between the CH_2 groups and the iminic N atoms. The chloride anions are nested between the methyl groups of the cationic tail of the complex molecules, so that in the overall packing (Figure 5), the moieties with different polarity are compartmentalized in a slice of phenyl groups, a slice of stacked coordination planes, and a slice of trimethylammonium moieties alternating with chloride anions. This organization leaves large voids that in the crystal are occupied by disordered solvent ready

to leave the solid and to decompose upon X-ray exposure. It has not been possible to build a sensible chemical model for this contribution, whose overall electron density is presented in the Figure 6.
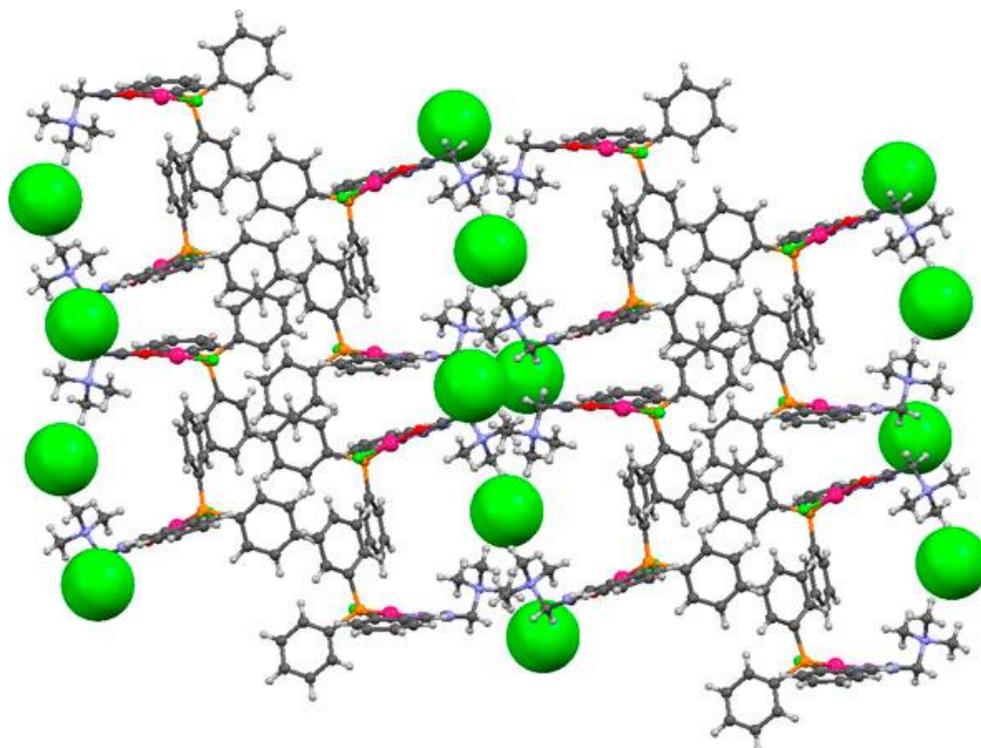
Figure 5. Crystal packing of the ordered part of the structure of (**1**), showing cations and anions.

Compound (**2**) crystallizes in the space group *Cc* in a huge cell, with a volume of 16841 $Å^3$ (Figure 7). The asymmetric unit contains three independent cations [Co**L₂**]$^{3+}$, and nine BF$_4^-$ anions, most of which were not visible in the electron density map. The structure is in fact highly disordered and the quality of diffraction data was not sufficient for an accurate determination of the molecular geometry and crystal packing. The connectivity of the complex cations is unambiguous and is shown in Figure 7. The complex has a bis(trischelate) PNO coordination on the metal center, giving an octahedral geometry, with

the formation of five-membered and six-membered chelation rings. The three cations in the asymmetric unit present different Δ/Λ absolute configurations on the metal, two being of the same configuration and the third being different; since the space group contains a symmetry plane, the compound is racemic.
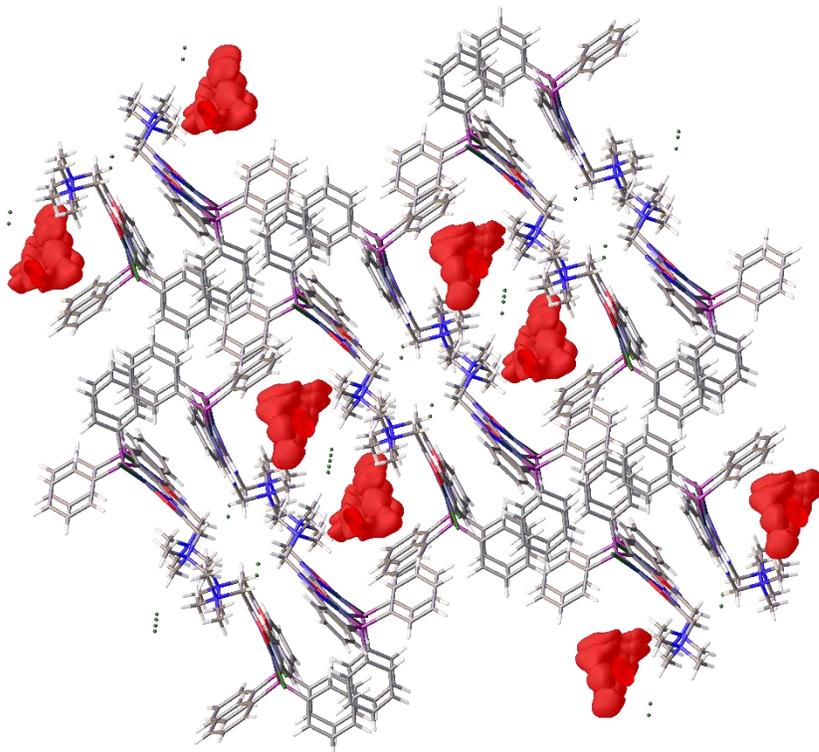
Figure 6. Crystal packing of compound (**1**), evidencing the volumes of undefined electron density residual after the refinement of the ordered part of the structure.
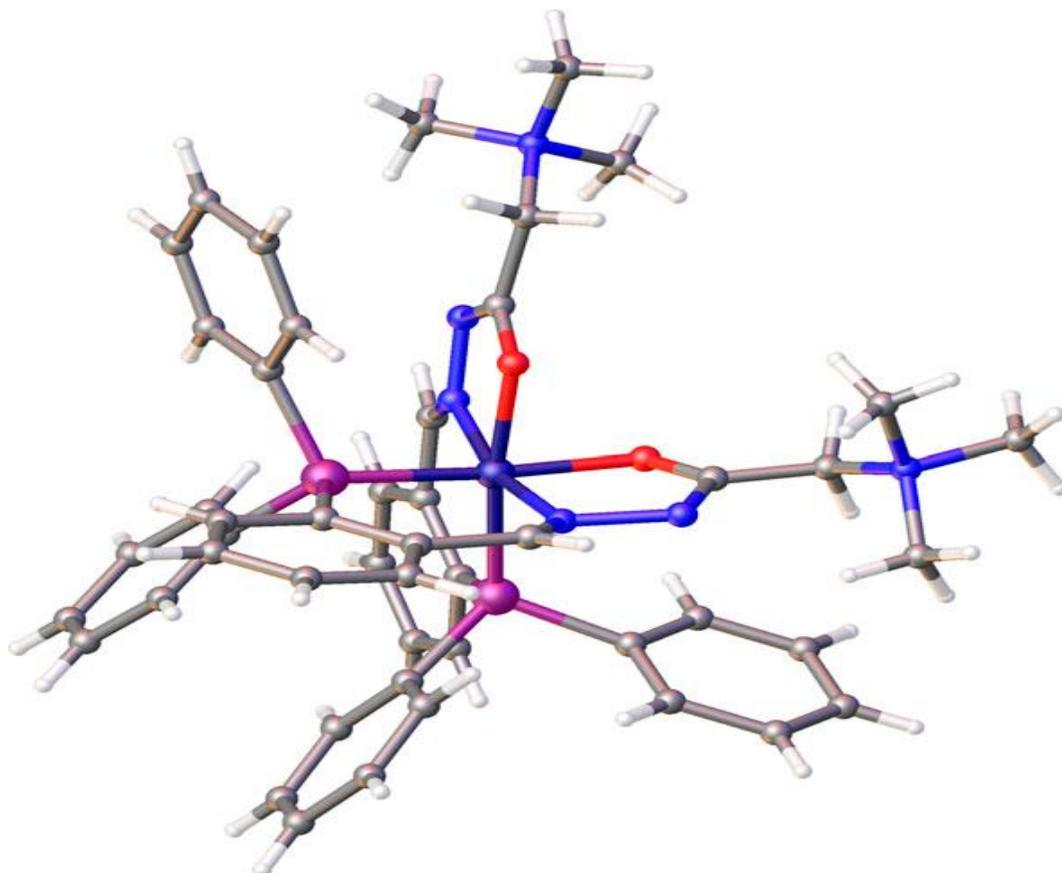
Figure 7. Molecular structure of [Co**L₂**]³⁺ cation in compound **(2)**, as determined by X-ray diffraction.

Crystals of products **(3)** and **(4)** suitable for X-ray analyses were prepared by slow evaporation of solvent at room temperature. Selected bond lengths and angles are given in Table 14. The structure of complex **(3)** possesses the tridentate ligand and complex **(4)** deprotonated tridentate **L** ligand, both coordinated to the nickel atom with a PNO set of donor atoms forming one five-membered and one six-membered chelate ring.

The structure of compound **(3)** is displayed in Figure 8. The three thiocyanate nitrogen atoms complete the distorted octahedral coordination mode of nickel atom in complex **(3)**. Intermolecular interactions that exist in the solid state of compounds **(3)** are depicted in Figure 9. N-H···O and O-H···S hydrogen bonds connect the complex molecules

and water molecules into an infinite chain. Hydrogen-bonding interactions for compound **(3)** are listed in Table 15.

The cationic complex in **(4)** consists of one tridentate molecule of deprotonated **L** ligand coordinated to the Ni(II) ion and thiocyanate anion coordinated through nitrogen atom forming a square planar geometry around the Ni(II) ion (Figure 10). The BF_4^- ion acts as counter-ion in the crystal structure. There are also two water molecules as solvate per one ionic formula unit. The sum of the nickel-containing angles in complex **(4)** is 360°. The position of the Ni(II) ion is 0.063(14) Å out of the best plane that contained the coordination sphere of four atoms. The observed elongation of O1–C5 and shortening of N1–C5 bond in complex **(4)** in comparison with the corresponding bonds in complex **(3)** (Table 14) indicates electron delocalization in the deprotonated hydrazine moiety and coordination of the ligand in enol form. In the structure of complex **(4)** there is no evidence for any significant non-covalent interactions.
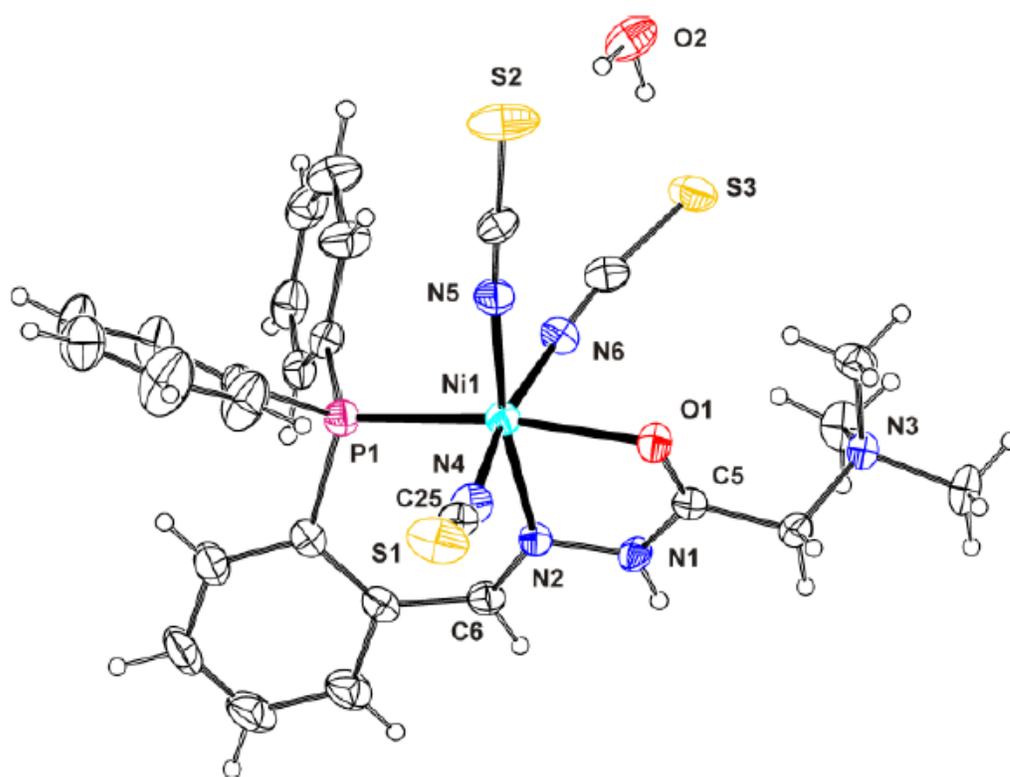
Figure 8. ORTEP plot of (**3**) with thermal ellipsoids at 30% probability for non-H atoms and open circles for H-atoms.
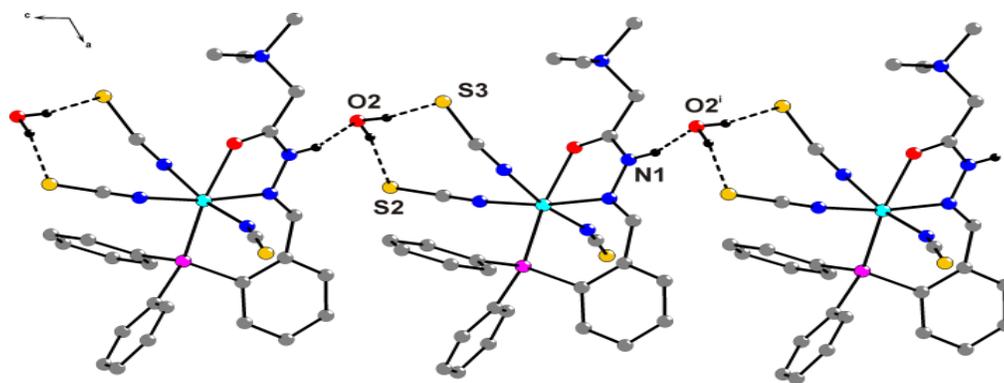
Figure 9. DIAMOND [8] view of (**3**) showing the polymeric chain in the crystal structure [Symmetry code: (i) x, –y+1/2, z–1/2].
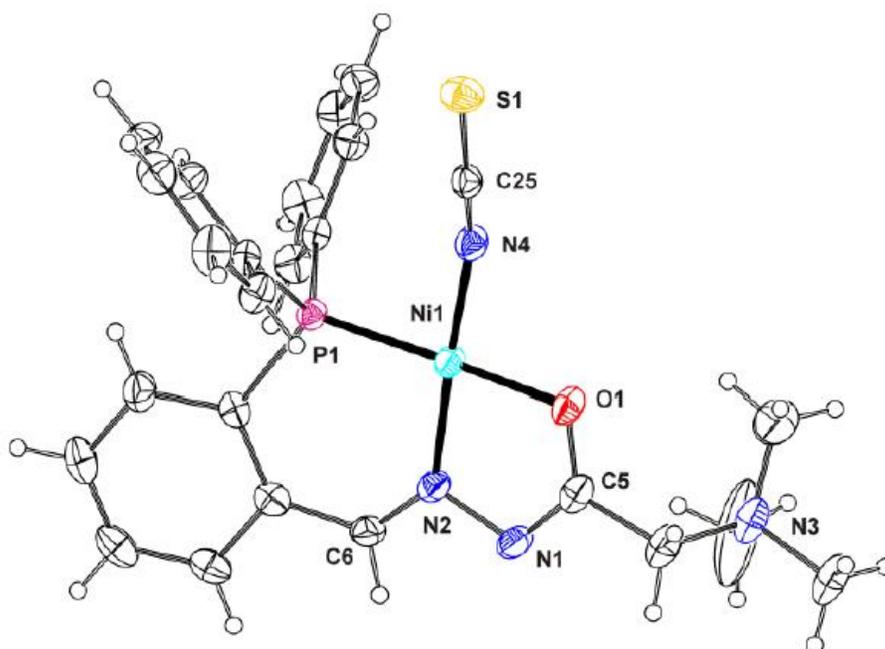
Figure 10. ORTEP plot of **(4)** with thermal ellipsoids at 30% probability for non-H atoms and open circles for H-atoms. BF_4^- and two water molecules were omitted for the reason of clarity.

Table 14. Selected bond lengths (Å) and angles (°) of compounds **(3)** and **(4)**.

	(3)	**(4)**
Ni1–P1	2.3724(10)	2.1469(10)
Ni1–O1	2.153(2)	1.903(3)
Ni1–N2	2.087(3)	1.863(3)
Ni1–N4	2.035(3)	1.859(3)
Ni1–N5	2.010(3)	–
Ni1–N6	2.099(3)	–
N1–N2	1.385(3)	1.415(4)
N1–C5	1.345(4)	1.291(5)
N2–C6	1.288(4)	1.280(5)
O1–C5	1.229(3)	1.290(5)
S1–C25	1.631(4)	1.616(4)
C25–N4	1.150(4)	1.159(5)
P1–Ni1–O1	166.64(6)	175.81(9)
P1–Ni1–N4	95.96(9)	88.63(10)
P1–Ni1–N5	98.35(9)	–
P1–Ni1–N6	93.64(9)	–
N2–Ni1–N4	92.11(11)	174.59(14)
N1–N2–C6	115.0(3)	112.8(3)
N1–C5–O1	121.7(3)	126.0(4)
N2–N1–C5	118.2(3)	109.2(3)

Table 15. Hydrogen bonding geometry for (3).

D – H $\cdots$ A	d(D – H)/ Å	d(H $\cdots$ A)/ Å	d(D $\cdots$ A)/ Å	<(DHA)/ °	Symmetry transformation for acceptors
N1–H1N$\cdots$O2	0.841(17)	1.94(2)	2.744(4)	159(3)	x, −y+1/2, z–1/2
O2–H1$\cdots$S2	0.954(19)	2.28(2)	3.218(3)	168(4)	
O2–H2$\cdots$S3	0.947(19)	2.37(2)	3.295(11)	165(4)	

4.5. Magnetic measurements

The data were corrected for the contributions of the sample holder and for the diamagnetism of the sample estimated from Pascal's constants. Magnetic data for complex (**3**) are shown in Figure 11, where temperature dependence of inverse magnetic susceptibility ($1/\chi$) and effective magnetic moment (μ_{eff}), per mole of Ni(II) complex are presented. It can be seen linear behavior of inverse magnetic susceptibility in the whole temperature range showing paramagnetic behavior of the investigated sample. Fitting the susceptibility data to the Curie–Weiss law $\chi = C/(T\text{-}\theta)$ (where C and θ present Curie constant and Weiss temperature, respectively), gave $C = 1.20$ cm^{3}mol^{-1}K^{-1}, and $\theta = -0.1$ K. The effective magnetic moment $\mu_{eff} = 3.1\mu_B$, obtained from Curie constant C, is slightly higher than the spin-only value for Ni^{2+} ion ($\mu_{eff} = 2.82\mu_B$), but it is in a good agreement with literature data for Ni^{2+} in octahedral environment [14, 15]. Small negative value obtained for Weiss constant is within the experimental error. Curve μ_{eff}(T) shows that magnetic moment is almost constant, starting from room temperature (3.12 μ_B) to 8 K, and for lower temperature (T = 2 K) slightly decreases to 2.85 μ_B, which is only 9% of the nominal value at 293 K.
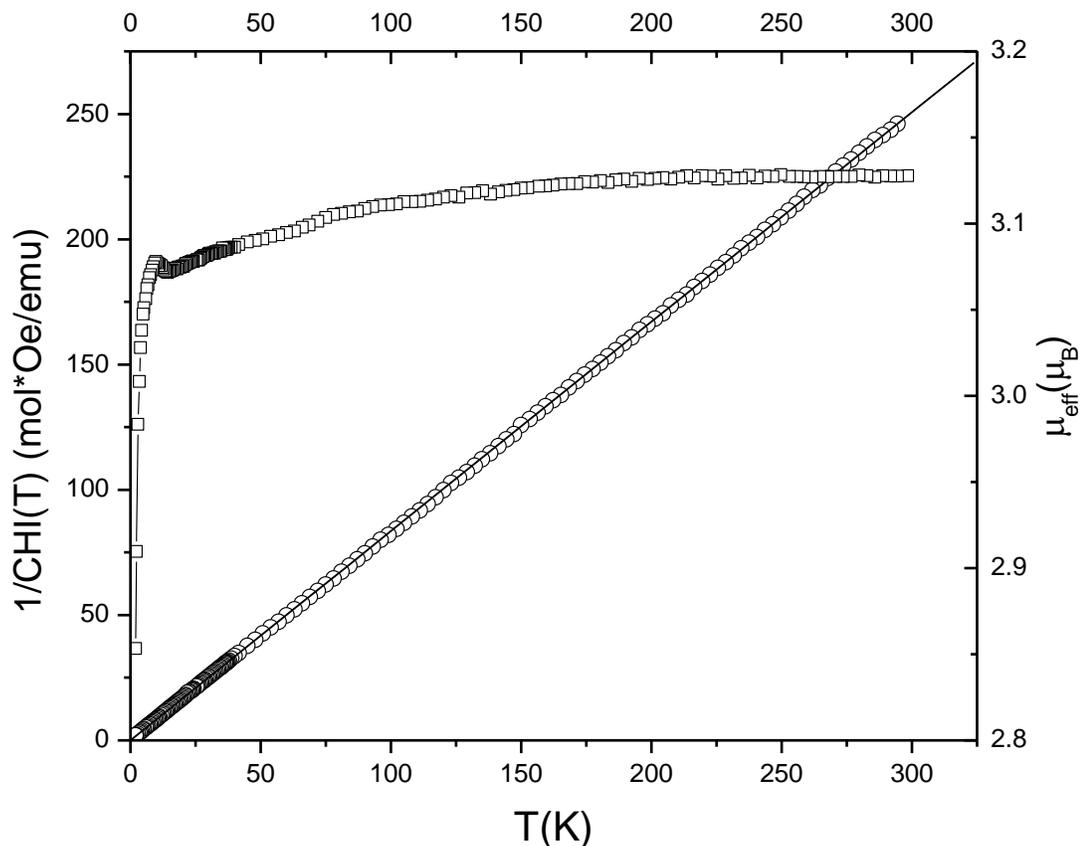
Figure 11. Temperature dependences of inverse magnetic susceptibility (open circles) and effective magnetic moment (open squares). Solid line is fit to Curie–Weiss law.

4.6. Antimicrobial activity

Antimicrobial activities of (**1**) and (**2**) were higher than the activity of ligand **HL**Cl·EtOH (Table 16). Complex (**2**) exhibited strong activity against Gram-positive bacterium *S. aureus* and Gram-negative bacteria *S.abony*, *P.aeruginosa*, and *K.pneumoniae*. A moderate activity of (**2**) was observed against the other examined bacterial strains. Complex (**1**) and ligand **HL**Cl·EtOH showed moderate activity on most of

the tested bacterial strains.The most pronounced activity of (1) was observed against Gram-negative bacteria *P. aeruginosa* and *S. abony*. The strongest antimicrobial activity of ligand **HL**Cl·EtOH was noted against *S. abony*. Compounds **HL**Cl·EtOH, (1) and (2) are not good antifungal agents, among them the highest antifungal activity was observed for compound (2).

Comparison of antimicrobial activity of compounds **HL**Cl·EtOH, (1) and (2) with the activity of previously investigated condensation product of 2-(diphenylphosphino)benzaldehyde and ethylcarbazate and corresponding complexes of Pd(II) [12] and Co(III) [5] gives insight into the influence of hydrophobicity, charge, and geometry of complexes on biological activity. The highest antibacterial activity was observed for octahedral electrolytic Co(III) complexes,while the best antifungal activity was observed for neutral square-planar Pd(II) complex with condensation product of 2-(diphenylphosphino)benzaldehyde and ethyl carbazate. The presence of positively charged ligand molecule in Pd(II) complex results in decreased antifungal activity and better antibacterial activity. An opposite situation was observed in the case of octahedral Co(III) complexes for which better antibacterial activity was observed for complex with uncharged ligand. Complex (1) showed better antimicrobial activity in comparison with previously synthesized Pd(II) complexes with similar PNO donor ligands [4, 10].

Table 16.The antimicrobial activity of ligand **HL**Cl·EtOH and complexs (**1**) and (**2**) (MIC values are given in mM).

Microorganisms	**HL**Cl·EtOH	(**1**)	(**2**)	$K_2[PdCl_4]$	$Co(BF_4)_2·6H_2O$	Cefotaxime	Amphotericin B
Staphylococcus aureus ATCC 6538	0.514	0.430	0.106	3.06	2.935	0.027	–
Pseudomonas aeruginosa ATCC 9027	0.514	0.430	0.212	3.06	2.935	0.055	–
Bacillus subtilis ATCC 6633	0.257	0.430	0.106	3.06	2.935	0.014	–
Salmonella abony ATCC 6017	0.257	0. 430	0.106	3.06	2.935	0.055	–
Klebsiella pneumoniae NCIMB 9111	0.514	0.430	0.106	3.06	2.935	0.027	–
Escherichia coli ATCC 10536	0.514	0.430	0.212	3.06	1.467	0.014	–
Candida albicans ATCC 10231	0.514	0.430	0.212	3.06	2.935	–	0.007

References of Results and Discussion

[1] V. Radulović, A. Bacchi, G. Pelizzi, D. Sladić, I. Brčeski, K. Andjelković, *Monatsh. Chem.* **137** (2006) 681.

[2] M. Milenković, A. Pevec, I. Turel, M. Vujčić, M. Milenković, K. Jovanović, N. Gligorijević, S. Radulović, M. Swart, M. Gruden-Pavlović, K. Adaila, B. Čobeljić, K. Anđelković, *Eur. J. Med. Chem.* **87** (2014) 284.

[3] A. Barandov, U. Abram, *Z. Anorg. Allg. Chem.* **633** (2007) 1897; (g) S.B. Novaković, G.A. Bogdanović, I.D. Brčeski, V.M. Leovac, *Acta Crystallogr. C* **65** (2009) 263; (h) V.M. Leovac, B. Ribár, G. Argay, A. Kálmán, I. Brčeski, *J. Coord. Chem.* **39** (1996) 11.

[4] M. Milenković, A. Bacchi, G. Cantoni, J. Vilipić, D. Sladić, M. Vujčić, N. Gligorijević, K. Jovanović, S. Radulović, K. Anđelković, *Eur. J. Med. Chem.* **68** (2013) 111.

[5] M. Milenković, A. Bacchi, G. Cantoni, S. Radulović, N. Gligorijević, S. Aranđelović, D. Sladić, M. Vujčić, D. Mitić, K. Anđelković, *Inorg. Chim. Acta* **395** (2013) 33.

[6] T.R. Todorović, U. Rychlewska, B. Warżajtis, D.D. Radanović, N.R. Filipović, I.A. Pajić, D.M. Sladić, K.K. Anđelković, *Polyhedron* **28** (2009) 2397.

[7] K. Nakamoto, Infrared and Raman Spectra of Inorganic and Coordination Compounds, Wiley-Interscience, New York, 2009.

[8] K. Brandenburg, DIAMOND, Crystal and Molecular Structure Visualization Version 3.2, Crystal Impact GbR, Bonn, Germany.

[9] Z. Kuodis, A. Rutavičius, A. Matijoška, O. Eicher-Lorka, *Cent. Eur. J. Chem.* **5** (2007) 996.

[10] M.M. Đorđević, D.A. Jeremić, M.V. Rodić, V.S. Simić, I.D. Brčeski, V.M. Leovac, *Polyhedron* **68** (2014) 234.

[11] M. Hagar, S.M. Soliman, F. Ibid, S.H. El Ashry, *J. Mol. Struct.* **1049** (2013) 177.

[12] M. Milenković, G. Cantoni, A. Bacchi, V. Spasojević, M. Milenković, D. Sladić, N. Krstić, K. Anđelković, *Polyhedron* **80** (2014) 47.

[13] A. Bacchi, M. Carcelli, M. Costa, A. Fochi, C. Monici, P. Pelagatti, C. Pelizzi, G. Pelizzi, L.M.S. Roca, *J. Organomet. Chem.* **180** (2000) 593.

[14] B. Čobeljić, B. Warżajtis, U. Rychlewska, D. Radanović,V. Spasojević, D. Sladić, R. Eshkourfu, K. Anđelković, *J.Coord.Chem.* **65:4** (2012) 655.

[15] S. Wöhlert, T. Runčevski, R.E. Dinnebier, S.G. Ebbinghaus, C. Näther, *Cryst.Growth Des.* **14** (2014) 1902.

5. CONCLUSION

In this thesis synthesis and structural characterization of (*E*)-2-(2-(2-(diphenylphosphino)benzylidene)hydrazinyl)-*N*,*N*,*N*-trimethyl-2-oxoethan-1-aminium chloride, as well as, its Pd(II), Co(III) and Ni(II) complexes were described. From the condensation reaction of the Girard's T reagent with 2-(diphenylphosphino)benzaldehyde, an ammonium quaternary chloride salt of the ligand was obtained. Square-planar Pd(II) complex is in the cationic form with the deprotonated ligand being tridentately coordinated via the phosphorus, the imine nitrogen and the carbonyl oxygen atoms, and the one chloride occupying the fourth coordination site; the other chloride acts as a counter-ion. The octahedral Co(III) complex cation consists of two tridentate PNO coordinated deprotonated ligands counterbalanced by three BF_4^- anions. Antimicrobial activities of Pd(II) and Co(III) complexes were higher than the activity of ligand. Complex of Co(III) exhibited strong activity against *S. aureus*, *S. abony*, *P. aeruginosa*, and *K. pneumoniae*. Complex of Pd(II) and ligand showed moderate activity on most of the tested bacterial strains. The most pronounced activity of Pd(II) complex was observed against *P. aeruginosa* and *S. abony*. Depending on the reaction conditions *i.e.* the source of Ni^{2+} and SCN^- ions three different isothiocyanato complexes of Ni(II) containing the condensation product of Girard's T reagent and 2-(diphenylphosphino)benzaldehyde were obtained. Coordination of deprotonated phosphine ligand results in formation of square-planar complexes, while the octahedral complex was formed with protonated ligand. In all the complexes of Ni(II) one molecule of organic ligand was coordinated in tridentate fashion through PNO donor atom set and the remaining coordination positions were occupied with thiocyanate ions. Magnetic data were analyzed by Curie-Weiss law from which effective magnetic moment (μ_{eff} = 3.1 μ_B) for Ni^{2+} was obtained. $1/\chi$(T) and μ_{eff}(T) curves show paramagnetic behavior of the investigated Ni(II) complex.

6. Supplementary material
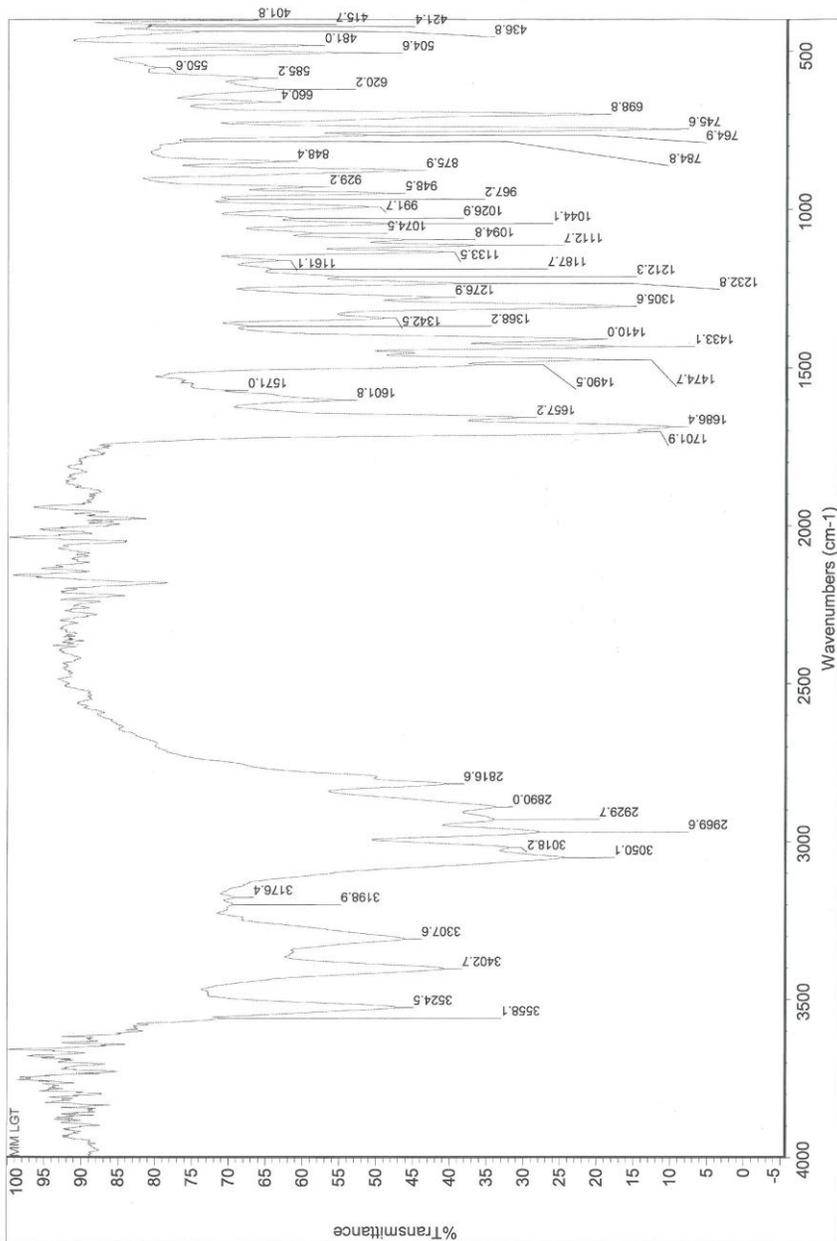
Figure S1. IR spectrum of **HL**Cl·EtOH.
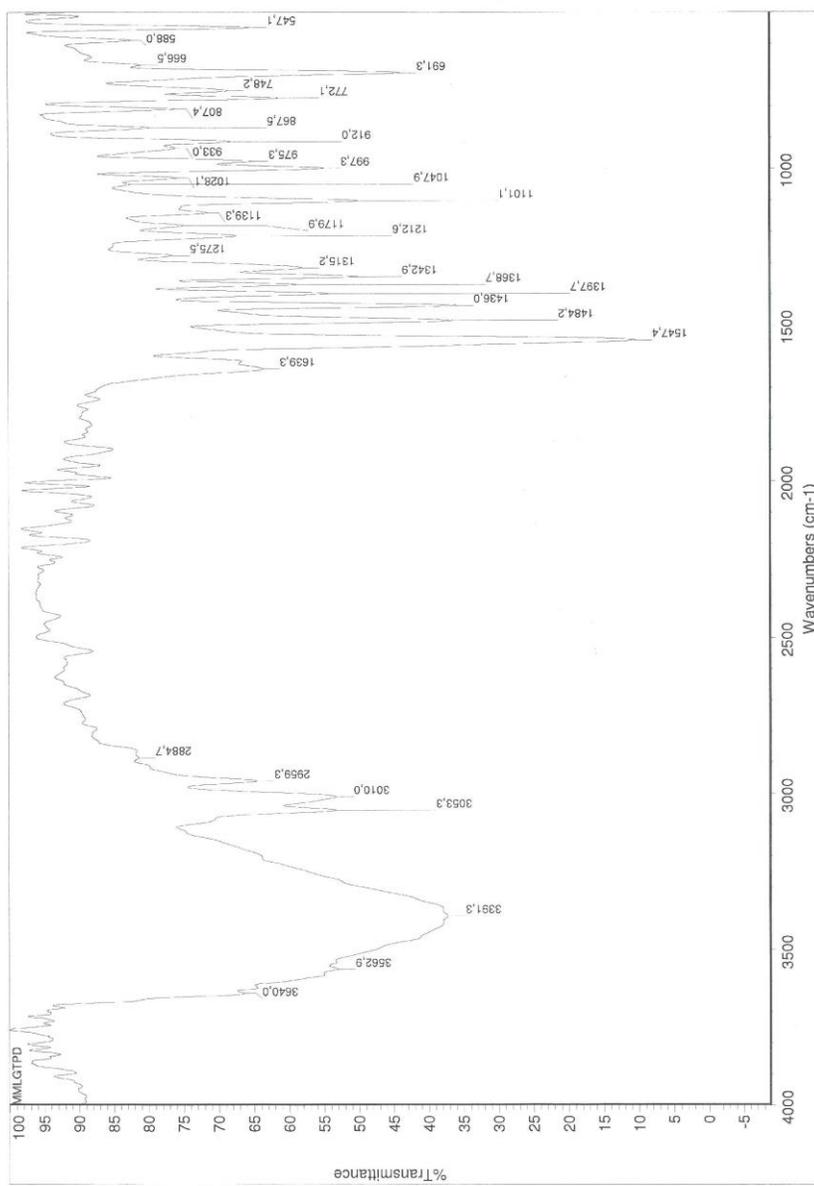
Figure S2. IR spectrum of complex **1**.
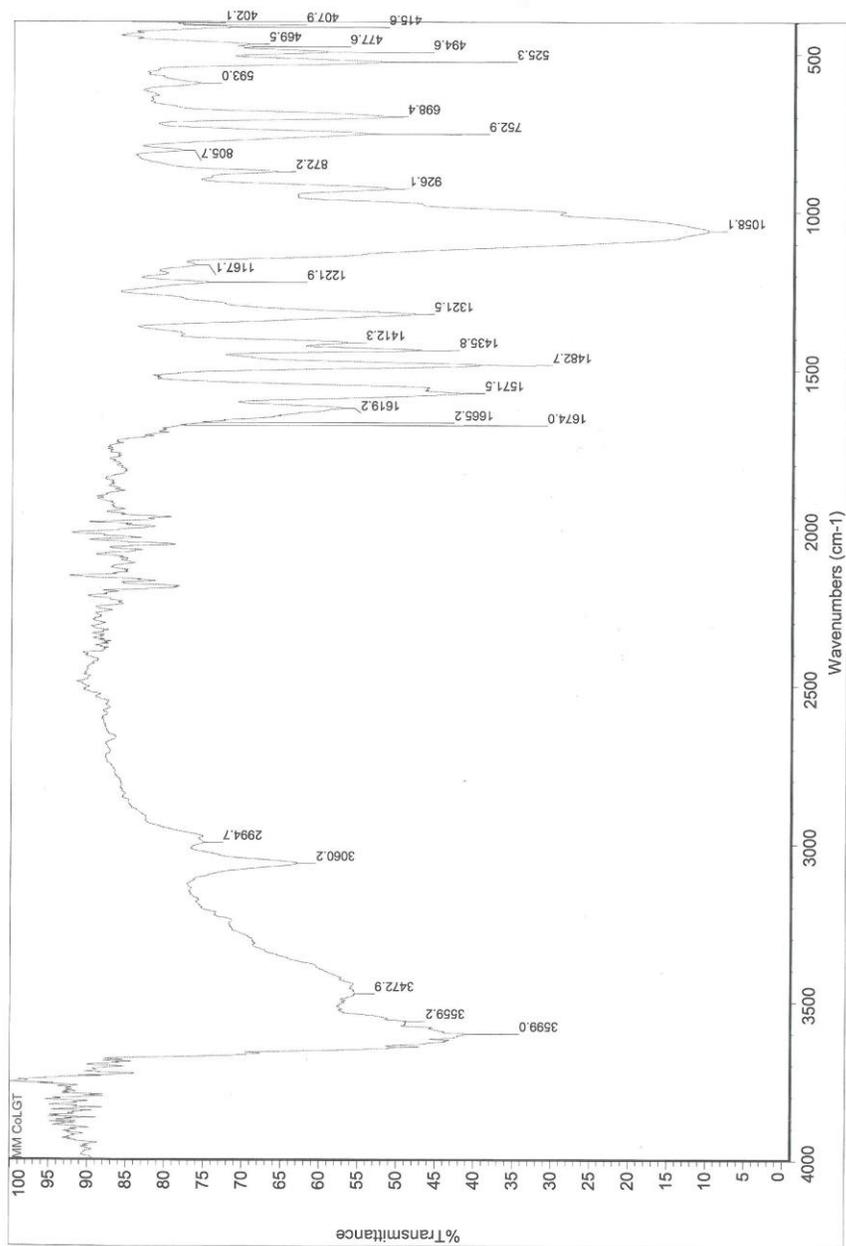
Figure S3. IR spectrum of complex **2**.
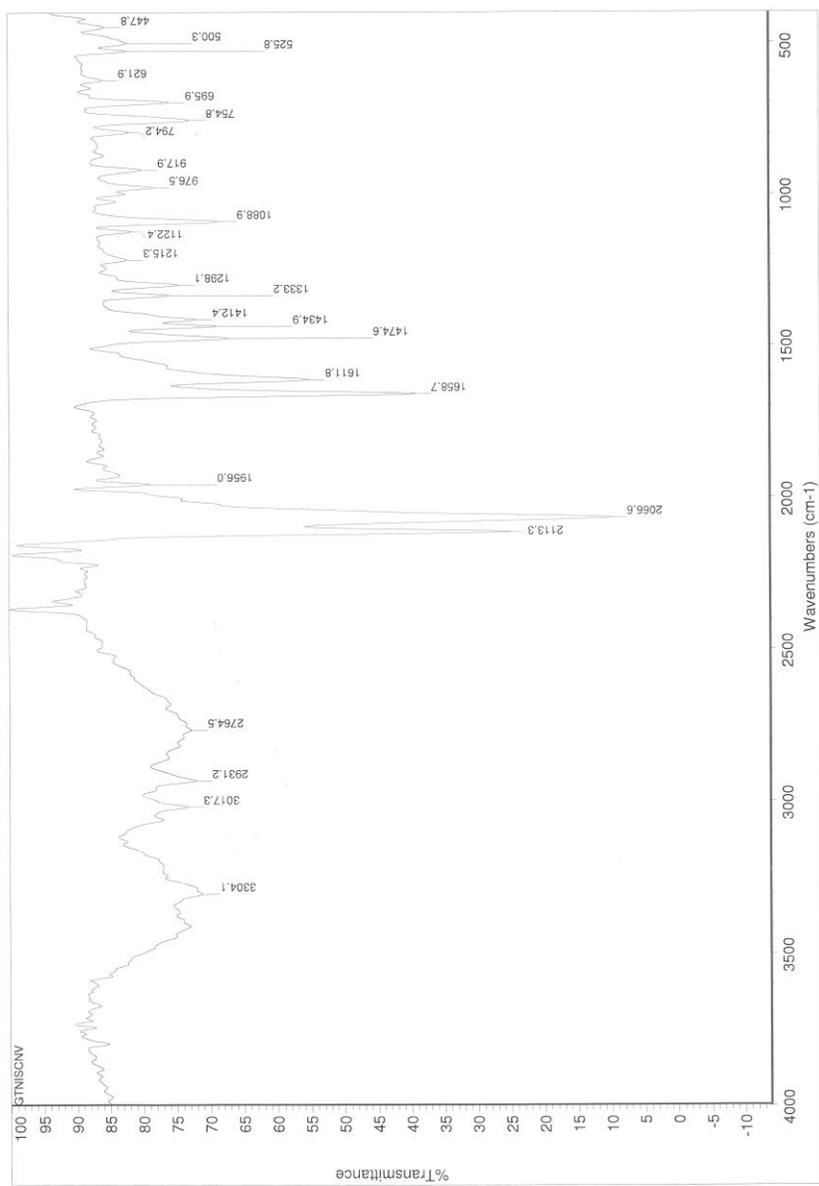
Figure S4. IR spectrum of complex **3**.
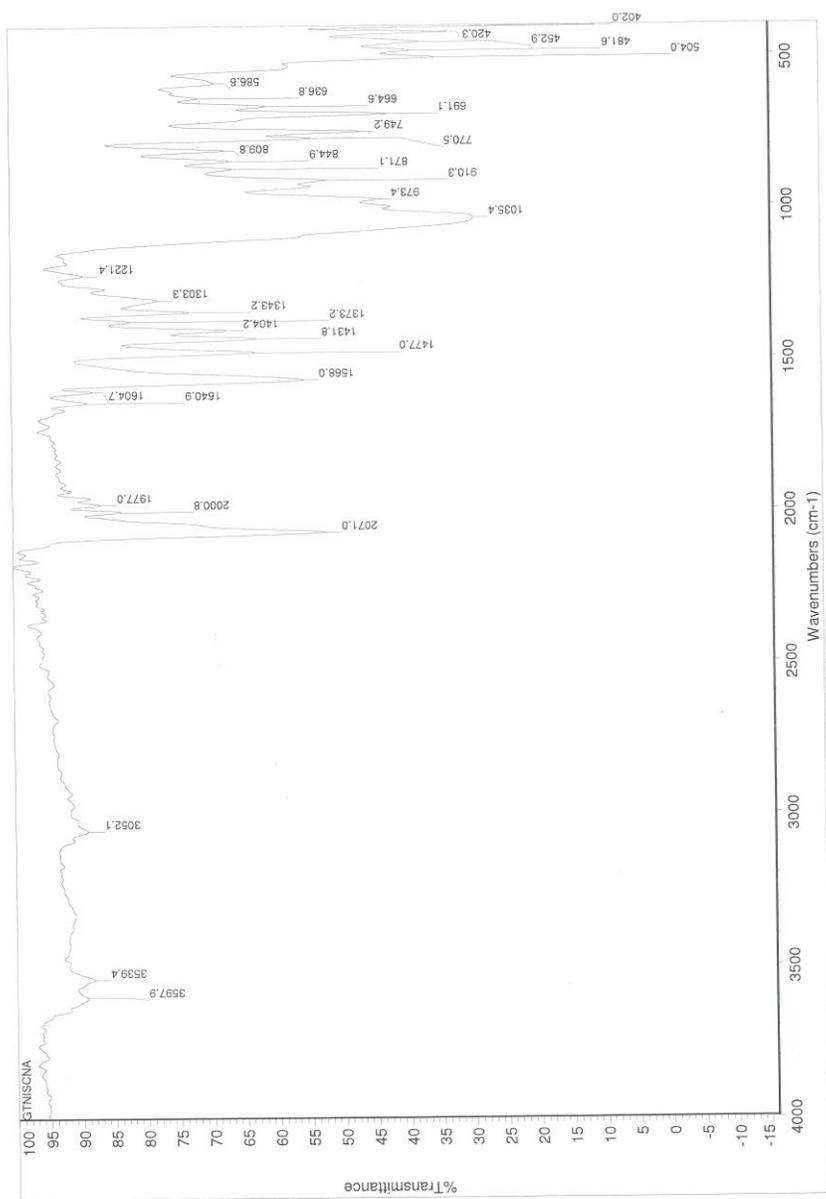
Figure S5. IR spectrum of complex **4**.
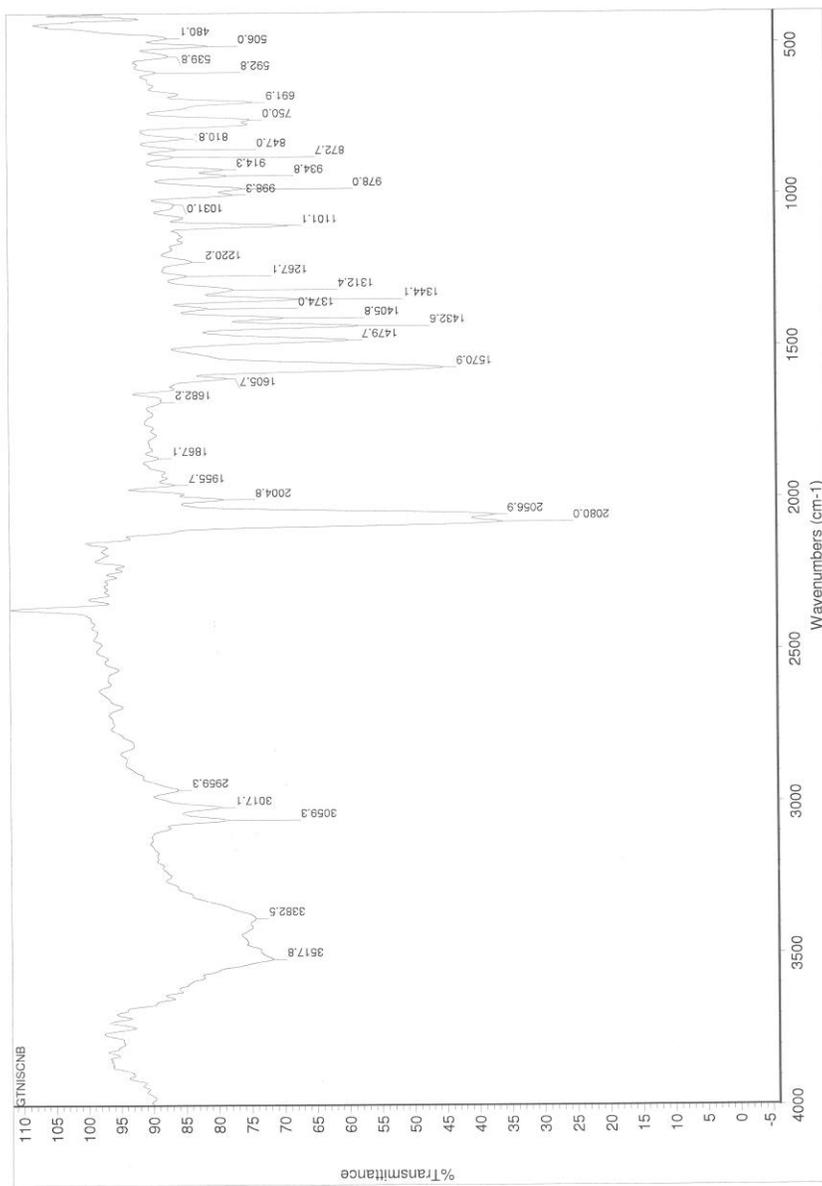
Figure S6. IR spectrum of complex **5**.
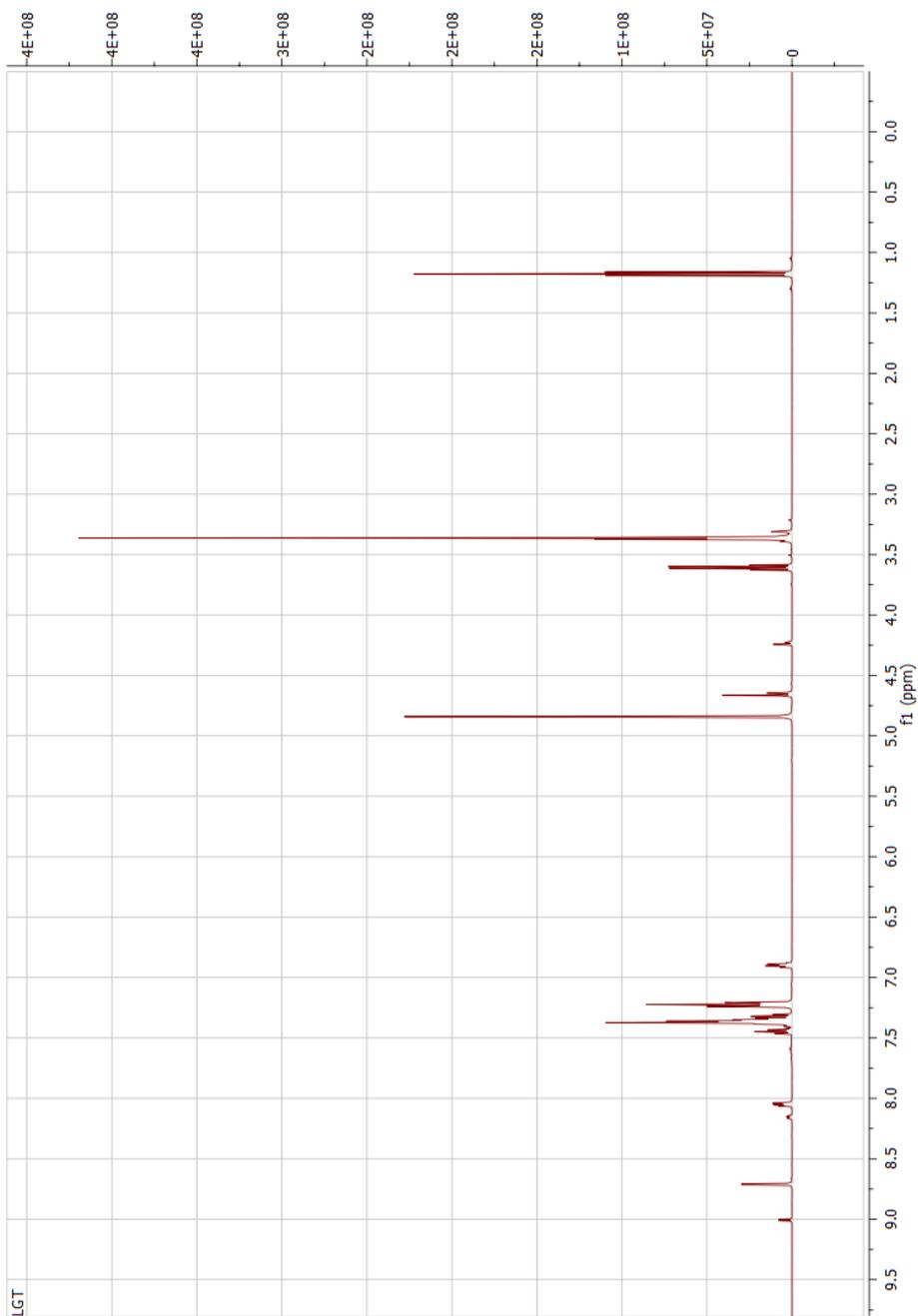
**Figure S7.** ^{1}H NMR spectrum of **HL**Cl·EtOH.
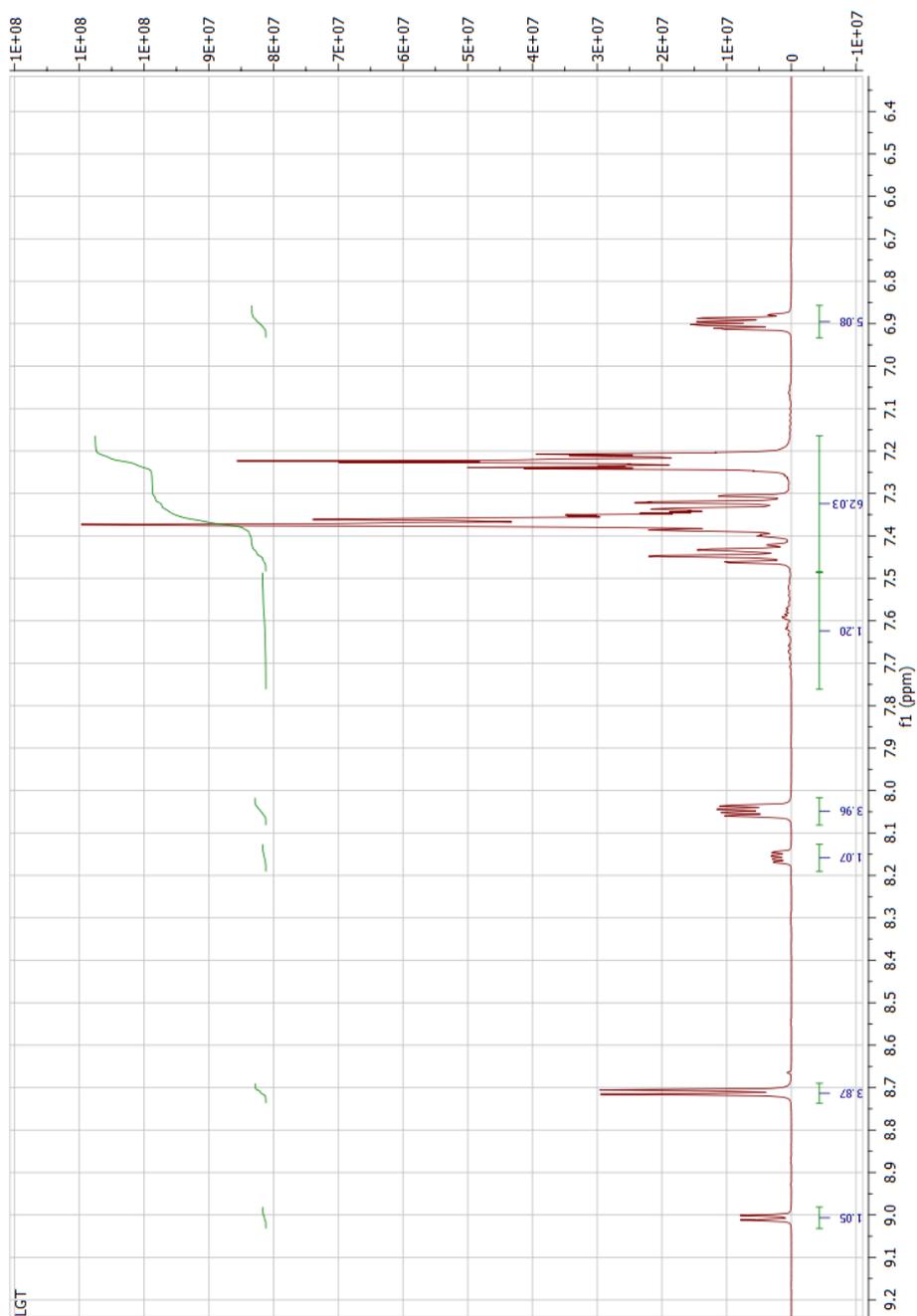
Figure S8. ^{1}H NMR spectrum of **HL**Cl·EtOH.
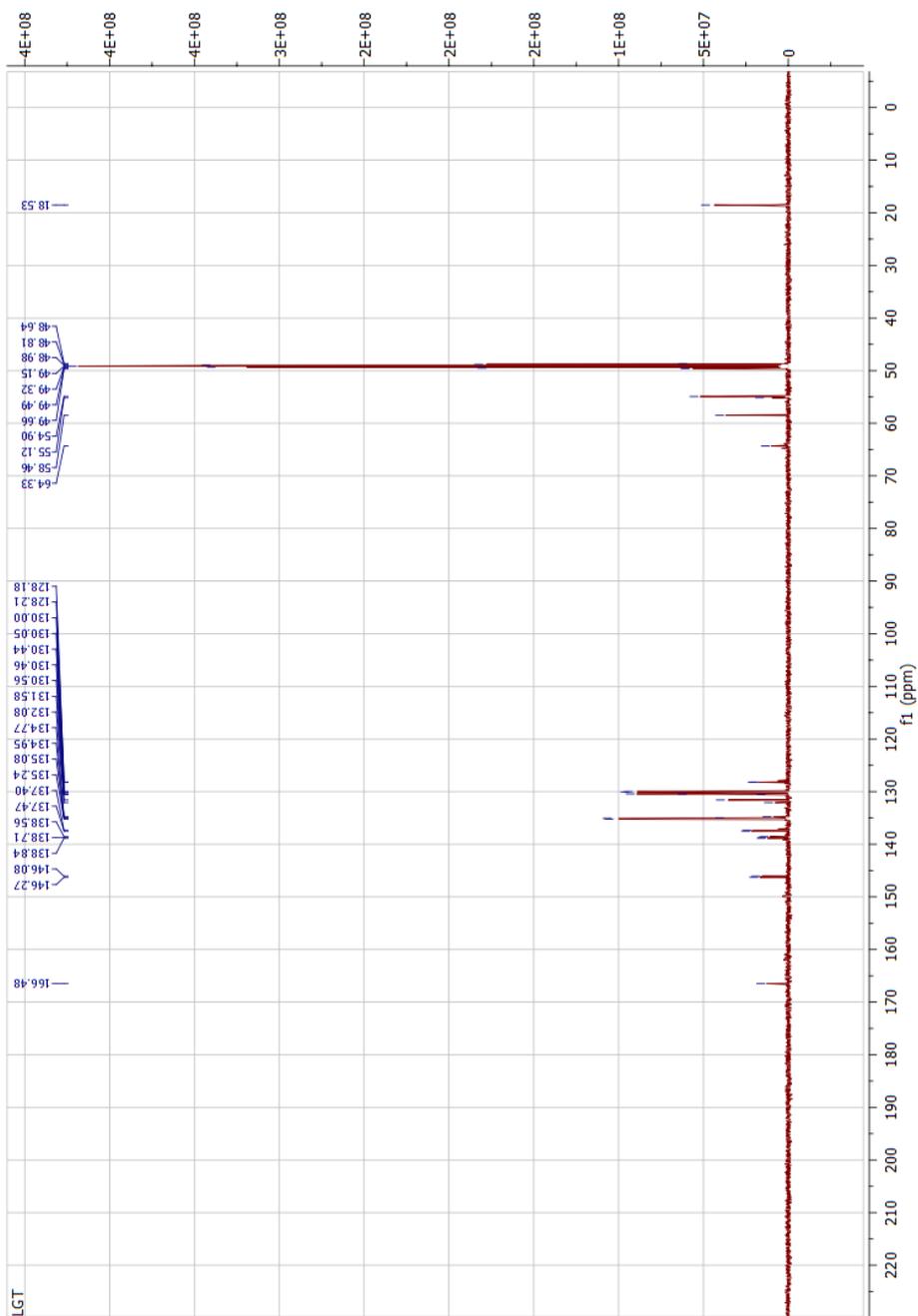
Figure S9. ^{13}C NMR spectrum of **HL**Cl·EtOH.
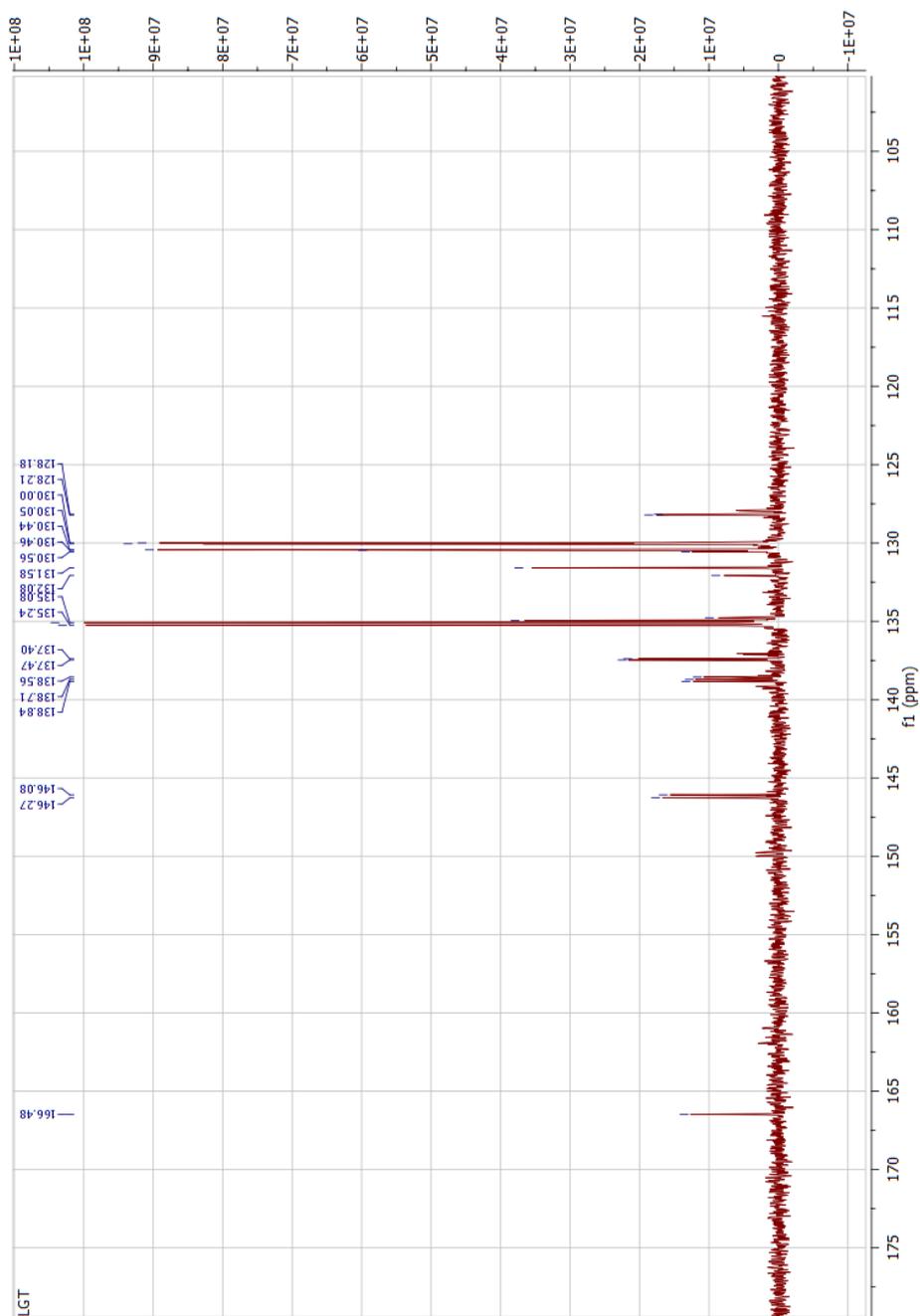
Figure S10. ^{13}C NMR spectrum of **HL**Cl·EtOH.
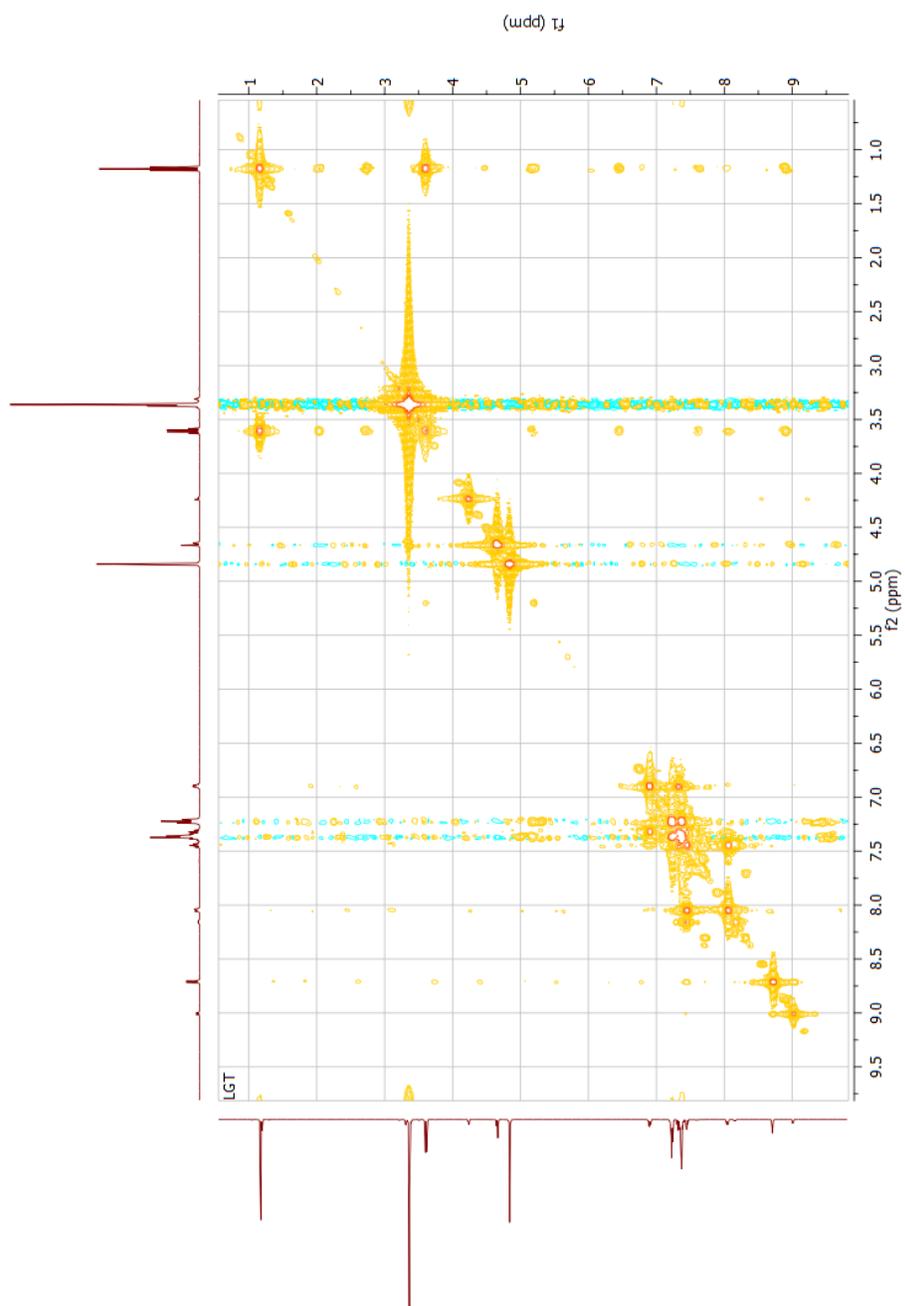
Figure S11. COSY spectrum of **HL**Cl·EtOH.
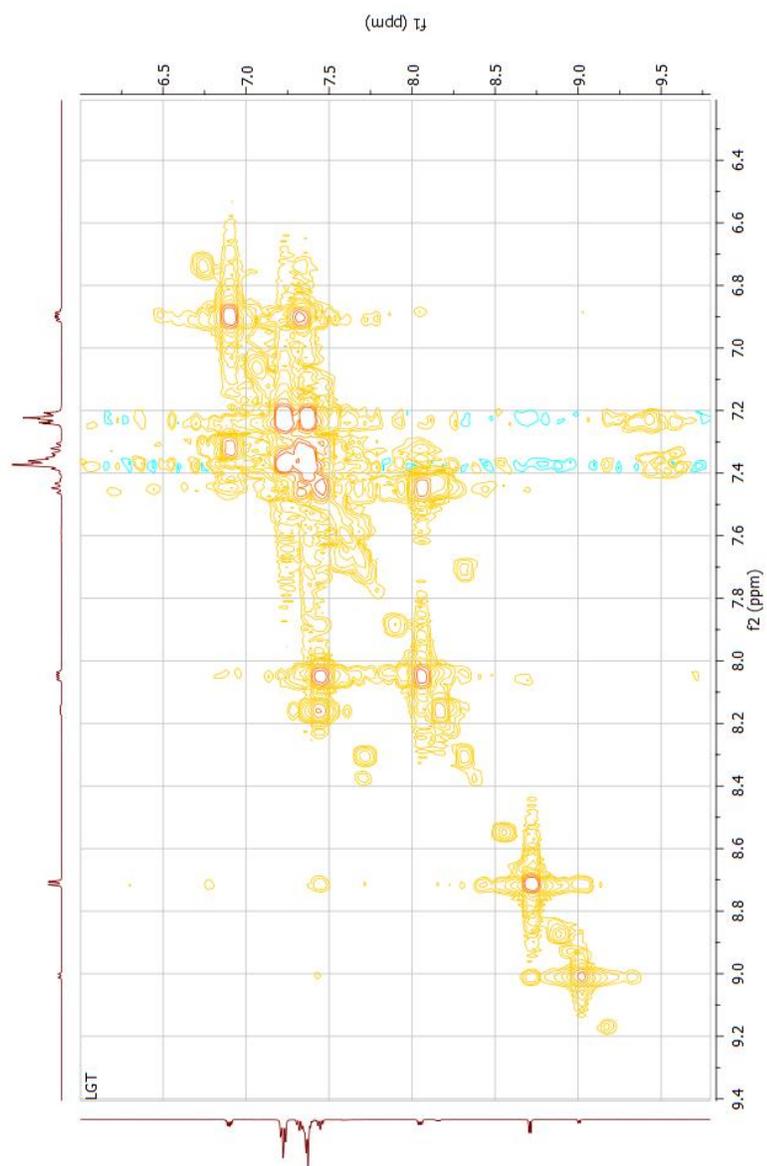
Figure S12. COSY spectrum of **HL**Cl·EtOH.
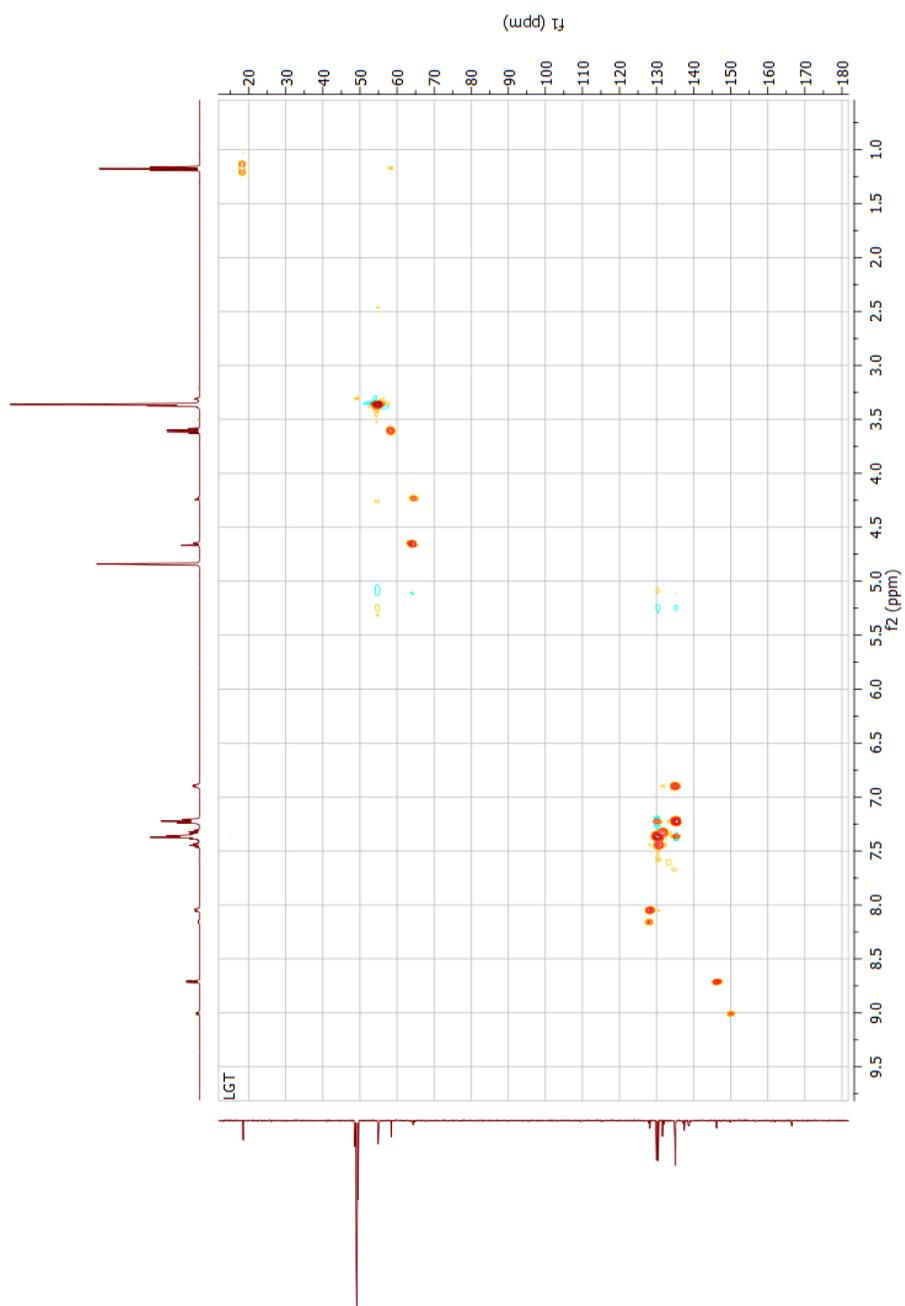
Figure S13. HSQC spectrum of **HL**Cl·EtOH.
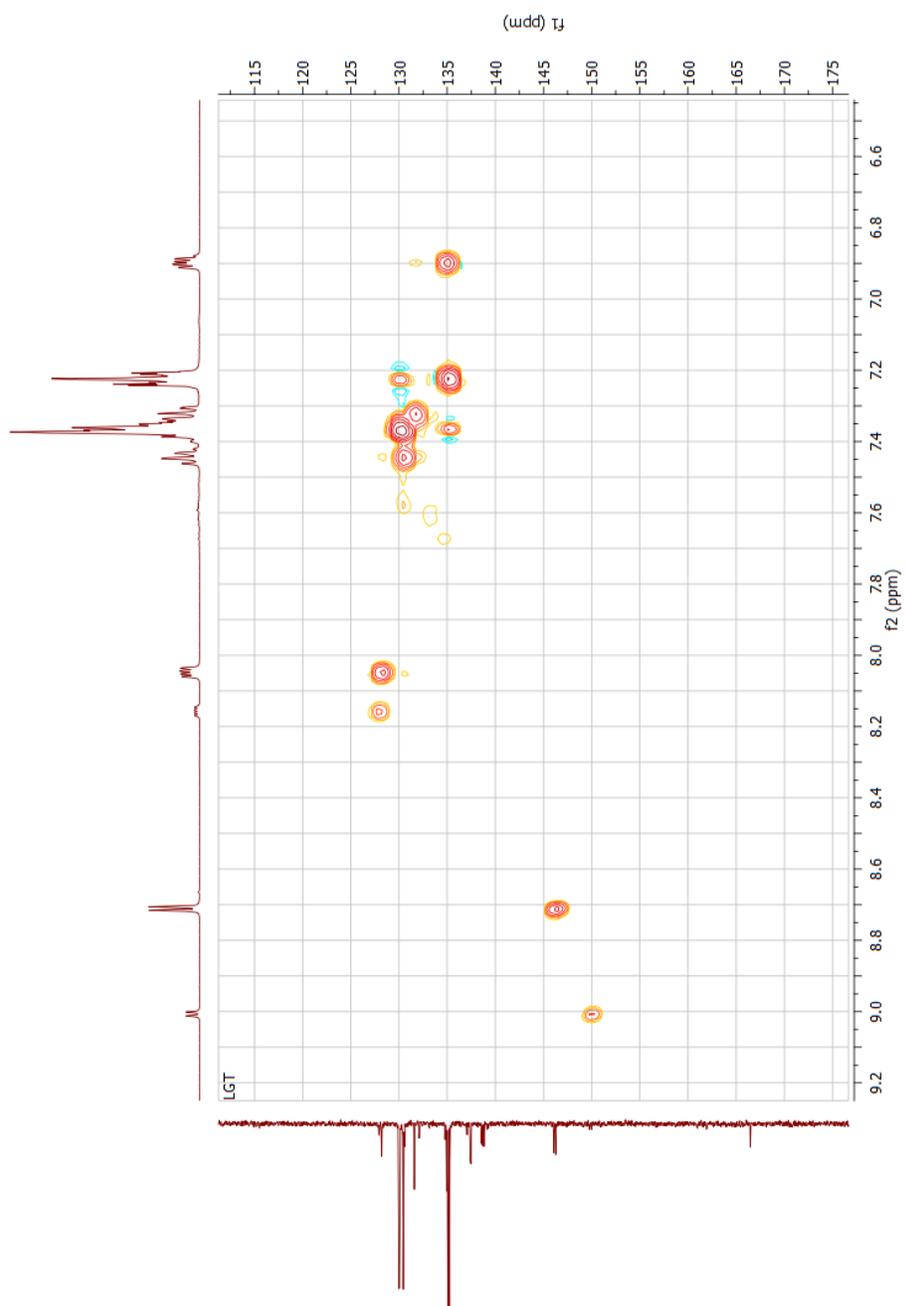
Figure S14. HSQC spectrum of **HL**Cl·EtOH.

Figure S15. ^{1}H NMR spectrum of complex **1**.
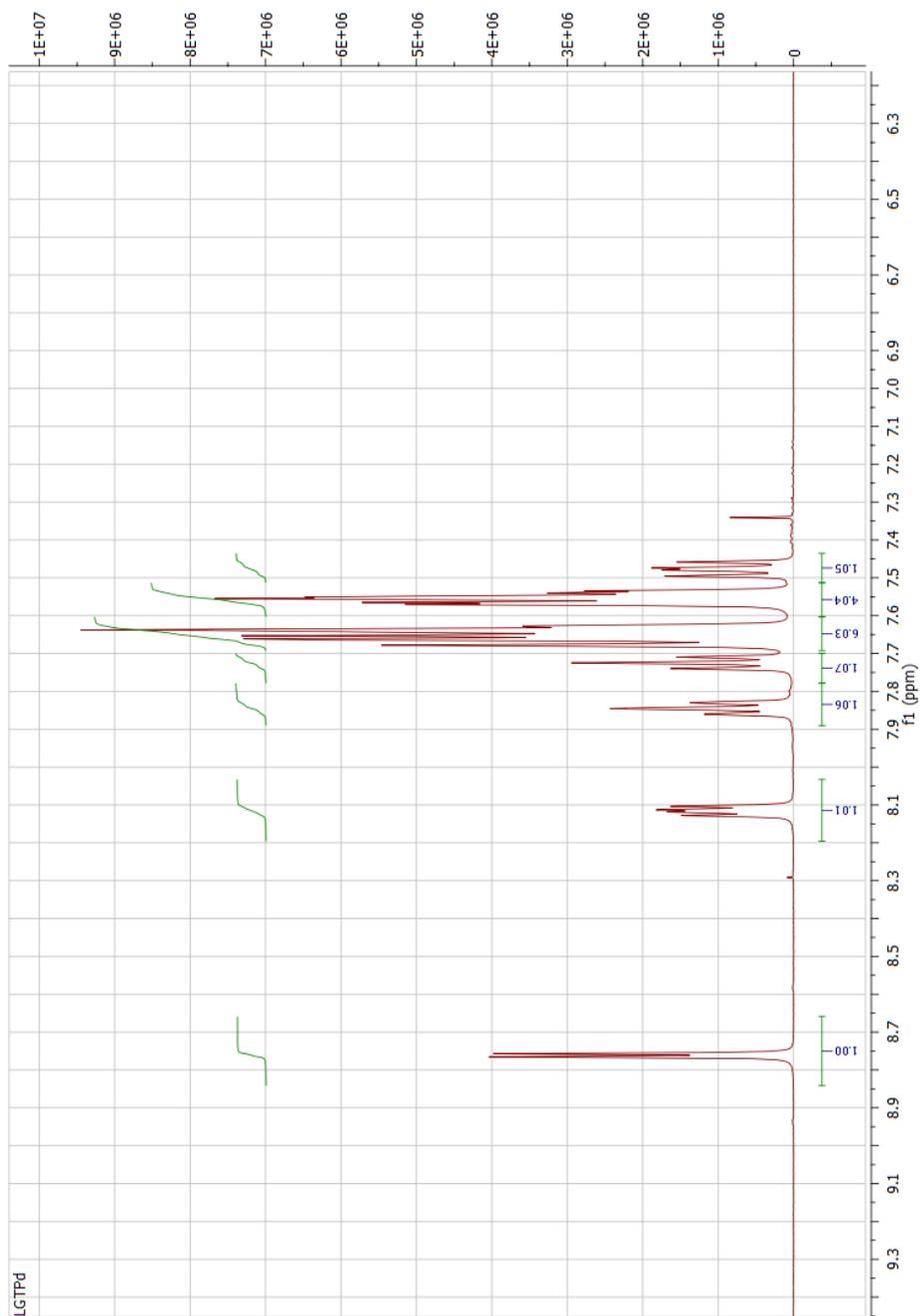
Figure S16. ^{1}H NMR spectrum of complex **1**.
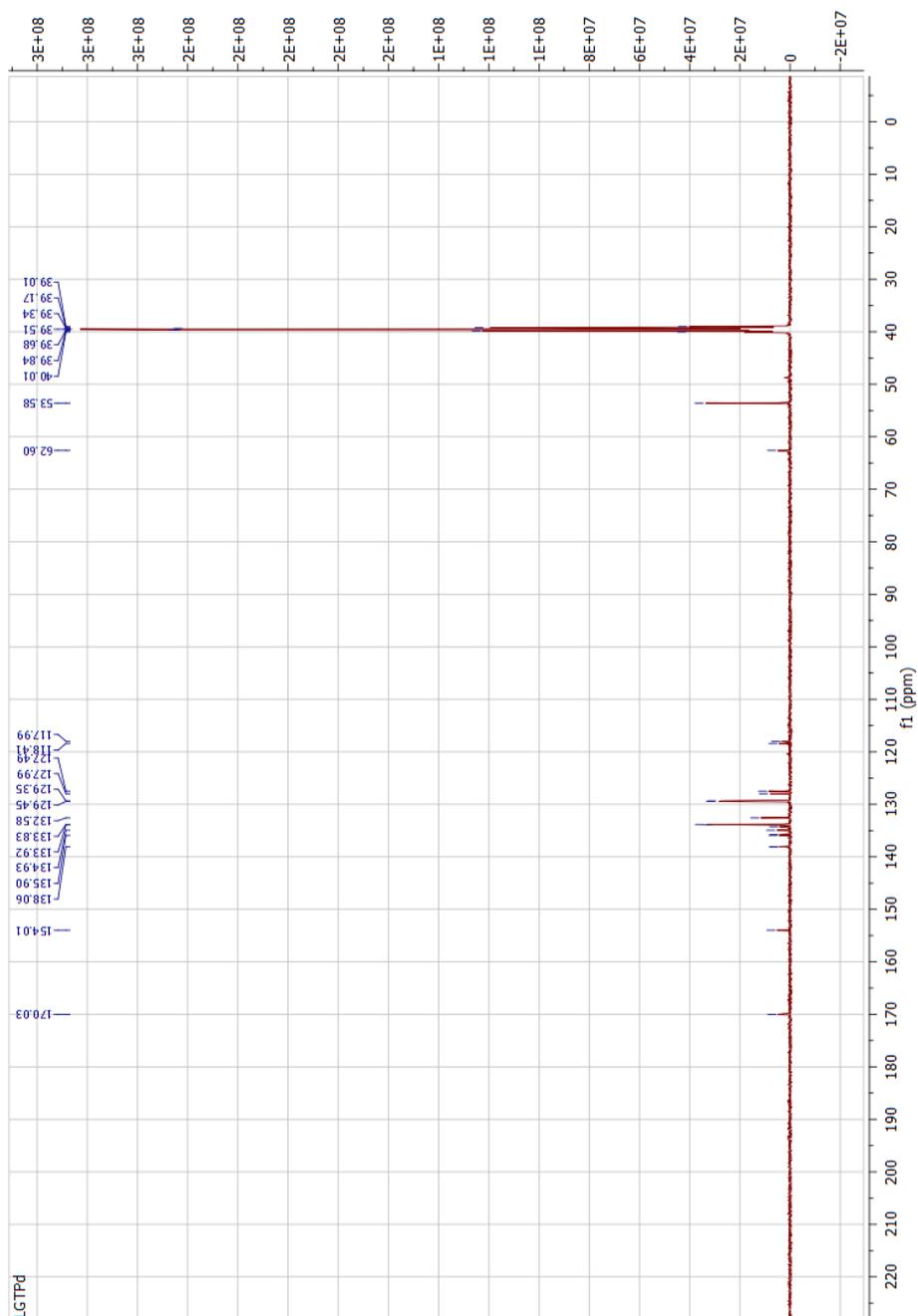
Figure S17. ^{13}C NMR spectrum of complex **1**.
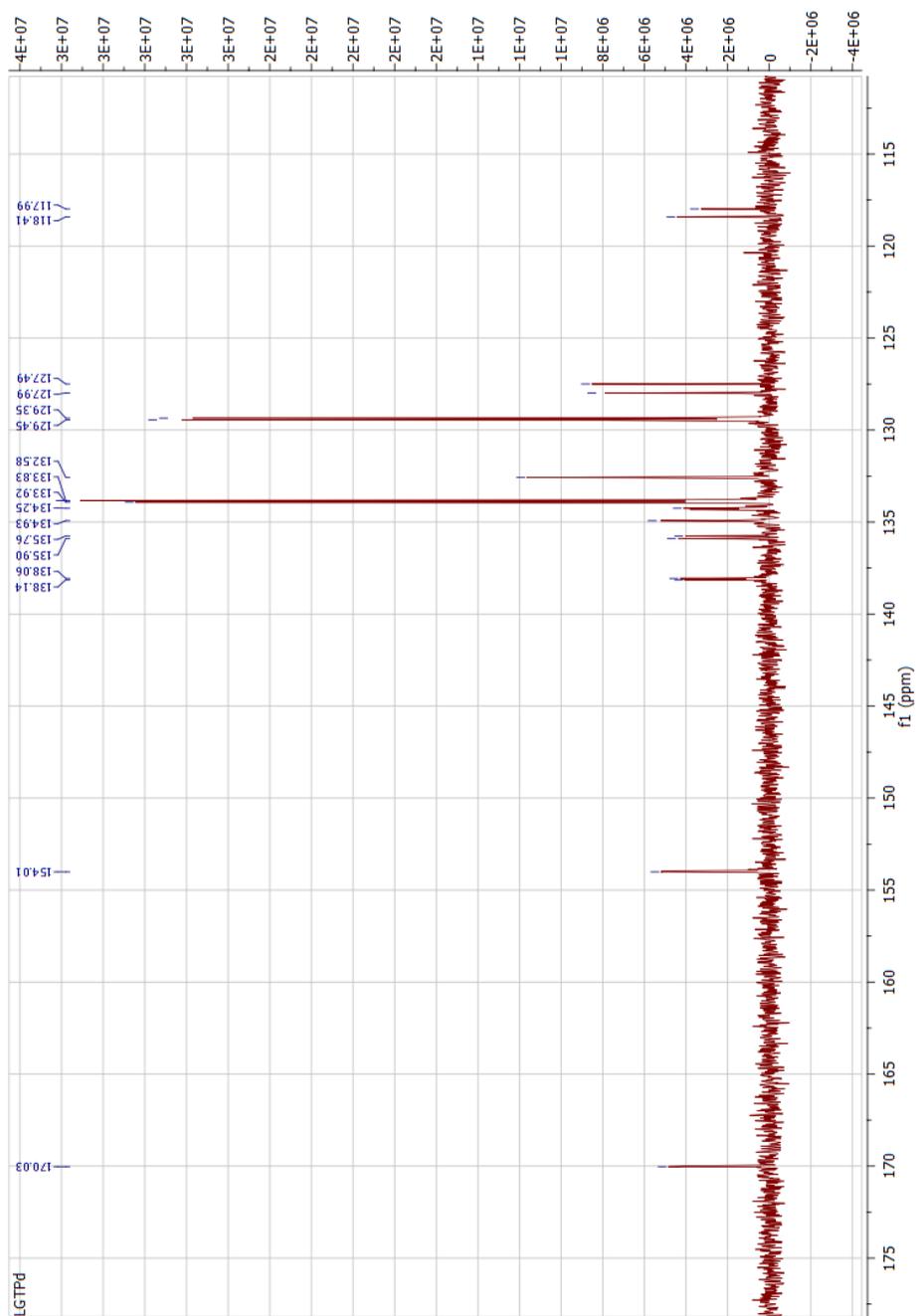
**Figure S18.** ^{13}C NMR spectrum of complex **1**.
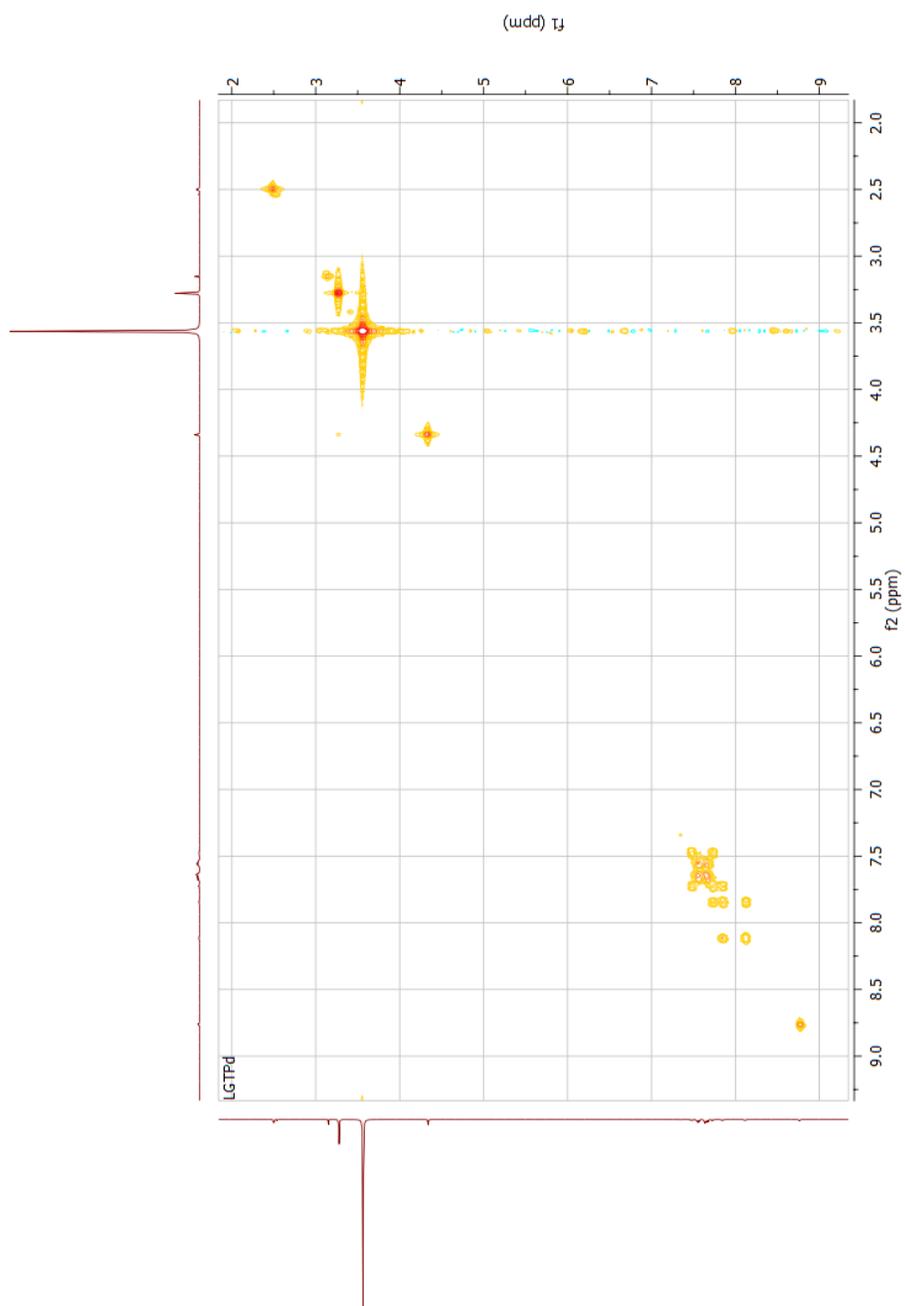
Figure S18. COSY spectrum of complex **1**.
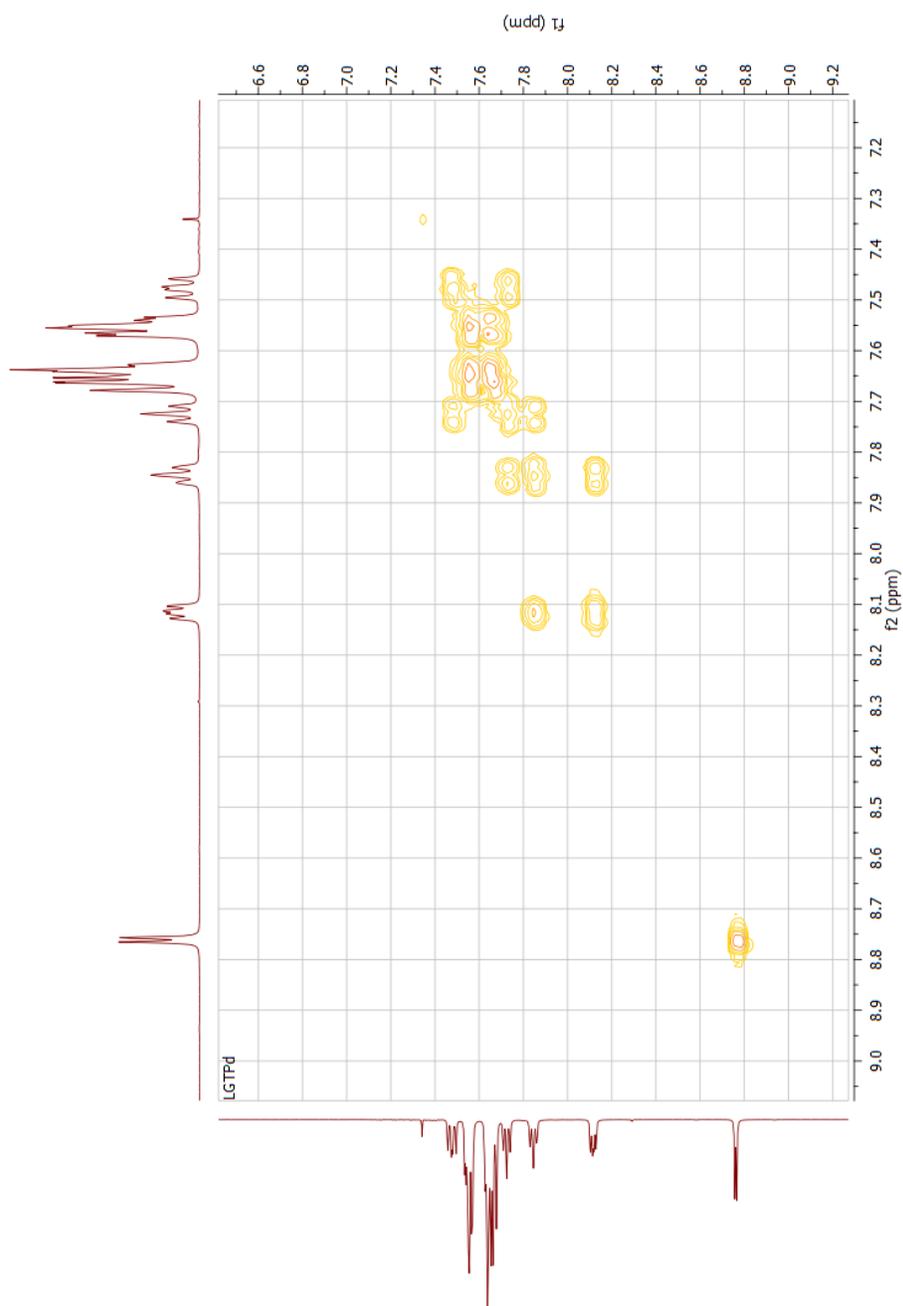
Figure S19. COSY spectrum of complex **1**.
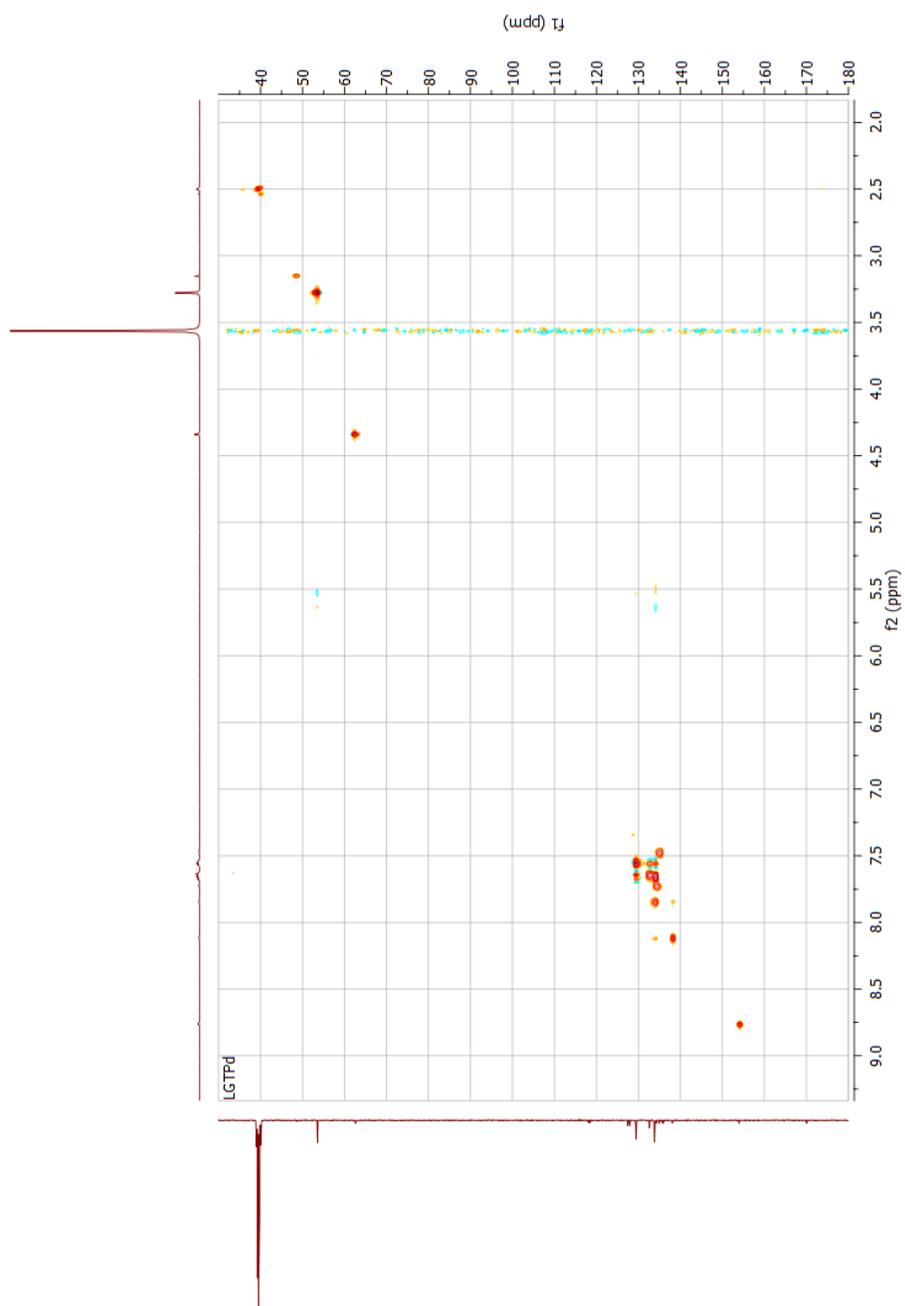
Figure S20. HSQC spectrum of complex **1**.
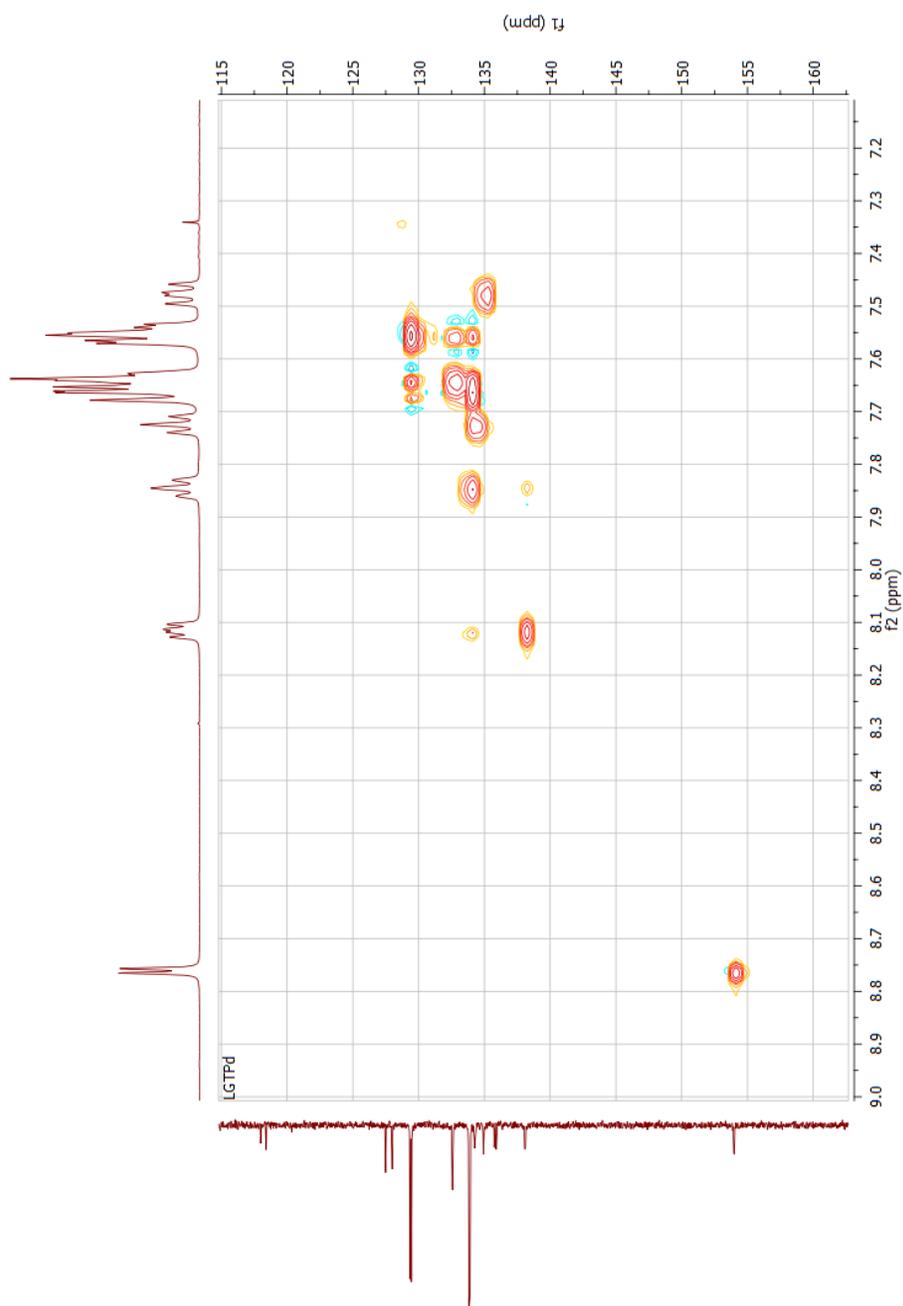
Figure S21. HSQC spectrum of complex **1**.
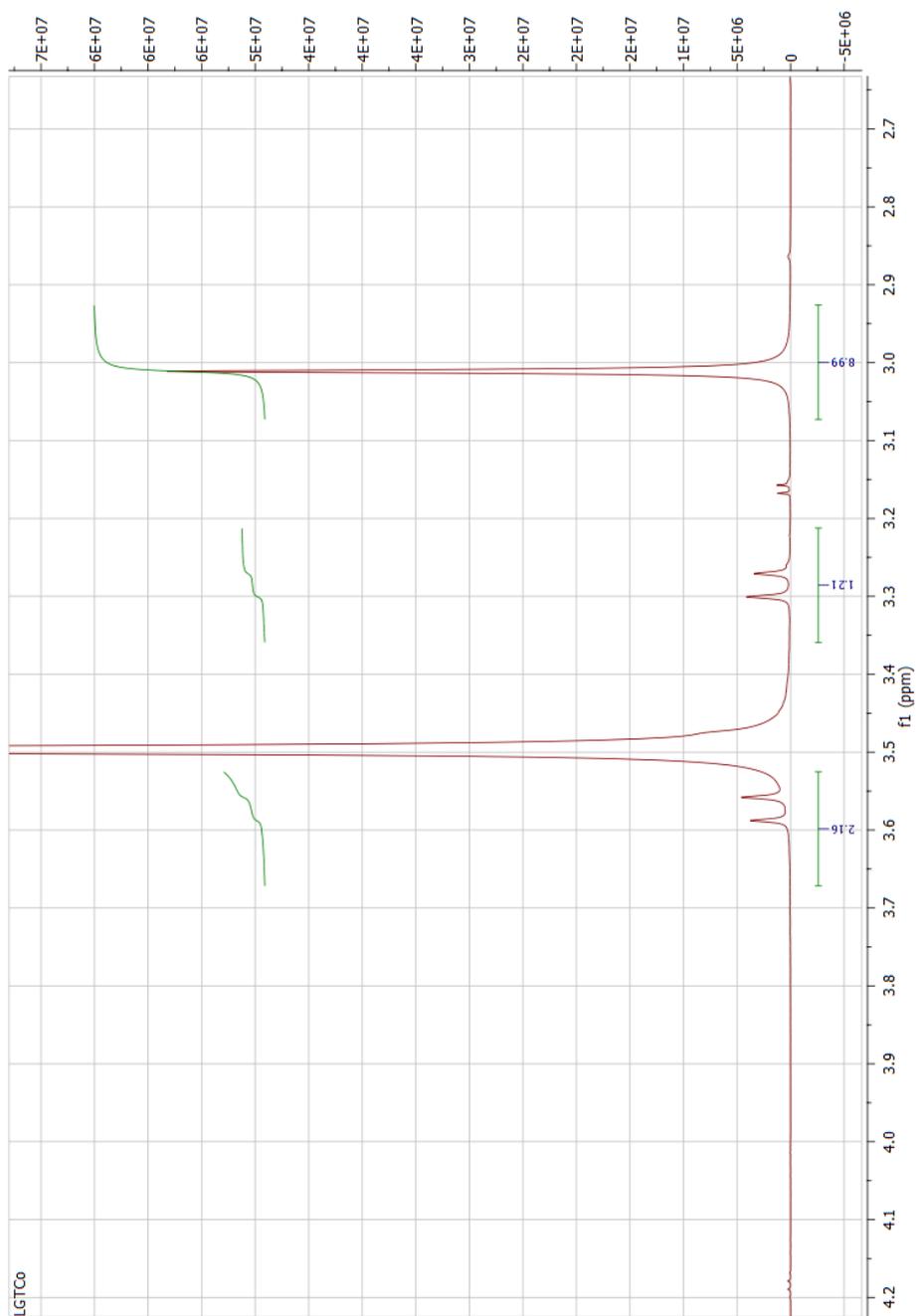
Figure S22. ^{1}H NMR spectrum of complex **2**.
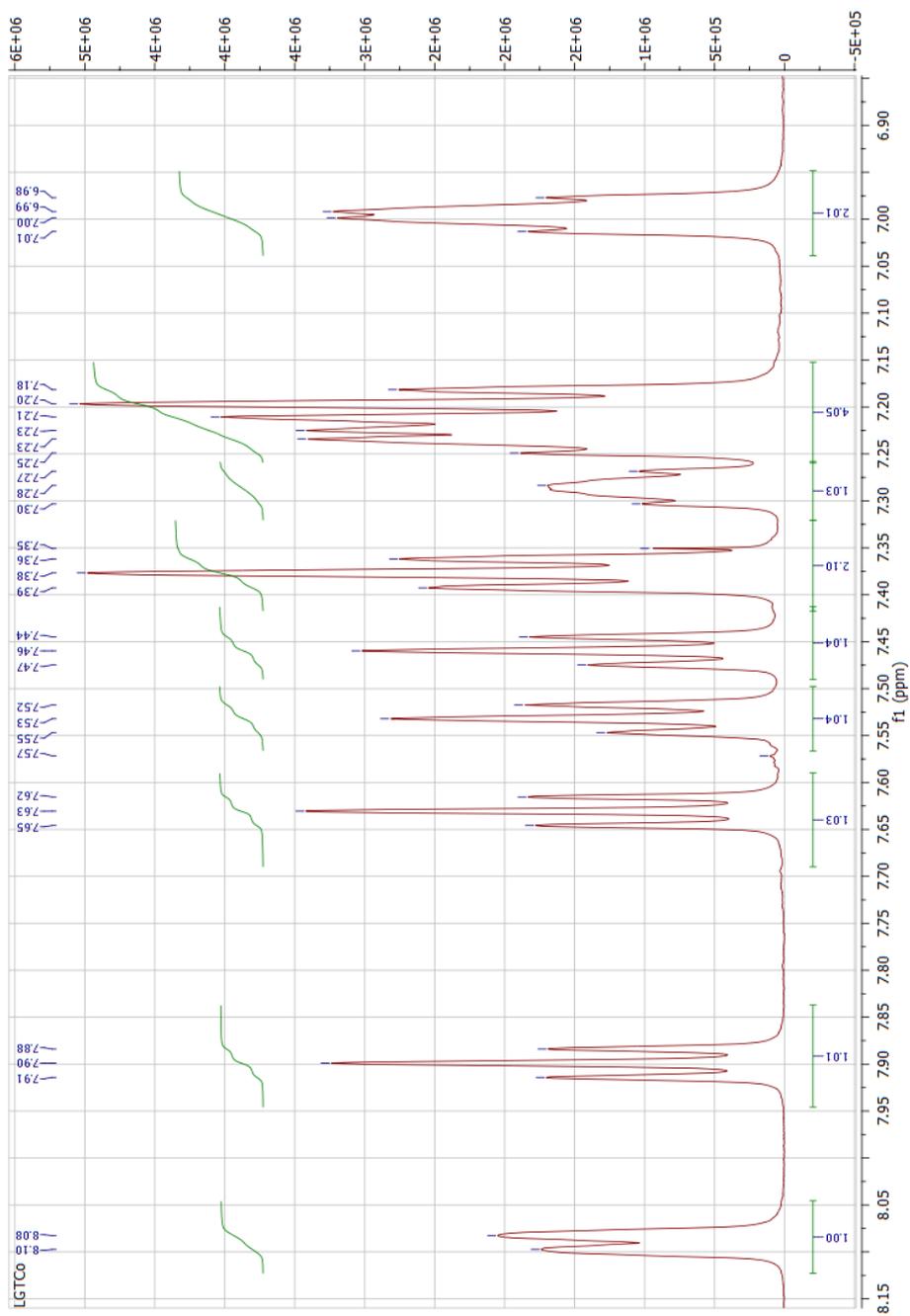
Figure S23. ¹H NMR spectrum of complex **2**.
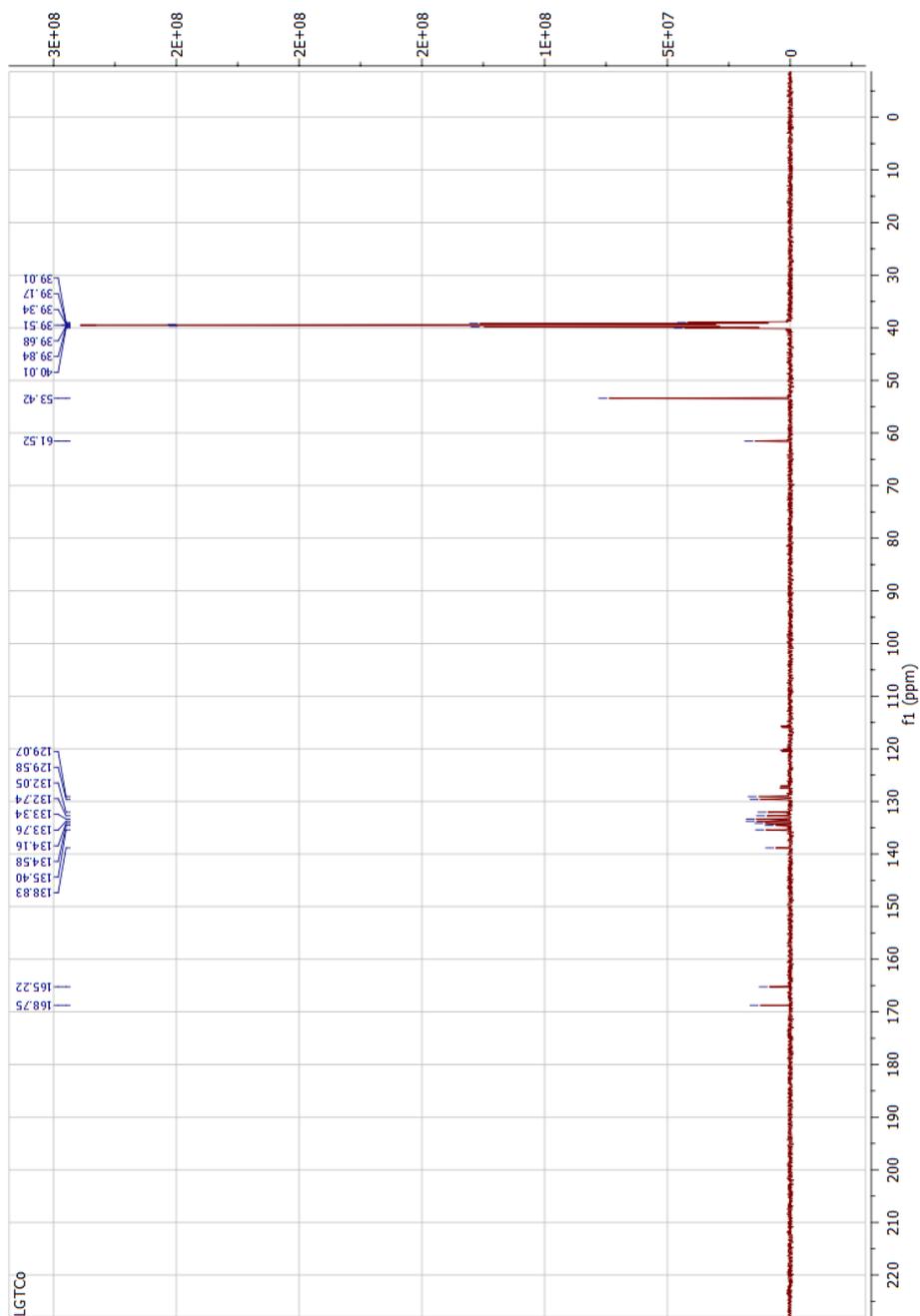
Figure S24. ^{13}C NMR spectrum of complex **2**.
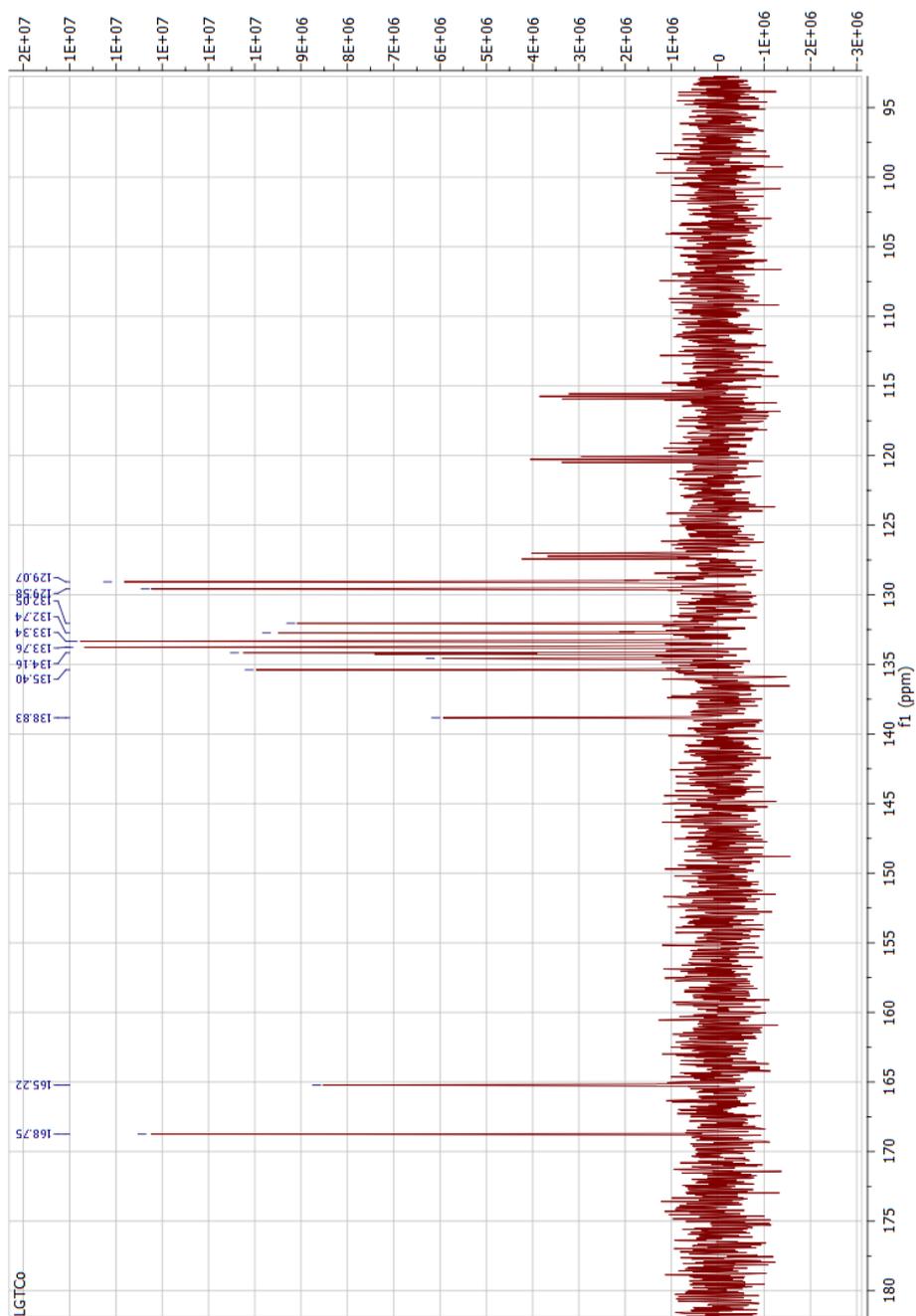
Figure S25. ^{13}C NMR spectrum of complex **2**.
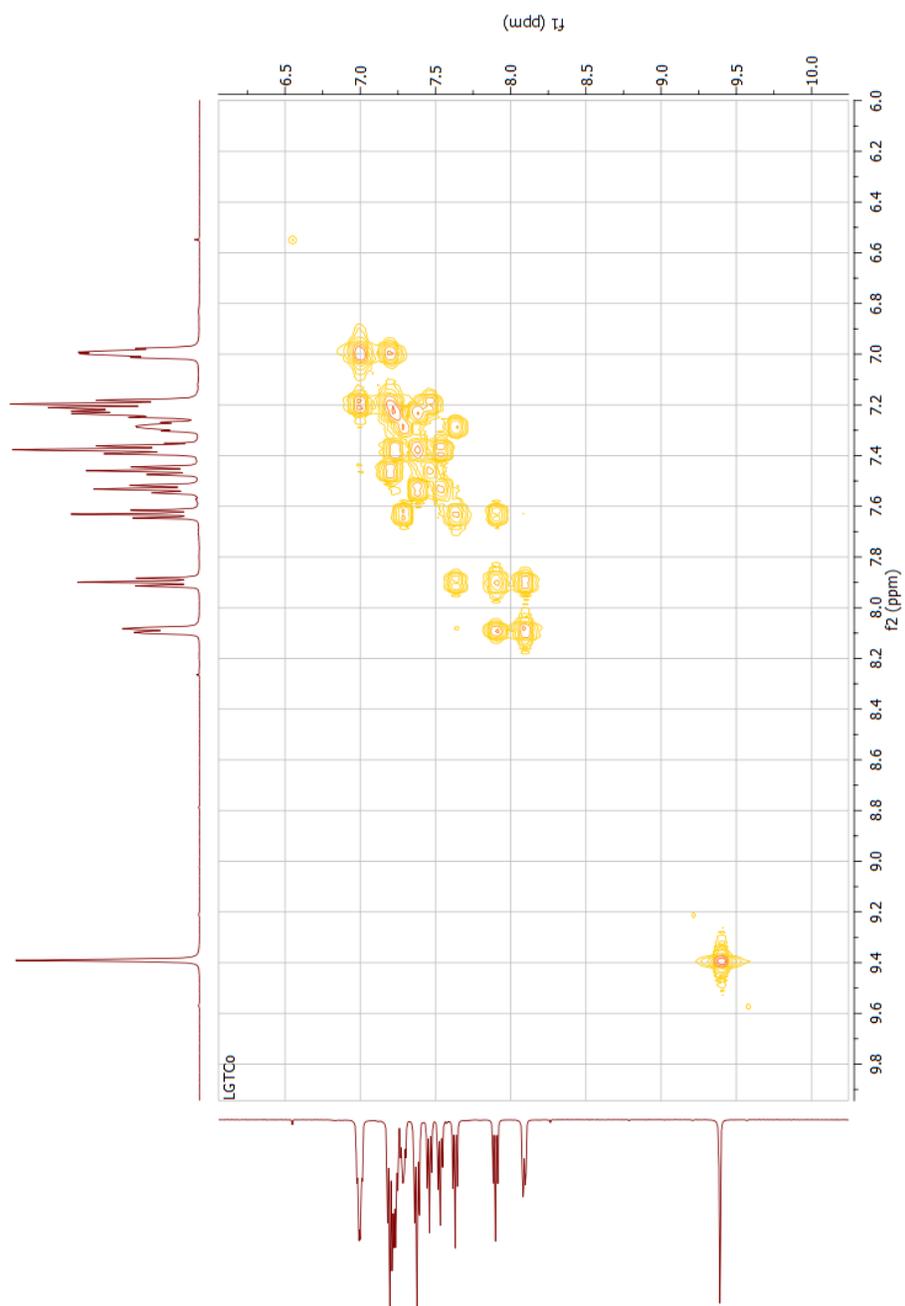
**Figure S26.** COSY spectrum of complex **2**.
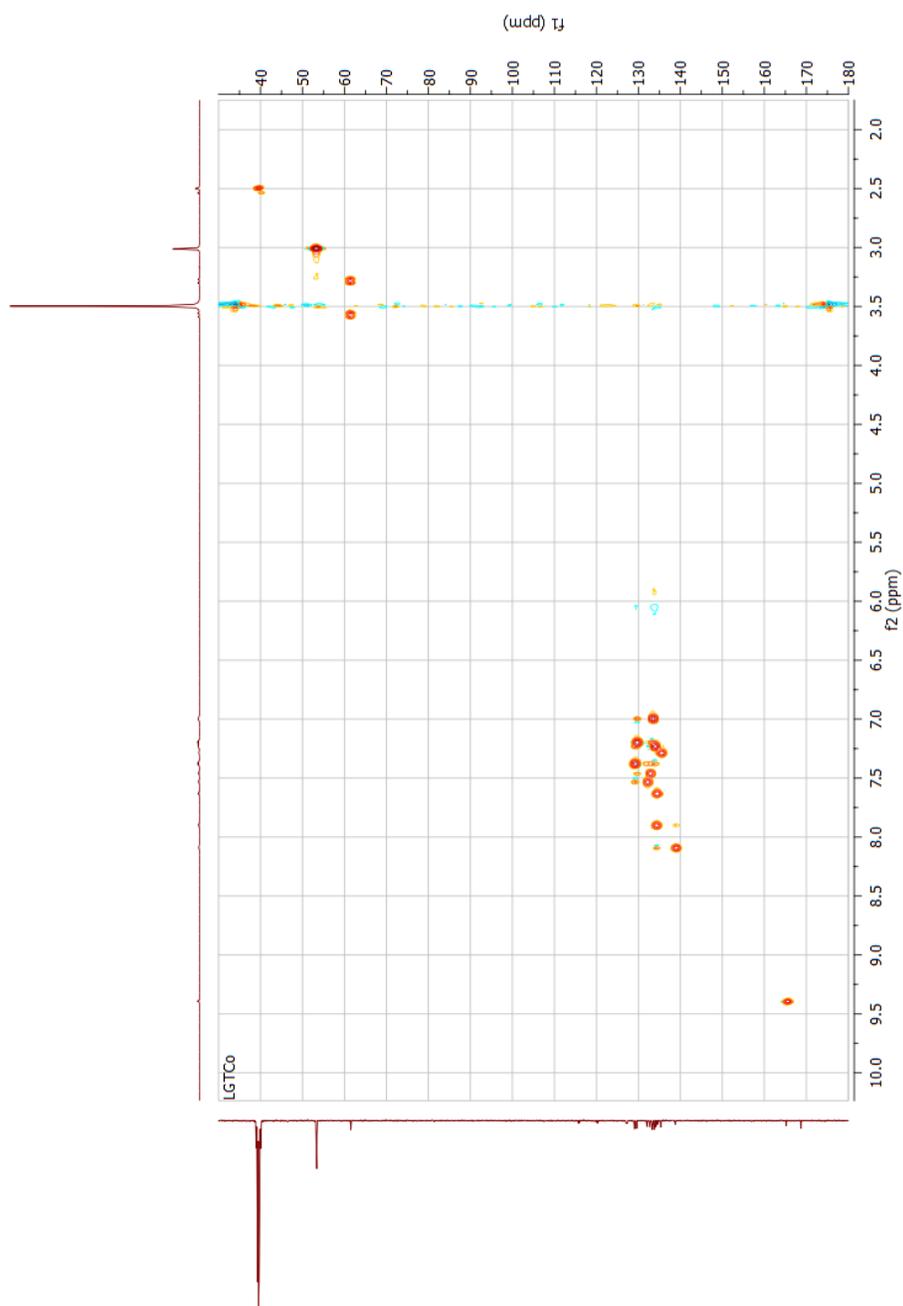
Figure S27. HSQC spectrum of complex **2**.
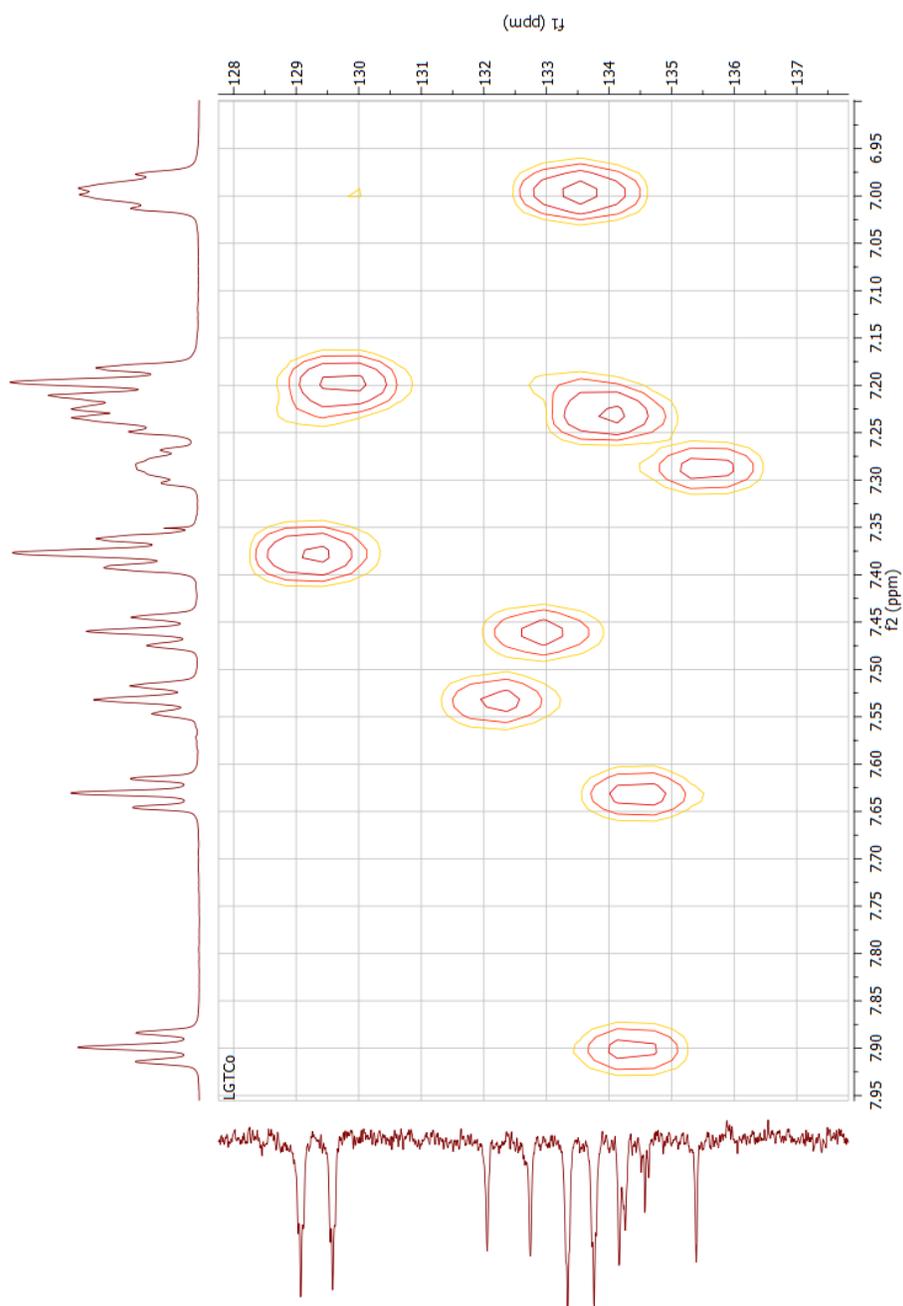
Figure S28. HSQC spectrum of complex **2**.

7. Curriculum Vitae

Kawther Adaila, MSc in Chemistry

Date of birth: 24th June 1986

Place of birth: Tripoli, Libya

Education

2012 –	PhD student at Faculty of Chemistry, University of Belgrade
December 2012	Master of Science degree in Chemistry, Faculty of Chemistry, University of Belgrade
2010-2012	MSc studies, Faculty of Chemistry, University of Belgrade
December 2008	Bachelor of Science degree in Chemistry, Faculty of Science, University of Al.jabal Al.garbi, Gharian, Libya
2005-2008	Chemistry studies, Faculty of Science, University of Al.jabal Al.garbi, Gharian, Libya
2001-2005	High school, Gharian, Libya
1998-2001	Elementary school, Gharian, Libya

Publications

K. Adaila, M. Milenković, A. Bacchi, G. Cantoni, M. Swart, M. Gruden-Pavlović, M. Milenković, B. Čobeljić, T. Todorović, K Anđelković,

Synthesis, characterization, DFT calculations, and antimicrobial activity of Pd(II) and Co(III) complexes with the condensation derivative of

2-(diphenylphosphino)benzaldehyde and Girard's T reagent,

Journal of Coordination Chemistry, **67**(22) (2014) 3633–3648.

B. Čobeljić, A. Pevec, S. Stepanović, V. Spasojević, M. Milenković, I. Turel, M. Swart, M. Gruden-Pavlović, <u>K. Adaila,</u> K. Anđelković,

Experimental and theoretical investigation of octahedral and square-planar isothiocyanato complexes of Ni(II) with acylhydrazones of 2-(diphenylphosphino)benzaldehyde,

Polyhedron, **89** (2015) 271–279.

Прилог 1.

Изјава о ауторству

Потписани-а <u>Каутер Адаила</u>

број индекса <u>ДХ19/2012</u>

Изјављујем

да је докторска дисертација под насловом

<u>Синтеза и карактеризација комплекса Pd(II), Co(III) i Ni(II) са кондензационим производом 2-(дифенилфосфино)бензалдехид и Жираровог Т реагенса</u>

- резултат сопственог истраживачког рада,
- да предложена дисертација у целини ни у деловима није била предложена за добијање било које дипломе према студијским програмима других високошколских установа,
- да су резултати коректно наведени и
- да нисам кршио/ла ауторска права и користио интелектуалну својину других лица.

Потпис докторанда

У Београду, _____

_____

Прилог 2.

Изјава о истоветности штампане и електронске верзије докторског рада

Име и презиме аутора <u>Каутер Адаила</u>

Број индекса <u>ДХ19/2012</u>

Студијски програм <u>доктор хемијских наука</u>

Наслов рада <u>Синтеза и карактеризација комплекса Pd(II), Co(III) i Ni(II) са кондензационим производом 2-(дифенилфосфино)бензалдехид и Жираровог Т реагенса</u>

Ментор <u>др Катарина Анђелковић, редовни професор Хемијског факултета Универзитета у Београду</u>

<div align="center">Потписани/а <u>Каутер Адаила</u></div>

Изјављујем да је штампана верзија мог докторског рада истоветна електронској верзији коју сам предао/ла за објављивање на порталу **Дигиталног репозиторијума Универзитета у Београду.**

Дозвољавам да се објаве моји лични подаци везани за добијање академског звања доктора наука, као што су име и презиме, година и место рођења и датум одбране рада.

Ови лични подаци могу се објавити на мрежним страницама дигиталне библиотеке, у електронском каталогу и у публикацијама Универзитета у Београду.

<div align="right">Потпис докторанда</div>

У Београду, _____

<div align="right">_____</div>

Прилог 3.

Изјава о коришћењу

Овлашћујем Универзитетску библиотеку „Светозар Марковић" да у Дигитални репозиторијум Универзитета у Београду унесе моју докторску дисертацију под насловом:

<u>Синтеза и карактеризација комплекса Pd(II), Co(III) i Ni(II) са кондензационим производом 2-(дифенилфосфино)бензалдехид и Жираровог Т реагенса</u>

која је моје ауторско дело.

Дисертацију са свим прилозима предао/ла сам у електронском формату погодном за трајно архивирање.

Моју докторску дисертацију похрањену у Дигитални репозиторијум Универзитета у Београду могу да користе сви који поштују одредбе садржане у одабраном типу лиценце Креативне заједнице (Creative Commons) за коју сам се одлучио/ла.

1. Ауторство

2. Ауторство - некомерцијално

3. Ауторство – некомерцијално – без прераде

4. Ауторство – некомерцијално – делити под истим условима

5. Ауторство – без прераде

6. Ауторство – делити под истим условима

(Молимо да заокружите само једну од шест понуђених лиценци, кратак опис лиценци дат је на полеђини листа).

<div align="right">

Потпис докторанда

</div>

У Београду, _____

<div align="right">

_____

</div>

1. Ауторство - Дозвољавате умножавање, дистрибуцију и јавно саопштавање дела, и прераде, ако се наведе име аутора на начин одређен од стране аутора или даваоца лиценце, чак и у комерцијалне сврхе. Ово је најслободнија од свих лиценци.

2. Ауторство – некомерцијално. Дозвољавате умножавање, дистрибуцију и јавно саопштавање дела, и прераде, ако се наведе име аутора на начин одређен од стране аутора или даваоца лиценце. Ова лиценца не дозвољава комерцијалну употребу дела.

3. Ауторство - некомерцијално – без прераде. Дозвољавате умножавање, дистрибуцију и јавно саопштавање дела, без промена, преобликовања или употребе дела у свом делу, ако се наведе име аутора на начин одређен од стране аутора или даваоца лиценце. Ова лиценца не дозвољава комерцијалну употребу дела. У односу на све остале лиценце, овом лиценцом се ограничава највећи обим права коришћења дела.

4. Ауторство - некомерцијално – делити под истим условима. Дозвољавате умножавање, дистрибуцију и јавно саопштавање дела, и прераде, ако се наведе име аутора на начин одређен од стране аутора или даваоца лиценце и ако се прерада дистрибуира под истом или сличном лиценцом. Ова лиценца не дозвољава комерцијалну употребу дела и прерада.

5. Ауторство – без прераде. Дозвољавате умножавање, дистрибуцију и јавно саопштавање дела, без промена, преобликовања или употребе дела у свом делу, ако се наведе име аутора на начин одређен од стране аутора или даваоца лиценце. Ова лиценца дозвољава комерцијалну употребу дела.

6. Ауторство - делити под истим условима. Дозвољавате умножавање, дистрибуцију и јавно саопштавање дела, и прераде, ако се наведе име аутора на начин одређен од стране аутора или даваоца лиценце и ако се прерада дистрибуира под истом или сличном лиценцом. Ова лиценца дозвољава комерцијалну употребу дела и прерада. Слична је софтверским лиценцама, односно лиценцама отвореног кода.